Creep and Shrinkage Prediction Models for Concrete Water Retaining Structures in South Africa

By

Edson Silva David Mucambe

Thesis presented in partial fulfilment of the requirements for the degree of Master of Science in Engineering at the University of Stellenbosch

Supervisor: Professor Gideon P.A.G. van Zijl

Faculty of Engineering
Department of Civil Engineering

Date of Award: December 2010

ABSTRACT

Concrete water retaining structures (WRS) in South Africa are under scrutiny due to the numerous durability problems that they have experienced lately; despite the efforts by local and national authorities in conserving these structures. At the heart of these problems are the creep and shrinkage phenomena. While shrinkage is the reduction of concrete volume with time, creep is defined as the time-dependent increase of concrete strain under constant or controlled stress. Both phenomena are affected by conditions to which WRS are exposed hence their accurate prediction is required.

Numerical models have been developed to calculate the extent to which concrete creeps or shrinks over time. The objective of this thesis is to identify which of these models is better equipped to be used in South African WRS design. This is achieved through a systematic method that involves an investigation into the contents of these models and a statistical comparison of model calculations to WRS representative data.

In partnership with reputable universities, a pioneer experimental creep and shrinkage data base is created in this project from which the WRS related data is selected. While investigating the contents of the numerical models, their applicability to South African WRS is identified and the integrity of model contents is assessed. Indeed, a few irregularities are found in the process and are presented in this thesis.

The model calculations are statistically compared to data in the form of individual experiments as well as in the form of groups of experiments with similar concretes to find the ideal prediction model for different types of concretes as well.

Also pioneered in this project is a weighted criteria and point system in which the findings of the model content assessment and statistical evaluations are incorporated. It is based on this system that conclusions are drawn and the most suitable prediction model for WRS design in South Africa is selected.

To my loved mother (Alina Estrela da Silva Ranchaze), my dear father (Anastácio David Faiela Mucambe), my sisters (Ivânia Vanessa da Silva Mucambe and Shelsea L. David Mucambe), my brother (Ivan Claudio David Mucambe) and my nephew (Annelka Nikolaus Tácio Mucambe)

DECLARATION

This research was carried out in the Civil Engineerig Department of the University of Stellenbosch, under the supervision of Professor Gideon P.A.G. van Zijl. This thesis represents original work done by the author (Edson S.D. Mucambe) and has not otherwise been submitted in any form for any degree or diploma to another university. Duly acknowledgement in the text is made for cases where the work of others has been used.

………………………………………… ……………………..

Edson Silva David Mucambe Date

ACKNOWLEDGEMENTS

My sincere thanks to my supervisor Prof. G.P.A.G. van Zijl, whose vast knowledge, and belief in my abilities were fundamental in the completion of this thesis. I thank him for the opportunities that he created for me, the intense hours of research discussion where he taught me how to think critically. Leaded by him, I felt encouraged to give my best and I hope that one day I may grow to be more like him.

I would also like to thank Prof. Jan Wium for everything that he has done for me. His unmatched generosity and belief in my abilities gave me confidence to work through the nights and most importantly, his constant smile reminded me that life is not all about work. He represents to me “the Stellenbosch way of living”: a friendly town where everyone gets along, a true source of inspiration. Not to mention his amazing ability to simplify every problem into a small challenge.

This work would not be completed without the help of Prof. Yunus Ballim and Mrs Petra Gaylard, for the data provided, constant correspondence and for hosting me in the big city of Johannesburg and University of Witswatersrand. Similarly my gratitude is extended to Prof. Mark Alexander and Dr. Hans Beushausen of the University of Cape Town. Thank you all.

I am also grateful to Dr. Robert Vollum of the Imperial College of London; Dr. John Forth of the University of Leeds; Mr Charles Goodchild and Dr. Chris Clear of the Concrete Centre of London; for the information provided and for making me feel welcome. My trip to the United Kingdom was productive and delightful due to their contribution.

The ultimate “thanks” goes to GOD, for the strength provided, the dreams achieved, the opportunity to meet these generous people and much more. May his glory shine through always …

TABLE OF CONTENTS

LIST OF TABLES

LIST OF FIGURES

LIST OF SYMBOLS

A

a	constant that accounts for different cement types
a/c	aggregate-cement ratio

B

b	constant that accounts for different cement types

C

c	cement content in kg/m^3
$C_0(t,t_0)$	compliance function for basic creep
$C_d(t,t_0,t_c)$	additional compliance function due to simultaneous drying

E

$E_{cm}(t)$	elastic modulus at different concrete ages
E_{cmto}	modulus of elasticity at the time of loading
E_{cm28}	elastic modulus at the age of 28 days

F

f_{cm28}	mean cylinder compressive strength at 28 days
f_{cukt}	characteristic cube compressive strength at different concrete ages
f_{cuk28}	characteristic cube compressive strength at the age of 28 days

H

h	variable regarding geometry of the structure
$H(t)$ *and* $H(t_0)$	are spatial averages of pore relative humidity

K

k_{RH}	constant to account for humidity effects
K_0	constant closely related to the modulus of the aggregate

N

N	number of data sets under observation

O

$\overline{O}_j$	mean value of observed results given in equation 3.3.

Q

q_1	instantaneous strain due to unit stress

$Q(t,t_0)$	binomial integral term

R

RH	relative humidity
R	Molar gas constant

S

$S(t,t_c)$	shrinkage development with time
s	concrete slump in mm
s_j	unbiased estimate of variance of a model versus a visually hand-smoothed experimental curve.
ST	Surface tension

T

T	temperature
t	age of concrete, days
t_c	curing time
t_o	loading age of the concrete specimen
t_T	temperature adjusted concrete age which replaces *t* in the corresponding equations

U

U_w	unit weight of concrete

V

V/S	volume over surface area ratio
Vm	Molar volume

W

w	water content in kg/m^3
w/c	water-cement ratio
$\overline{w}$	overall coefficient of variation relative to the mean value of creep or shrinkage
w_j	coefficient of variation of data set j, defined in equation 3.2

GREEK ALPHABET

α	power which depends on the type of cement
α_5	constant to account for cement type effects
α_6	constant to account for curing conditions
α_a	air content in percentage of total volume
$\beta(t)$	correction term to account for curing time and volume to surface ratio

$\beta_c(t,t_0)$	function that takes into account the development of creep with time after loading
β_{RH}	correction term to account for humidity effects
β_{sc}	constant to take into account the cement type
Δt_i	number of days where a temperature T prevails
$\varepsilon_{cc}(t)$	creep strain at time $t > t_o$
$\varepsilon_{ci}(t_0)$	initial strain at loading
$\varepsilon_{cn}(t)$	stress independent strain ($\varepsilon_{csh}(t)+\varepsilon_{cT}(t)$)
$\varepsilon_{csh}(t)$	shrinkage strain
$\varepsilon_{csp}(t)$	specific creep strain
$\varepsilon_{cT}(t)$	thermal strain
$\varepsilon_{c\sigma}(t)$	stress dependent strain ($\varepsilon_{ci}(t_0)+\varepsilon_{cc}(t)$)
ε_{shu}	ultimate shrinkage strains
$\phi(t,t_0)$	creep coefficient
$\phi_{(t_c)}$	correction factor to account for drying before loading
ϕ_u	ultimate creep coefficient
ϕ_0	notional creep coefficient
ϕ_{30}	30 year creep factor
γ_c	cumulative product of applicable ultimate creep coefficient correction factors
$\gamma_{c,sh}$	cement content correction factor of ultimate shrinkage
$\gamma_{RH,c}$	relative humidity correction factor of ultimate creep coefficient
$\gamma_{RH,sh}$	relative humidity correction factor of ultimate shrinkage
$\gamma_{s,c}$	Slump correction factor of ultimate creep coefficient
γ_{sh}	cumulative product of applicable ultimate shrinkage correction factors
$\gamma_{s,sh}$	slump correction factor of ultimate shrinkage
$\gamma_{tc,sh}$	curing time correction factor of ultimate shrinkage
$\gamma_{to,c}$	loading age correction factor of ultimate creep coefficient
$\gamma_{v/s,c}$	V/S correction factor of ultimate creep coefficient
$\gamma_{v/s,sh}$	V/S correction factor of ultimate shrinkage
$\gamma_{\alpha a,c}$	air content correction factor of ultimate creep coefficient
$\gamma_{\alpha a,sh}$	air content correction factor of ultimate shrinkage
$\gamma_{\psi,c}$	fine aggregate percentage correction factor of ultimate creep coefficient
$\gamma_{\psi,sh}$	fine Aggregate percentage correction factor of ultimate shrinkage
τ_{sh}	shrinkage half-time
ψ	fine aggregate percentage

LIST OF ACRONYMS

A

ACI	American Committee Institute
ASTM	American Society for Testing and Materials

B

BP-COV	Bažant and Panula coefficient of variation
BS	British Standard

C

$CaCO_3$	Calcium carbonate (Calcite)
$Ca(OH)_2$	Calcium hydroxide
CEB-FIP	Comite Euro-International du Beton
CEB- MSE	CEB Mean Square Error
CO_2	Carbon dioxide
CS	Chemical Shrinkage
C_3A	Tricalcium Aluminate, also known as $3CaO{\times}Al_2O_3$
C_2S	Carbon disulfide
C_3S	Tricalcium Silicate, also known as $3CaO{\times}SiO_2$
C_4AF	Tetracalcium Aluminoferrite, also known as $4CaO{\times}Al_2O_3{\times}Fe_2O_3$

E

EN	Eurocode (European Standard)

G

GL 2000	Gardner and Lockman model of 2000

H

H_2O	Water
hcp	Hardened cement paste

R

RH	Ambient relative humidity
RILEM	International Union of Testing and Research Laboratories for Materials and Structures
RSA	Republic of South Africa

S

SABS	South African Bureau of Standards

U

UCT	University of Cape Town

UK	United Kingdom
USA	United States of America

W

WITS	University of Witwatersrand
WRS	Water Retaining Structures

CHAPTER 1
INTRODUCTION

1.1. Motivation

The National Water Policy for South Africa (NWP) was preceded by the development of 28 fundamental Principles and Objectives for a New South African Water law. The 7th Principle is of particular relevance to this research project as it states that:

The objective of managing the quantity, quality and reliability of the Nation's water resources is to achieve *__optimum, long-term, environmentally sustainable__* *social and economic benefit for society from their use.*

Three fundamental objectives for managing South Africa's water resources, which are firmly grounded in the provisions of the Bill of Rights of the Constitution of South Africa, 1996 (No. 108 of 1996) arise from these Principles. These are:

1. *To achieve equitable access to water,* that is, equity of access to water services, to the use of water resources, and to the benefits from the use of water resources.

2. *To achieve sustainable use of water* by making progressive adjustments to water use with the objective of striking a balance between water availability and legitimate water requirements, and by implementing measures to protect water resources.

3. *To achieve efficient and effective water use* for optimum social and economic benefit.

The above may be found on the National Water Resource Strategy of 2004. Consequently, Water retaining structures (WRS) are one of the most essential structures in the efforts to achieve this strategy. These structures supply water to cities and communities and its conservation is of outmost importance.

Despite the efforts by local and national authorities in conserving water retaining structures, these structures are still the object of early deterioration and leakage problems. These problems are aggravated by the fact that South Africa is semi-arid country, where water conservation is critical.

While water conservation campaigns may be used to reduce the water usage at consumer level, a more elaborate effort is required to accomplish sustainability at reservoir level. To achieve sustainability, water retaining structures (e.g. reservoirs) must be made more durable. This is obtainable through a better design approach (i.e. design standards), better quality of concrete and site workmanship, as well as improved knowledge of concrete response to WRS conditions.

Concrete water retaining structures in South Africa are designed using BS 8007, due to lack of an existing National code. Recently, a draft code was prepared for the design of water retaining structures in South Africa SANS 10100-3. Quality of concrete and site workmanship has also been subject to scrutiny by the researcher, however not much investigation has taken place with regard to understanding the behaviour of concrete when subjected to the conditions experienced by WRS.

Additionally, early deterioration of WRS make evident that these structures are facing durability problems. At the heart of these problems are the creep and shrinkage phenomena which are the focus of investigation in this project.

Concrete is a material used thoroughly in construction and it has proven durability against many surrounding hazards. However, the ability of concrete to resist constant water pressures, but also variable pressures due to variable water levels is an uncertainty. Concrete creep (which is the deformation of concrete under constant load), occur under these circumstances. Therefore, it is relevant to study the creep experienced by these structures due to permanent and fluctuating load and the designer’s ability to predict it.

Shrinkage takes place in concrete structures despite the quality of workmanship or design approach. This phenomenon may cause damage to the concrete and increase of crack width, from which leakage of stored water can occur. The prediction of the extent to which shrinkage takes place, is an important tool to guarantee the sustainability of water retaining structures and its study is duly required.

A.M. Neville (2000) reported that the longest time of deformation measurement to date indicating that a small increase in creep still takes place, is 30 years. A similar consideration may be taken on shrinkage as it continues over a long period of time as well. This emphasizes the importance of predicting creep and shrinkage if durability problems are to be reduced. Despite the large number of experimental investigations into shrinkage and creep, no widely accepted prediction method exists (Gardner & Lockman, 2001).

To date, concrete creep and shrinkage in South Africa are predicted using SABS 0100-1 Annex C, which is a direct replication of the method used in BS 8110. This has been the case despite the difference in climatic conditions, aggregate type or even workmanship quality to name a few. Significant errors can be incurred if models developed in other countries are adopted into local design specifications without consideration of the climatic and material differences which may affect the prediction (Ballim, 1999). Therefore the applicability of the BS 8110 Model (as well as other models) to predict creep and shrinkage of concrete subjected to South African climatic conditions is a question worthy of discussion.

To conclude, this study into the creep and shrinkage of concrete water retaining structures specifically, can be seen as one of more steps towards the compilation of a better South African code for the design of these structures.

1.2 Objectives of the research

The main objective of this research is to determine the most suitable creep and shrinkage prediction model to be used in concrete water retaining structures in South Africa.

Along with that objective three others are drawn, namely:

1) To compare the different prediction models available in literature, whilst evaluating their significance to South African WRS.
2) To evaluate the performance of these prediction models against South African data related to WRS.
3) To provide a conclusion (and or solution) that can be used in the compilation of a new South African code for the design of WRS.

1.3 Outline of dissertation

The next chapter of this thesis contains the review of the literature on creep and shrinkage of concrete. In this chapter the different forms of creep and shrinkage, the micro-mechanisms and macro-mechanisms of these phenomena are explained.

Chapter three introduces the methodology that was employed to perform this research. It explains the methods used for experimental data acquisition and processing; for prediction model selection and processing; as well as the statistical methods used to compare the models' predictions to the experimental data.

Chapter four deals with the prediction models individually. The contents of each model are exposed and explained accordingly.

In chapter five, the programming of these models into the selected software package is verified. A series of techniques are employed to identify programming errors or model limitations to respond according to the expected physical behavior of concrete. The programming of statistical indicators is also under scrutiny in this chapter.

Chapter six assesses the prediction models with respect to required input parameters, characteristics and their applicability to WRS design. It is in this chapter that advantages and disadvantages of the models are identified.

Chapter seven compares the model predictions to the different sets of experimental data. This is done visually through a series of graphs and statistically using the statistical indicators, which provides sets of results.

The analysis of these comparison results is accessible in chapter eight. This chapter summarizes the results into groups of data, from which the most accurate model to particular groups is observed.

In chapter nine, the criteria for selecting the most suitable model for creep and shrinkage calculation are developed and using these criteria, the most suitable model is selected.

Finally, in chapter ten, a brief summary of the research is presented and conclusions are drawn. Also, recommendations for further research are found in this chapter.

CHAPTER 2
LITERATURE REVIEW

2.1 Introduction

Identification of the most suitable model to predict concrete creep and shrinkage of South African water retaining structures (WRS) is crucial for the design industry. At present, several prediction models are available in the literature, yet none has achieved unanimous acceptance by designers throughout the country. This is further accentuated by the lack of a South African Standard for WRS. This literature review aims at clarifying the mechanisms that cause and influence creep and shrinkage whilst laying a platform from which such identification can take place.

The design of WRS is normally carried out according to limit state principles (Bhatt *et al*. 2006). However, unlike regular reinforced concrete structures, design is often governed by serviceability limit state considerations of limiting crack rather than ultimate limit state consideration. Therefore as Jaufeerally (2001) suggests, it is of vital importance to predict realistically the creep and shrinkage deformations of concrete structures as they impact on the durability and long term serviceability.

Although several models have been developed for creep and shrinkage prediction, these models are developed using either historical precedents or results of a large number of tests which are used to shape the model (Ballim, 1999). Thus, a problem arises when models which have been developed in other countries are incorporated into local design codes without thought being given to the difference in materials, environments and applications of concrete technology in the two countries or regions (Ballim, 1999). For example, British Standards apply particularly to UK conditions, and although the principles are applicable to design in other part of the world, the designer should take account of local conditions, particularly variations in climate" (BS: 8007).

Apart from the models used, the designer must have comprehensive knowledge of creep and shrinkage in order to avoid errors in the prediction of these phenomena. The complexity of creep and shrinkage is noted by various researches and not many agree on the mechanisms that cause these phenomena. For this reason, this literature review explains fundamental concepts of creep and shrinkage that may be needed during prediction.

2.2 Shrinkage

Shrinkage is the decrease of concrete volume with time. The inverse process of shrinkage is *swelling* which denotes volumetric increase due to moisture gain in the hardened concrete. Several types of shrinkage exist, however the early age volume changes are typically ignored in design of concrete structures since their magnitude can be much less than shrinkage resulting from drying (Holt 2001). For particular concretes, the early age behaviour may however be very important, for instance due to high early temperature caused by hydration for certain cement and supplementary binding materials, which may lead to early age crack formation (Bamforth 2007). This research focuses on the long term deformations of concrete which are used in the design phase.

Shrinkage can be firstly separated into two stages: Early age shrinkage (which occurs in the first 24 hours) and long term shrinkage (which occurs after the first 24 hours and beyond) (e.g. Holt 2001). However, within the long term shrinkage stage, different types of shrinkages have been identified as shown in figure 2.1.

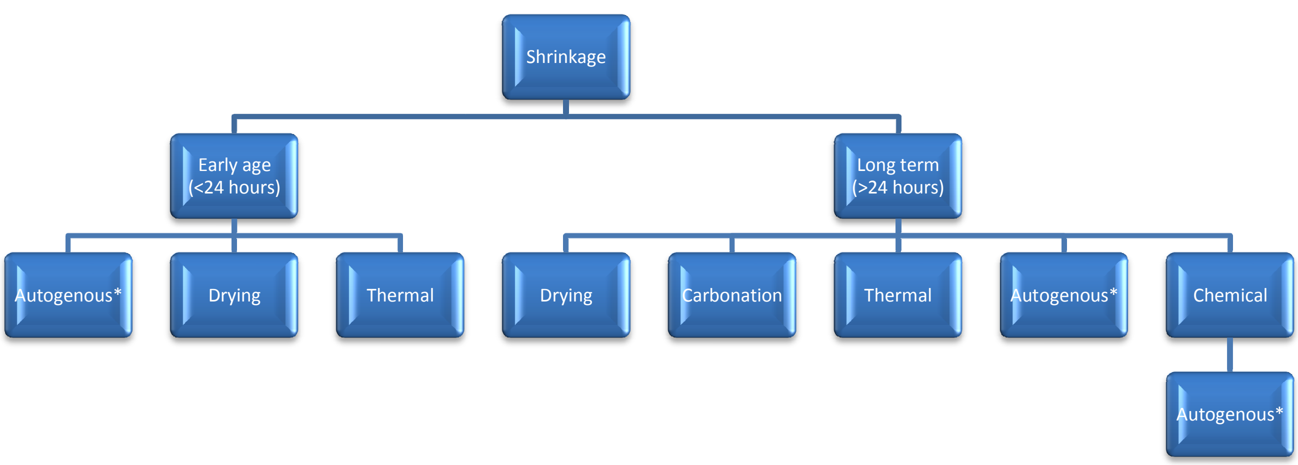

*Legend: * - Repeated citation of autogenous shrinkage is explained in section 2.2.1*

Figure 2.1: Diagram of shrinkage stages and types (Adapted from Holt, 2001)

2.2.1 Autogenous Shrinkage

Autogenous shrinkage is the decrease of concrete volume that occurs without moisture being transferred to the exterior environment. With no moisture movement to or from the cement paste, self desiccation leads to removal of water from capillary pores and to autogenous shrinkage. The magnitude of the autogenous shrinkage is often an order of magnitude less than that of drying shrinkage except for cases of concretes with very low water/cement ratios, where it may be significantly larger (e.g. Illston and Domone, 2006).

The use of modern admixtures, such as super-plasticizers and silica fume permit the utilization of such low water/cement ratios in search of high strength concretes, and therefore a bigger risk of impact of autogenous shrinkage exists. However, in the case of water retaining structures, normal strength concrete is mostly used. Also, strength is not the determining factor but rather the serviceability limit state considerations of limiting crack width as mentioned before. Thus, a lower emphasis is given to autogenous shrinkage for the design of these structures. For the purposes of elucidation only, this type of shrinkage is explained below.

Figure 2.1 shows the relationship between chemical and autogenous shrinkage. In the early stages, while the concrete is still liquid, the autogenous shrinkage is equivalent to the chemical shrinkage, hence only the autogenous shrinkage is mentioned in the figure (at that stage). As the concrete hardens the autogenous shrinkage becomes a part of the chemical shrinkage as shown in figure 2.2. Once concrete has hardened, autogenous shrinkage may no longer be the result of chemical shrinkage but rather the result of self-desiccation.

.

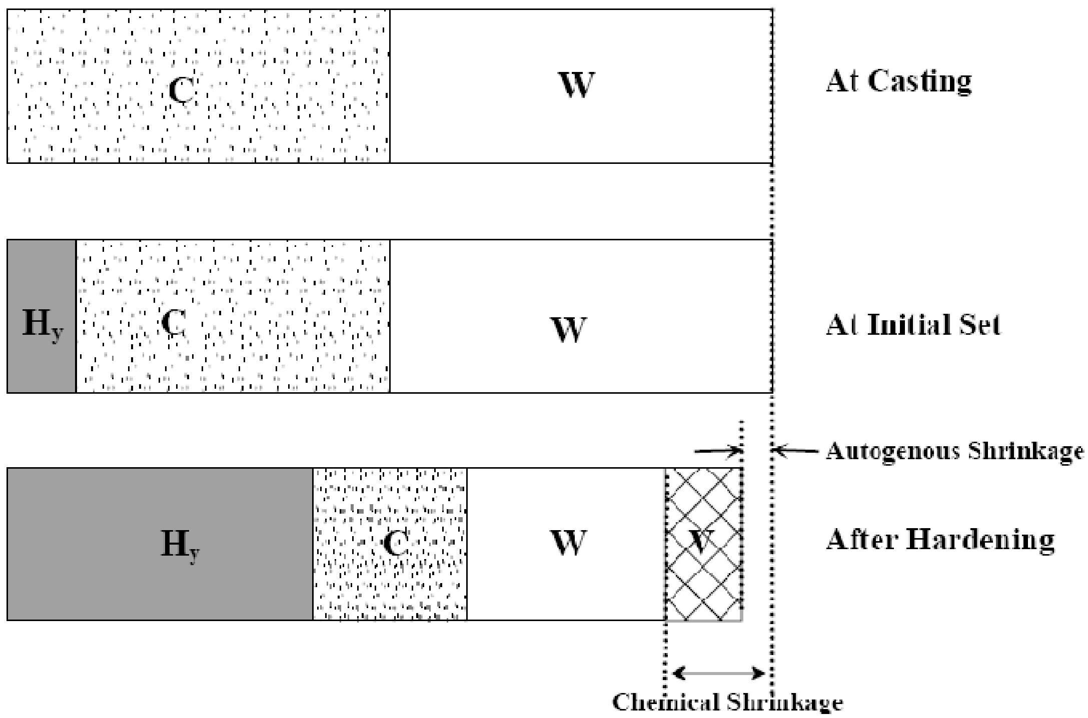

Legend: C = unhydrated cement, W = unused water, H_y = hydration products, and V = voids generated by hydration

Figure 2.2: Reactions causing autogenous and chemical shrinkage (Japan Concrete Trust, 1999)

The forces that drive autogenous shrinkage change over time as reported by Hammer (1999). Immediately after casting, the autogenous shrinkage is only due to chemical shrinkage (region AB of figure 2.3). Still in the early stage, the skeleton structure within the concrete starts to form and the influence of chemical shrinkage into autogenous shrinkage reduces which is shown in region BC of figure 2.3. Once the concrete has hardened (Region beyond point C of figure 2.3), the autogenous shrinkage is systematically less influenced by the chemical shrinkage and more a function of self desiccation. Bearing in mind that self desiccation increases as the degree of hydration increases, figure 2.3 may be used to elucidate the concept of evolution of autogenous shrinkage driving forces with time.

Self desiccation is the localized drying resulting from a decreasing relative humidity, where the lower humidity is a result of cement requiring extra water for hydration (e.g. Holt 2001). Although it may not begin immediately after casting, self desiccation occurs for a longer period than chemical shrinkage ensuring that the autogenous shrinkage continues into the long term shrinkage stage.

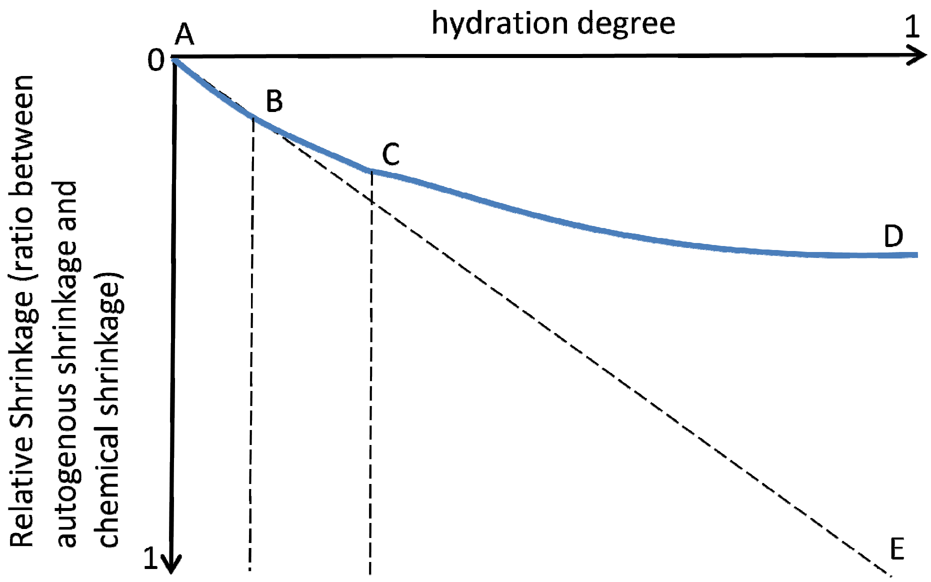

Figure 2.3: Schematic evolution of autogenous shrinkage as a function of hydration degree (Acker, 1988).

2.2.2 Chemical shrinkage

A fundamental difference between autogenous and chemical shrinkage is that autogenous shrinkage is an external volume change whilst chemical shrinkage is an internal volume change. This is seen from figure 2.2 above. Also, while autogenous shrinkage is firstly driven by chemical shrinkage and later by self desiccation, the chemical shrinkage is the result of reactions between cement and water, which lead to volume reduction.

Chemical shrinkage is defined as the type of shrinkage that results from difference in volume of the initial and final products of the hydration process. Because the hydration process will always take place whenever concrete is mixed, this type of shrinkage cannot be prevented by casting, placing or curing methods, but must be addressed when proportioning the concrete mixture.

Paulini (1992) described the basic reactions of the cement clinker that occur during the cement-water interaction, through the following symbolic equations of the clinker phases:

C_3S : $$2C_3S + 6H \rightarrow C_3S_2H_3 + 3CH \quad [2.1]$$

C_2S : $$2C_2S + 4H \rightarrow C_3S_2H_3 + CH \quad [2.2]$$

C_3A : $$C_3A + 6H \rightarrow C_3AH_6 \quad [2.3]$$

C_4AF : $$C_4AF + 2CH + 10H \rightarrow C_3AH_6 + C_3FH_6 \quad [2.4]$$

The magnitude of chemical shrinkage is calculated by equation 2.5. Holt (2001) clarifies that this equation may be unrealistic as the exact volume of various components might prove difficult to compute.

$$CS = \frac{(V_c + V_w) - V_{hy}}{V_{ci} + V_{wi}} \times 100 \quad [2.5]$$

where

CS = chemical shrinkage

V_{ci} = volume of cement before mixing

V_c = volume of hydrated cement

V_{wi} = volume of water before mixing

V_w = volume of reacted water

V_{hy} = volume of hydrated products

Despite the stumbling block of determining the parameters of equation 2.5, the above knowledge may still be used to determine chemical shrinkage reduction. For example, the use of a concrete with lower C_3A content would result in less reactions involving C_3A which is known to lead to less chemical shrinkage. It is also agreed that some compounds such as C_2S and C_3S may combine to produce lower shrinkage values. According to Holt (2001) a cement with higher C_2S content and lower C_3S would result in lower overall chemical shrinkage as compared to regular cement chemical shrinkage.

2.2.3 Carbonation Shrinkage

Carbonation shrinkage is the reduction of concrete volume that occurs due to the reaction between the products of the hydration process and the carbon dioxide available in the atmosphere. This type of shrinkage is irreversible and has the effect of reducing the reversible component of the total shrinkage (e.g. Ballim, 1983).

In order to understand carbonation shrinkage the process of carbonation within the concrete has to be understood. *Carbonation* Is the process by which carbon dioxide, CO_2, from the atmosphere slowly transforms calcium hydroxide into calcium carbonate in concrete (e.g. Bhatt *et al*. 2006). It is agreed that both CO_2 and humidity need to be present for carbonation to occur, and that the carbonation reaction follows the chemical formula shown below (Ferreira, 2004)

Calcium hydroxide + Carbon dioxide $\rightarrow$ Calcite + water [2.6]

This reaction occurs in three phases (Ferreira, 2004):

1. CO_2 Diffuses inwards
2. CO_2 Reacts with H_2O
3. Resulting carbonic acids react with alkaline components of the concrete

The process of carbonation is schematically represented in figure 2.4.

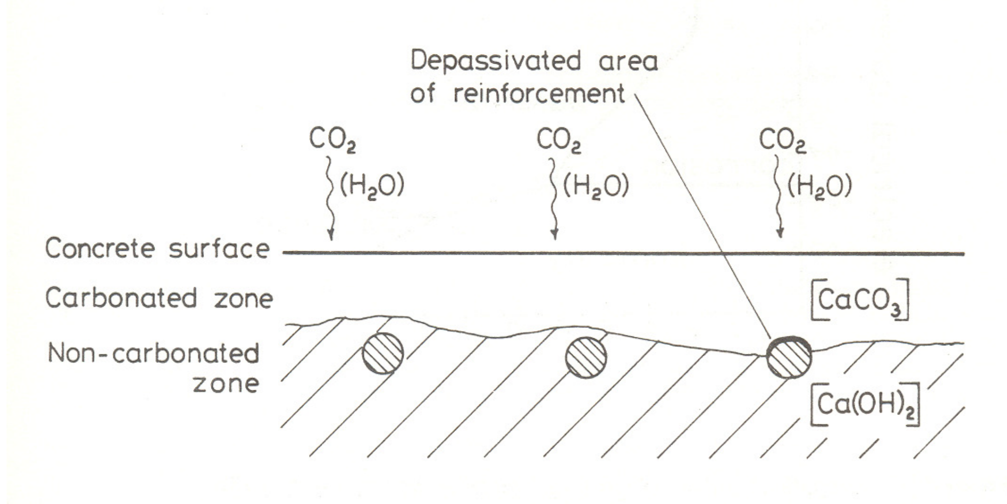

Figure 2.4: Diagram showing a schematic representation of the carbonation process (Richardson, 1988)

Carbonation is a fairly well understood process. It is known that it increases concrete strength and reduces permeability of the concrete as the calcite crystallises out in the pores, closing the concrete voids. Conversely, it is also known that it reduces the pH value of concrete considerably, which affects negatively the passive corrosion environment surrounding the steel reinforcement within the concrete. However, this literature review will not study these aspects further and will focus on the shrinkage caused by this process.

As water is released from the reaction described by equation 2.6, it increases the weight of the cement paste and dissolves the calcium hydroxide from more highly stressed regions, resulting in shrinkage (e.g. Illston & Domone, 2006).

It is reasonable to believe that carbonation shrinkage reaches its maximum when carbonation process is at its maximum. Many researchers such as Ballim (1983) believe that this maximum occurs at a relative humidity of 50% and that no carbonation occurs at humidities below 25% or if the concrete is fully saturated. Ferreira (2004) provided the expected rates of carbonation (hence, carbonation shrinkage) for different humidity ranges. This is presented in table 2.1:

Table 2.1: Rate of carbonation as a function of relative air humidity

Relative air Humidity (%)	Rate of carbonation
Below 30	Low
40 to 70	High
Above 75	Low

(Ferreira, 2004)

In addition to the relative humidity of the environment, the rate at which carbon dioxide will react with the hydration products of cement depends on factors such as the permeability and moisture content of the concrete, the concentration of carbon dioxide in the atmosphere and the exposed surface area of the concrete member (Ballim,1983).

Illston & Domone (2006) explained further that carbonation front will only penetrate a few centimetres over the years, for an average strength concrete, provided it is compacted and cured properly. However, much greater penetration can occur with poor quality concrete or in regions of poor compaction. Thus, it is highly important to keep the permeability of the concrete to gases low in order to avoid high values of carbonation shrinkage.

A study by the author in 2007 into the quality of concrete and workmanship used in particular WRS in the KwaZulu-Natal region, revealed that the concrete has low permeability to gases. Bearing in mind that the study was done according to South African durability index test specifications and that similar concretes may be used in throughout the country, it can be expected that carbonation shrinkage of WRS will remain low.

2.2.4 Thermal shrinkage or expansion

Thermal dilation is the volume change that occurs in concrete when temperature fluctuates. As in most materials concrete will expand when temperature rises and it will contract when cooled. Thermal expansion may occur at both early stages as well as late stages and it causes problems when the rate of temperature change is too severe or when thermal gradients exist over the concrete's cross sectional area.

At early ages, the concrete temperature rises due to the exothermic behaviour of the hydration process. This is likely to cause expansion, however some of this thermal expansion is elastic since the concrete returns to its original dimensions during subsequent cooling. It is important to note that some parts of the concrete may respond non-elastic and this will prevent the concrete to return to its original dimension resulting in early age damage. In the early and long term, care must be given to thermal expansion due to ambient temperature variations.

In order to anticipate the behaviour of a concrete under temperature variations it is important to know the concrete's *thermal expansion coefficient* which is the change in unit length per degree of temperature change (e.g. Metha & Monteiro,2006). The hardened cement paste (hcp) has a different thermal expansion coefficient to that of concrete due to the influence of aggregates in the concrete. The thermal expansion of hcp varies between 10 and 20 x 10^{-6} per ℃ and the maximum is reached when concrete is exposed to 70% relative humidity (Illston & Domone, 2006). This is further illustrated by figure 2.5 below.

The thermal expansion coefficient of the aggregate in the concrete varies between 6 and 10 x 10^{-6} per ℃ (Illston & Domone, 2006), which is lower than that of the hcp (also shown in figure 2.5). The combination of the two coefficients, gives rise to a lower thermal expansion coefficient of concrete. Because the aggregates occupy a larger volume in the concrete than the hcp, the influence of relative humidity on the thermal expansion coefficient of concrete is reduced when compared to its influence to hcp's coefficient alone.

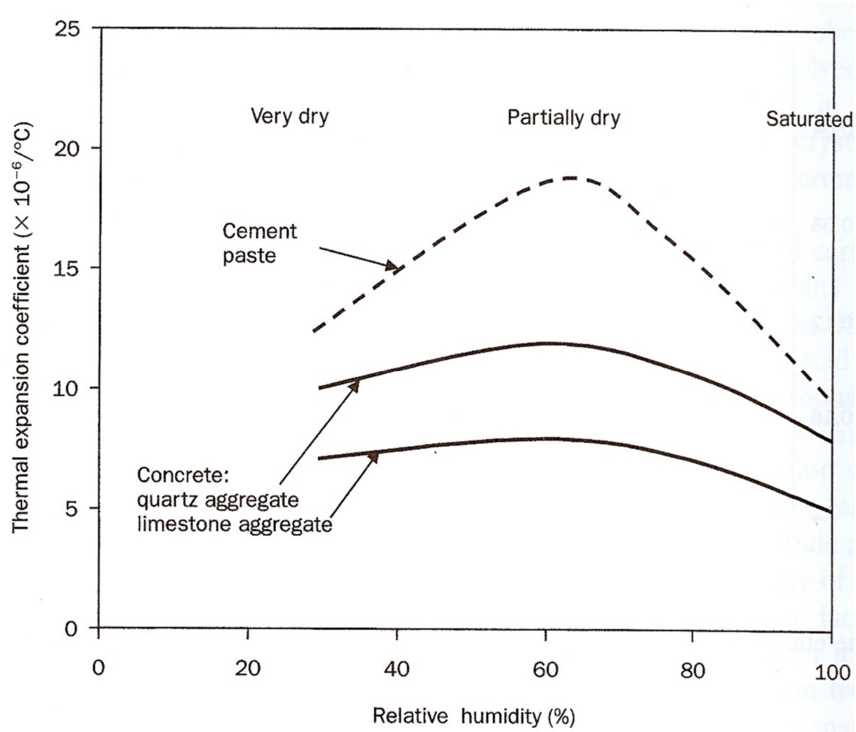

Legend: chart applicable to temperatures ranging from about 0 ℃ to 60 ℃

Figure 2.5: The effect of relative humidity on the thermal expansion coefficient of hardened cement paste and concrete (Illston & Domone, 2006)

2.2.5 Drying Shrinkage

Drying shrinkage is the decrease of concrete volume that occurs due to a physical loss of water from the concrete system to the exterior environment once the concrete has reached the hardened state. This type of shrinkage outweighs the other types of concrete shrinkage in most cases and a large part is reversible upon rewetting.

Not all losses of water lead to drying shrinkage. Water is present in the concrete in different forms and it may also leave the concrete system in a variety of ways. The ways in which water is contained in the system and how its loss may lead to shrinkage is explained below:

- *Water vapour:* The larger voids of concrete may be filled with water and water vapour at a pressure which is in equilibrium with the relative humidity and temperature of the environment.

- *Capillary water*: Water contained in voids larger than 50 nm is considered free water and it is not under the influence of surface forces. The water that is contained in the capillary and larger gel pores (i.e. wider than about 5 nm but less than 50nm) is denoted as capillary water (Mehta & Monteiro, 2006). The free water loss does not cause significant shrinkage but the loss of capillary water may lead to autogenous shrinkage as explained before in section 2.2.1. However, if this capillary water is eventually removed from the concrete system, then it may lead to drying shrinkage.
- *Adsorbed water*: This type of water is held close to solid surfaces, and contrary to capillary water, it is under influence of surface attractive forces. Up to five molecular layers of water can be held, giving a maximum total thickness of about 1.3nm (Illston & Domone, 2006). A large proportion of this water can be lost due to drying, and this water loss is the main contributor to drying shrinkage.
- *Interlayer water:* This is the type of water that exists in gel pores narrower than 2.6nm (Illston & Domone, 2006). Under such narrow space, it is agreed that the water is under the influence of attractive forces by two solid surfaces and therefore strongly held. With strong drying such as elevated temperatures and/or low relative humidities (i.e. less than 11%, Mehta & Monteiro, 2006) it is possible to remove this water causing drying shrinkage. After the water is removed, Van der Waals forces are able to keep the solid surfaces together which completes the shrinkage process.
- *Chemical combined water:* This is the water that has combined with the fresh cement during the hydration process. This water as an integral part of various cement hydration products. *However,* chemical combined water is not lost on dying and it only evolves when the paste is decomposed by heating to high temperatures in excess of 900-1000 °C (Illston & Domone, 2006). Therefore, it is not a concern for the serviceability of water retaining structures.

The free drying shrinkage (i.e. the stress-free drying shrinkage) cannot be measured directly because the moisture content in the concrete is not uniform. This non uniformity is caused by the slow nature of the drying process in concrete in which the material close to an exposed area dries faster than the interior material (see figure

2.6a for non uniform drying representation). As van Zijl (1999) explains, if the concrete was made of independent layers, each would have a different shrinkage length as shown in the dotted lines of figure 2.6b. Van Zijl further explains that since this is not the case, the connection between these layers of concrete prevents this deformation from taking place as it is shown by the solid lines of figure 2.6b. Shorter layers are therefore extended, going into tension whilst the longer layers are compressed, generating compressive stresses. The distribution of internal stresses (i.e. eigenstresses) is shown in figure 2.6c.

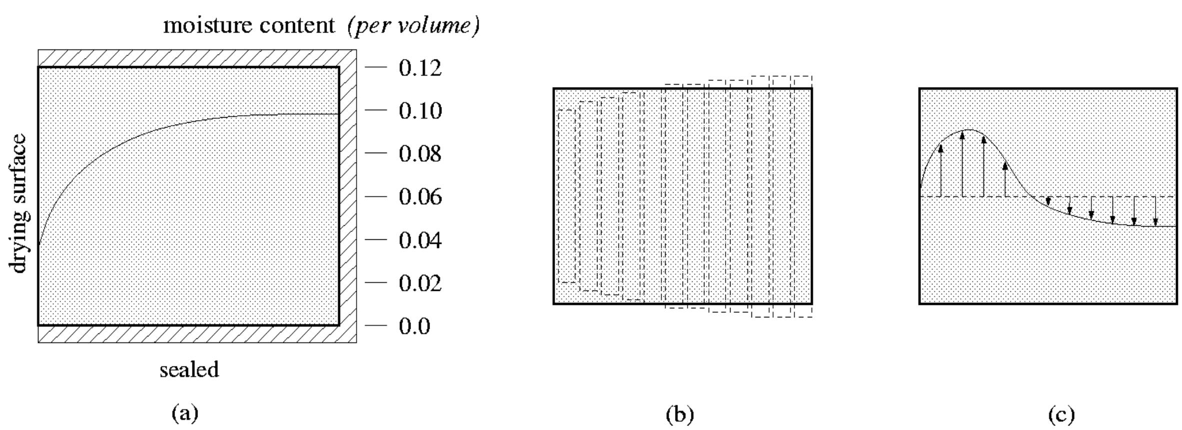

Figure 2.6: (a) Non uniform drying; **(b)** shrinkage **(c)** eigenstressing due to slow drying process of concrete (Van Zijl,1999)

Van Zijl (1999) suggests that a very thin specimen with no hygral gradient should be used to avoid these internal stresses in the measurement of the free drying shrinkage. Alternatively, a model of the interacting phenomena should be used through iteratively modifying the model parameters until acceptable agreement is found.

Simpler shrinkage prediction models are unable to differentiate between the different types of shrinkage. More complex models may distinguish the drying shrinkage from the autogenous shrinkage. From this separation it is possible to observe the order of magnitude to which drying shrinkage exceeds the autogenous. For example, from a graphical representation of the formulae presented in the EuroCode (EN 1992-1-1:2004), shown in figure 2.7, it is possible to observe this aspect in more detail.

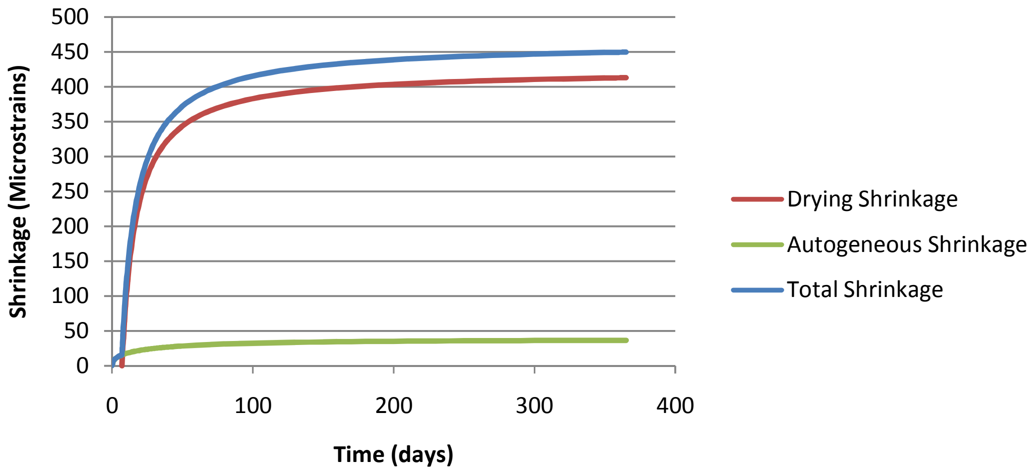

Figure 2.7: Magnitude of drying shrinkage to autogenous shrinkage according to EuroCode, EN 1992-1-1:2004

For this reason, drying shrinkage prediction and minimization thereof is emphasized by designers and it is the focus of this study with regard to shrinkage. Section 2.4 (Macro-mechanisms of creep and shrinkage), will concentrate on the influence of the properties of concrete to drying shrinkage in particular. Section 2.2.6 (Micro-mechanisms of shrinkage) however, will describe the mechanisms that lead to shrinkage in general.

Note that, for classes of especially very high strength concrete, the autogeneous shrinkage may become more dominant than shown in Figure 2.7. This is not of consequence for WRS, which mostly are constructed with moderate strength concrete.

2.2.6 Micro-mechanisms of shrinkage

The following is a description of mechanisms that allow the different types of shrinkage explained above to exist. Four different mechanisms have been suggested and are explained from sub-section 2.2.6.2 to 2.2.6.5.

Before explanation can proceed, reference is made to figure 2.8 which might aid the reader in understanding the concepts to follow and is mentioned throughout this section.

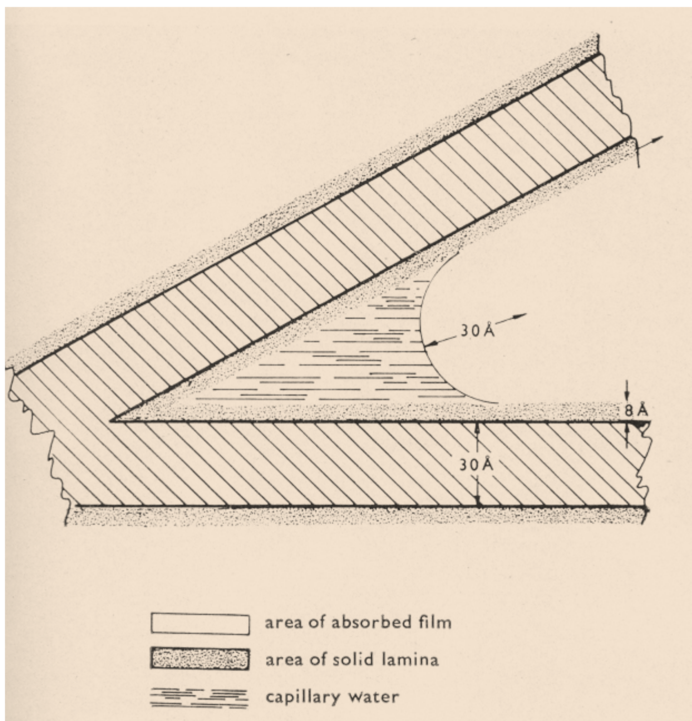

Figure 2.8: Hindered adsorption and capillary condensation (Powers, 1965)

2.1.6.1 Elastic and chemical assumptions of shrinkage micro-mechanisms

The volume of a liquid or solid material is determined by the volumes of the atoms of which it is composed, the molecular or crystal structure, temperature and atmospheric pressure. Consequently, a change in temperature and atmospheric pressure of a chemically uncomplicated material changes the thermal vibration of the atoms which changes the average interatomic distances, that in turn brings about volume change. Furthermore, Powers (1965) explains that a change in temperature may also change the structure of the material and in some cases its chemical composition. Therefore, the suggested shrinkage micro-mechanisms assume that the materials to be considered are mechanically elastic and chemical stable, and that the temperature remains constant.

2.2.6.2 Capillary tension

The free water surfaces in the capillary and larger gel pores (defined in section 2.2.5) are in surface tension. When the atmospheric pressure drops, water starts to evaporate, which yields the free surface to become more concave and subsequently the surface tension increases. The relationship between the radius of this concavity, *r*, and the corresponding atmospheric vapour pressure, *p*, is given by Kelvin's equation (e.g. Wittmann, 2009):

$$r = -\frac{2 \times ST \times V_m}{R\theta \ln\left(\frac{p}{p_0}\right)} \qquad \text{or} \qquad D_c = -\frac{4 \times ST \times V_m}{R\theta \ln\left(\frac{p}{p_0}\right)} \tag{2.7}$$

where,

$p/p_0 \leq 1$
p_0 = vapour pressure over a plane surface
ST = surface tension
θ = absolute temperature
V_m = molar volume
R= molar gas constant
r = radius of curvature
D_c = diameter of curvature
p = vapour pressure

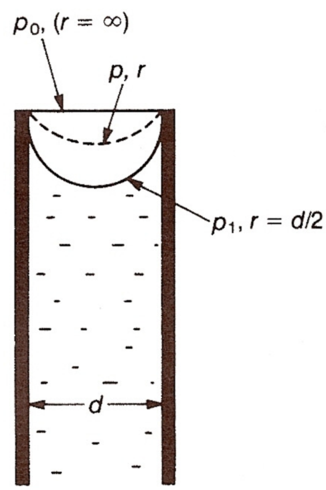

Figure 2.9: Relationship between the radius of curvature and vapour pressure for water in a capillary (Sokota, 1979)

It is also agreed that the tension within the water near the meniscus is 2ST/r. The water evaporation causes an increase of the tensile stresses in the water which must be balanced by an equivalent increase of the compressive stresses of the surrounding solid. This increase in the compressive stresses results in a decrease of volume, i.e. shrinkage.

The diameter of the curvature cannot be smaller than the pore diameter. Looking at Equation 2.7, when the atmospheric pressure drops, the absolute value of $\ln(p/p_0)$ increases, and consequently the diameter of the curvature decreases; hence a decrease of vapour pressure yields a decrease in the diameter of the curvature towards its limiting value (i.e. pore diameter). At a particular vapour pressure p_1, the diameter of the curvature reaches the diameter of the pore and at this stage the pore empties out. Looking at a system of pores, as the vapour pressure increases steadily, each pore gradually empties out according to their size, widest first. Thus, cement pastes with high water/cement ratios (which are more porous) will shrink more than other cement pastes.

With a pore emptying out, the tensile and compressive stresses associated with the pore reduce to zero. Therefore, full recovery of shrinkage would be expected on full drying however it is agreed that other mechanisms that are operative at lower humidities prevent full recovery from happening.

2.2.6.3 Surface tension or surface energy

A primary particle (such as an atom, ion or molecule) that is located far from the surface of a solid or liquid body is completely surrounded by other particles. The distance between a particle and its neighbouring particles is determined by three factors:

1. *Forces of attraction and repulsion between these particles*
2. *Static equilibrium*: the sum of all forces in each particle must be zero
3. *Minimum potential energy*: each particle must position itself with respect to its neighbouring particles at a position in which potential energy is minimized.

At the surface of a solid or liquid body, particles cannot be fully surrounded by other particles. As described by Powers (1965) the positions of minimum potential energy cannot be the same as for particles in the interior and these distances are not same for the tangential and normal direction to the surface. Powers (1965) indicates that the distance of minimum potential energy in the tangential direction is smaller than the actual distance between particles. The tendency of the particles to get closer to achieve the minimum potential energy is viewed as the reason for the tendency for the surface area of a body of liquid to diminish spontaneously. Due to these attractive forces between particles, the surfaces of both solid and liquid materials are in state of tension.

The tensile force in the surface zone of a liquid can be measured, but corresponding tensile stress cannot be calculated because the thickness of the tensile zone is not known. To increase surface area, work has to be done against this force, and the surface energy is defined as the work required to increase the surface by a unit area.

As stated in the previous sub-section, surface tension forces induce balancing compressive stresses in the material of value 2ST/r, assuming that Kelvin's equation (equation 2.7) is accurate enough to overcome the limitation explained in the paragraph above. The adsorption of water particles onto the surface of hardened cement paste (*hcp*) solids reduces these compressive stresses, leading to volume increase, i.e. swelling, which is reversible.

2.2.6.4 Disjoining pressure

Figure 2.8 shows a typical gel pore, narrowing from a wider section containing free water in contact with vapour (in which capillary forces apply) to a much narrower space between hcp solids (under the influence of surface forces). Water is subsequently adsorbed to form a layer (i.e. the adsorbed water layer) which is also under the influence of surface attractive forces. This results in a swelling or disjoining pressure (as explained in the previous sub-section) which is balanced by the tension inter-particle bond.

The thickness of the adsorbed water reduces when drying occurs, creating a reduction of the area where hindered adsorption takes places. This reduces the disjoining pressure and results in overall shrinkage.

2.2.6.5 Movement of interlayer water

The ways in which movement of interlayer water may cause shrinkage have been explained thoroughly in section 2.2.5 when the different forms of water in concrete were discussed. However it is important to note, that although strong drying at elevated temperatures and/or low relative humidities is required to move the interlayer water, this movement is likely to result in significantly higher shrinkage than the movement of an equal amount of free or adsorbed water.

2.2.6.6 Ranges of applicability of shrinkage micro-mechanisms

The extent to which these mechanisms determine the occurrence of shrinkage and their overall contribution to the total shrinkage is a debatable issue. Table 2.2 below shows the opinion of four main authors on the contribution of these mechanisms to total shrinkage and the relative humidity levels that these mechanisms can be observed.

Table 2.2: Proposed micro-mechanisms of shrinkage

	Relative humidity: 0 – 0.2 – 0.4 – 0.6 – 0.8 – 1
Powers (1965)	← Disjoining pressure → ← Capillary tension →
Ishai (1965)	← Surface energy →← Capillary tension →
Feldman & Serada (1970)	← Interlayer water →← Capillary tension and surface energy →
Wittmann (1968)	← Surface energy →← Disjoining pressure →

(Sokota, 1979)

This adds difficulty to the use of micro-mechanisms in the prediction of shrinkage and hence a more phenomenological approach based on macro-mechanisms is used. Although macro-mechanisms are used, the influence of different micro-mechanisms at different humidity ranges is considered in some prediction models (e.g. CEB-FIP 1990 and ACI 209 R-92) by adjusting the formulae or humidity correction factors for different humidity ranges.

2.3. Creep

Creep is the time-dependent increase of strain of a solid body under constant or controlled stress. The magnitude of creep strains can be significantly higher than the initial elastic strain and therefore it influences the structural behaviour of structures significantly.

Specific creep and creep coefficient are terms that have been defined to calculate or model creep. S*pecific creep* is the creep strain per unit of applied stress and *creep coefficient* as the ratio of creep strain to elastic strain (e.g. Mehta & Monteiro, 1993).

Figure 2.10 indicates that creep may last longer than 30 years, which is important for the durability assessment of structures required to perform beyond that period. That is the case for WRS in developing countries and even in some remote areas of South Africa. The figure also indicates that creep increases considerably when the concrete is simultaneously drying, i.e. creep and shrinkage are not independent.

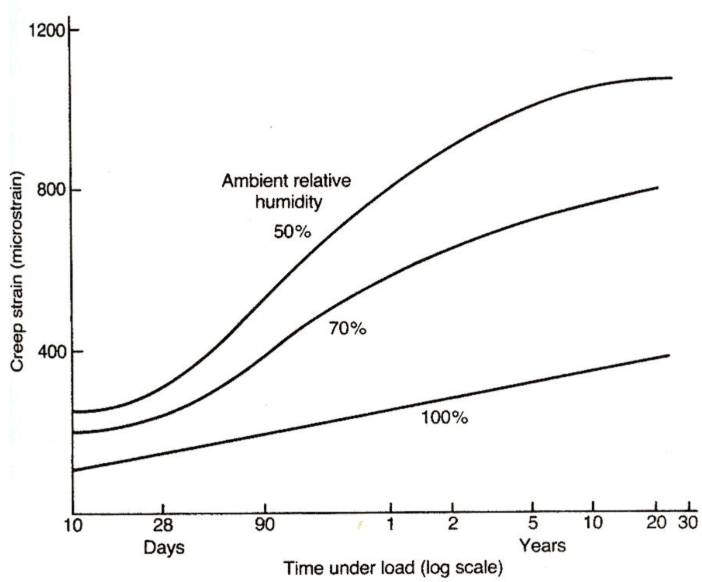

Figure 2.10: Creep of concrete moist-cured for 28 days, loaded at different relative humidities (Troxell et al, 1958)

.

Two types of creep are generally distinguished:

1. *Basic creep*, which is the time-dependent increase in strain under sustained load of a concrete specimen in which moisture losses or gains are prevented (sealed specimen) (e.g. ACI 209.2R, 2008).
2. *Drying creep*, which is the additional creep (added to the basic creep) that occurs when the specimen under load is also drying (e.g. Mehta & Monteiro, 2006).

The following sections discuss these two types of creep in more detail as well as micro-mechanisms in the concrete that allow creep to occur.

2.3.1 Basic creep

When stress is kept constant on a sealed specimen, the specimen displays an increase of strain over time, called *basic creep*. This condition may occur in concrete structures where drying shrinkage can be neglected, such as the inside face or the interior column of a water retaining structure.

2.3.2. Drying creep

When a specimen is under load and it is simultaneously exposed to relative humidities below 100%, the total strain observed is higher than the sum of elastic strain, free shrinkage strain and basic creep strain. Note that, the free shrinkage is the shrinkage of an unloaded specimen in a drying condition. The additional creep that is required for the sum of strains to reach the total strain under these conditions (drying and loaded specimen) is called *drying creep*. This is expressed mathematically in equation 2.8 and visually in figure 2.11.

$$\in_c(t) = \in_{el} + \in_{sh} + (\in_{bc} + \in_{dc}) \qquad [2.8]$$

where

$\in_c(t)$ = total strain at time t

$\in_{el}$ = elastic strain

$\in_{sh}$ = free shrinkage

$\in_{bc}$ = basic creep

$\in_{dc}$ = drying creep

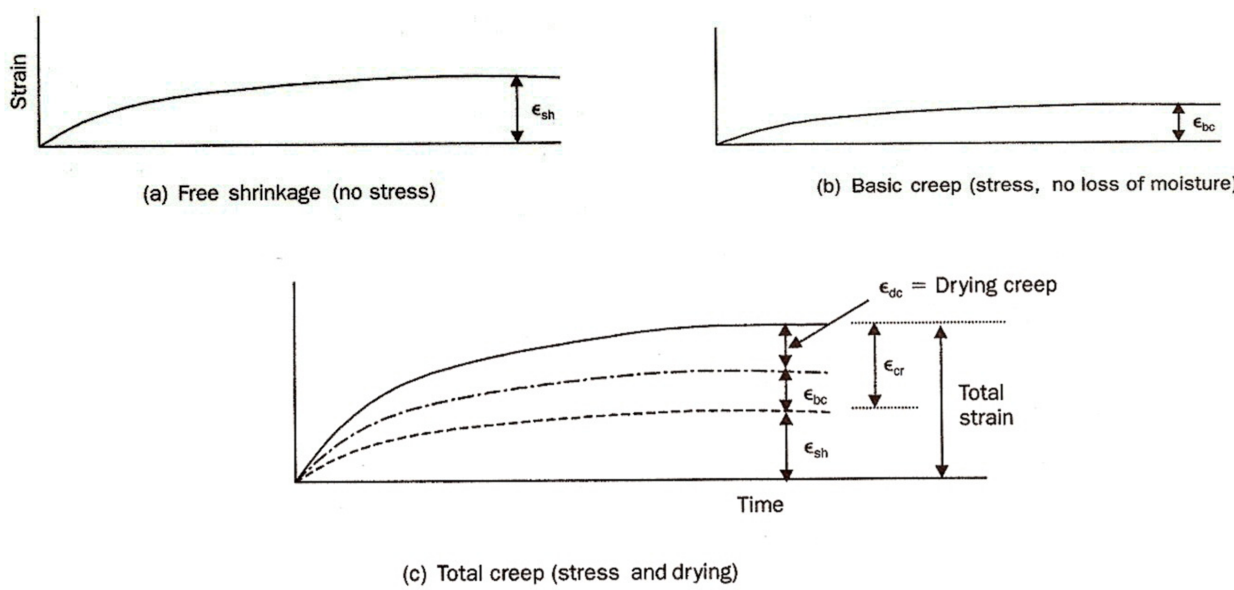

Legend: $\in_{cr}$ = total creep

Figure 2.11: Definitions of strains due to shrinkage, creep and combined shrinkage and creep (Illston & Domone, 2006).

2.3.3. Measurement of creep

The sum of basic and drying creep, $(\in_{bc} + \in_{dc})$, is called *total creep*, $\in_{cr}$. It is common practice for design standards not to distinguish these two types of creep, due to the number of test specimens required to objectively measure drying creep and basic creep, therefore creep is often considered as the deformation under loading in excess of the sum of elastic and free shrinkage strains.

Two specimens are required to measure creep: a loaded and an unloaded specimen. The free shrinkage is recorded from the unloaded specimens, whilst the elastic strain (immediately after loading) and total strains are recorded from the loaded specimen. A simple computation is therefore required to complete the process by subtracting the free shrinkage and elastic strains from the total strain. This is simply an arithmetic manipulation of equation 2.8, shown here in equation 2.9.

$$(\in_{bc} + \in_{dc}) = \varepsilon_c(t) - \in_{sh} - elastic\ \ strain \text{ or } total\ \ creep = \varepsilon_c(t) - \in_{sh} - elastic\ \ strain \qquad [2.9]$$

If only drying creep is to be measured, three specimens are required. One is left unloaded while drying (provides free drying shrinkage). The second is loaded, but sealed to prevent drying shrinkage (provides basic creep over time and elastic strain measured at loading). And the third specimen is loaded and allowed to dry in the same environment as the first specimen to provide the total time-dependent deformation (and elastic strain if desired). Trough a simple arithmetic manipulation equation 2.9, the basic creep may be obtained (shown in equation 2.10).

$$\in_{bc} = \varepsilon_c(t) - \in_{sh} - \in_{dc} - elastic\ \ strain \qquad [2.10]$$

2.3.4 Micro-mechanisms of creep

The following is a description of mechanisms by which the phenomenon of creep can be explained or enhanced. Four different mechanisms have been suggested and are explained from sub-section 2.3.4.1 to 2.3.4.4.

As for shrinkage, simplification is required to describe various mechanisms. The subsequent description of mechanisms assumes that the materials considered are mechanically elastic, chemical stable and that the temperature remains constant for the same reasons explained in sub-section 2.2.6.1.

The similarities of creep and shrinkage micro-mechanisms are evident due to the interdependency of these phenomena. This is further justified by the following factors:

- Both the shrinkage and creep originate predominantly from the same source, the hydrated cement paste.
- The strain-time curves appear to be very similar (this can be observed from figures 2.7 and 2.11).
- The factors that influence the drying shrinkage also influence the creep, generally in the same way (to be observed in section 2.4: Macro-mechanisms of creep and shrinkage).
- The magnitude of the creep and shrinkage strains cannot be ignored in structural design.
- Both phenomena are partially reversible.

2.3.4.1. Moisture diffusion

When pressure is applied to a body that contains water, the water is likely to move from the point of contact (where the stresses are more significant) towards zones of less pressure. In scientific terms, the applied stress cause changes in the internal energy of the body, causing the water to move along the induced energy gradient. Because concrete is made up of pores of different sizes, the water moves from smaller to larger pores at different levels:

- The movement of capillary water is rapid and reversible;
- The adsorbed water (that is subjected to surface attractive forces) moves more gradually, yet the movement is also reversible;

- The interlayer water (present in narrow spaces, held by the attractive forces of two solid surfaces) moves slower than the previous two. Solid bonding may develop between the solid surfaces and therefore the process may not be reversible.

2.3.4.2. Micro-cracking

The hcp and concrete contain defects and cracks at a microscopic level. The micro-cracking is relatively more common in the *interfacial zone* (i.e. the zone between aggregate and cement paste) than in the bulk cement paste and they play a crucial role in determining the stress-strain relations in concrete. In fact Hsu *et al*. (1963), attributed the non-linearity of the stress-strain relationship to the progressive micro-cracking in the concrete under load.

The stress-strain relationship is calculated by the *elastic modulus* which is the ratio between the applied stress and the instantaneous strain within an assumed proportional limit. In other words, it is a measure of how much strain can be expected under a certain level of stress or what stresses may be induced in the concrete by strains associated with environmental effects for example drying shrinkage.

Because the micro-cracks in the interfacial zone, affect the elastic modulus (i.e. stress-strain relationships), they eventually affect creep as they progress. In fact, The non-linearity of the stress-strain relation in concrete, at stress levels greater than 30 to 40 % of ultimate stress, clearly indicates the contribution of the interfacial zone micro-cracking to creep (Mehta & Monteiro, 2006). At these stress levels, there is a significant influence of micro-cracking to the elastic modulus hence a sizeable contribution to creep strains.

2.3.4.3 Delayed elastic strain

The delayed elastic response of aggregate is another cause of creep in concrete. Since the cement paste and the aggregate are bonded together, the stress on the concrete decreases as load is transferred from the cement paste to the aggregate in time. Under the increased load, the aggregate deforms elastically and the resulting strain (i.e. *delayed strain*) contributes to creep. This process is reversible, to enable the material to return to its original unstressed state upon removal of the load. Note that this mechanism is only due to aggregate delayed response, the hydrate structure also has a measure of recoverable strain, obtained similarly to that of aggregate.

2.3.4.4 Structural Adjustment

Powers (1965) explains that if a cylindrical specimen is exposed to compressive load in the longitudinal direction, the resulting longitudinal shortening and the associated deformation of internal spaces upsets the initial state of balance of internal forces and sets in motion the processes required to restore a state of equilibrium which includes the external force.

When this load is applied, stress concentrations also arise in the hcp structure because of its heterogeneous nature and re-organization of particles into a more stable state without loss of strength (to maintain the required equilibrium mentioned above) occurs at these stress concentrations. This re-organization is called *structural adjustment* and it occurs in the following ways:

- *Viscous flow:* adjacent particles sliding past each other;
- *Local bond breakage:* this is followed by immediate movement and re-connection of particles.

The moisture movement, explained before, is believed to disturb the molecular structure further, encouraging the structural adjustment to occur. This mechanism is irreversible.

2.4. Macro-mechanisms of creep and shrinkage

As van Zijl (1999) explains, the attempts to mathematically model the processes in the microstructure lead to better understanding of the mechanisms of shrinkage, but the complex nature of the microstructure and the still limited knowledge of the microstructural processes remain stumbling blocks. Furthermore, a viable practical analysis of shrinkage requires a macroscopical approach. Certainly, the same applies for the more complex creep phenomenon. In short, macro-mechanisms are the *input parameters* used by the prediction models due to limited knowledge of concrete microstructure and to simplify calculations.

In this section emphasis is given to factors that influence creep and shrinkage on an intrinsic level as well as on an extrinsic stage. Although the existing design/prediction models of creep and shrinkage do not consider all macro-mechanisms as input parameters, it is important to understand the influence of these mechanisms. However, attention is drawn to the fact that there are too many factors that influence creep and shrinkage to consider all of them, not all factors are known and some may be of negligible influence, therefore some factors may be excluded from this discussion.

The macroscopic factors affecting creep can be divided into two categories:

1. *Intrinsic factors:* resulting from the internal state of the material (e.g. mix proportions, materials within the concrete and curing*). Discussed from section 2.4.1.1 to 2.4.1.6;
2. *Extrinsic factors*: the external environment and the effect of member size, which influence the internal state of the material. Discussed from section 2.4.2.1 to 2.4.2.4

Legend: * - considering the possibility of internal curing

2.4.1 Intrinsic factors

2.4.1.1 Water/Cement ratio

Water/cement ratio (w/c), as the name suggests, is the ratio of water content to cement content in the concrete. Neville (1981) has shown that, for the same aggregate/cement ratio, the shrinkage strains increase with increasing w/c ratio.

The effect of w/c ratio in shrinkage becomes less pronounced as the aggregate content of the mix increases, due to the restraint of the cement paste by the aggregate. This is shown by work of Neville (1981) in figure 2.12. Moreover Ballim (1983) explains that for normal structural grade concretes (applicable to WRS), where the aggregate volume content may be approximately 70% (or 80% according to Illston & Domone, 2006), a change in w/c ratio has very small effect. This may justify the fact that many prediction models do not consider this factor as an input parameter of shrinkage prediction.

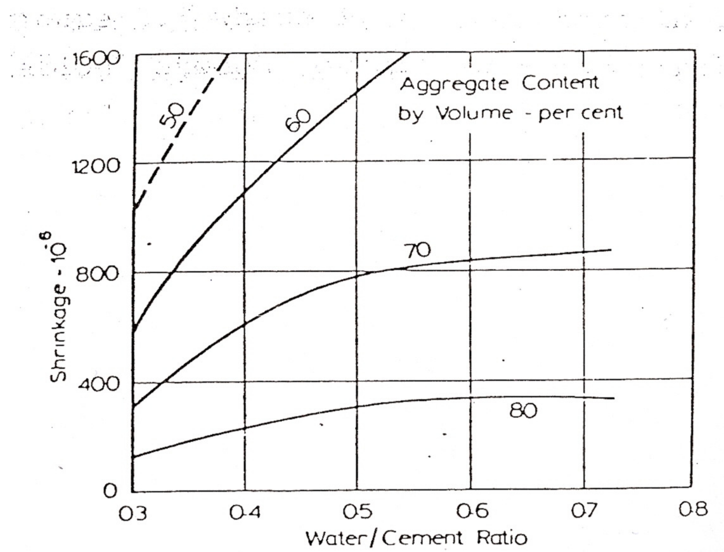

Figure 2.12: Shrinkage vs. w/c ratio for various aggregate concentrations (Neville 1981)

The Materials technology Division Committee of the British concrete society reported in 1973 that creep is greatly influenced by w/c ratio and that within the normal ranges of water cement ratio (0.4 to 0.6) an approximate linear relationship exists between w/c ratio and creep. This relationship is shown in figure 2.13.

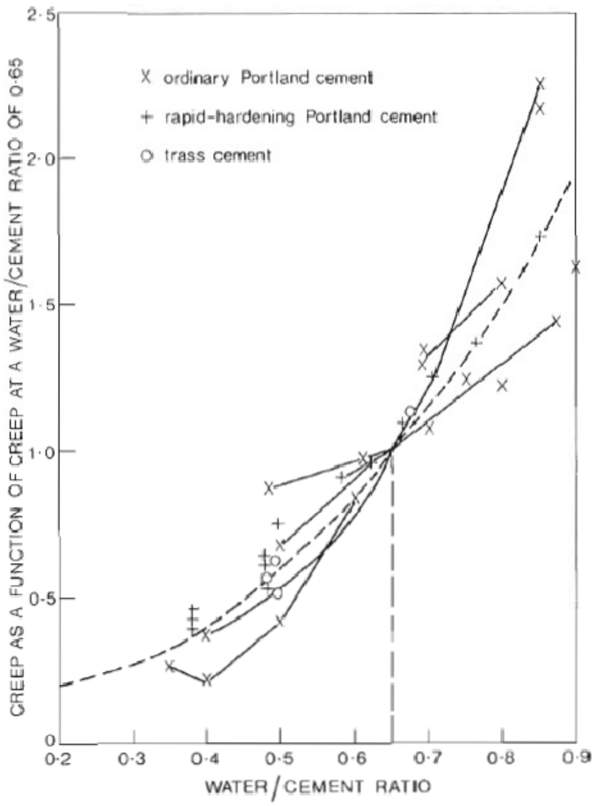

Figure 2.13: Effect of water/cement ration on concrete creep (Wagner 1958)

2.4.1.2 Water content

An increase in water content, increases the evaporable water and decreases the volume of restraining aggregate. Therefore its effect in creep might be significantly higher than that in shrinkage, however the overall direction of concrete volume change is the same, i.e. increase of strain.

2.4.1.3 Cement type

There is no agreement in the literature for the effect of cement type on creep or shrinkage. For example Hobbs & Parrott (1979), reports conflicts of the findings different researchers: While Meissner (1950), Swayze (1961), Blaine *et al* (1966), and Roper (1968) report that increments of C_3A content increases the shrinkage of concrete, Lerch (1946) suggest the opposite for some ranges of C_3A content.

As discussed in section 2.1.2, an increase in C_3A content result in an increase of concrete shrinkage.

Another contradiction arises as Hobbs & Parrot, (1979) conclude that for the purpose of shrinkage prediction, cement variations lead to a coefficient of variation of only about 10% in the magnitude of shrinkage and have little effect upon shape/form of the shrinkage versus drying period curve. However, Alexander (2001) reports that there are differences in shrinkage between different types of Portland cement and between cements of nominally the same types but other sources.

The conclusion by Alexander seams more appropriate, as different cements have different chemical compounds which react differently during the hydration phase.

Facing these contradictions, it is not surprising that the different prediction models adopt different approaches when considering the effect of cement on shrinkage or creep.

2.4.1.4. Aggregates

Aggregates (i.e. sand and stone in concrete) have a significant effect to creep and shrinkage. Its influence is divided in two categories:

A. Aggregate content
B. Aggregate type or physical characteristics of aggregate

<u>A. Aggregate content</u>

The aggregate provides restraint to creep and shrinkage as mentioned in the discussion on micro-mechanisms. The aggregate is also capable of shrinking, because the aggregate also contains pores capable of retaining and releasing water. Depending on the amount that the aggregate shrinks the restraint to overall shrinkage may be minimized. Therefore, the restraint is increased when the amount of aggregate is increased.

From figure 2.12 it can be observed that shrinkage decreases as the amount of aggregate increases. It is common for prediction models to recommend changes to the elastic modulus for creep and shrinkage calculation, which is understandably affected by aggregate due to the restraint it provides. However no direct input regarding aggregate attributes is made in such models.

The following equation (eq. 2.11) has been derived by Pickett (1956) to relate the ratio of shrinkage of concrete to the shrinkage of the cement paste which is dependable on volume of aggregates.

$$\frac{\varepsilon_{csh}}{\varepsilon_{cp}} = (1 - V_a)^{\beta} \qquad [2.11]$$

where,

ε_{csh} = shrinkage of concrete ;

ε_{cp} = shrinkage of cement paste

V_a = volume of aggregates

β = slope of the line of log $\frac{\varepsilon_{csh}}{\varepsilon_{cp}}$ plotted against log $\frac{1}{(1-V_a)}$

Note: β varies between 1.2 and 1.7

The restraint to movement provided by the aggregate affects creep considerably. Aggregate content affects creep through the concept of volume concentration. Greater concentration provides better restraint to movement hence reduces creep. Moreover, the aggregate may absorb water from the paste which reduces the effective water/cement ratio, hence reduces creep. The effect of aggregate content to creep is shown in figure 2.14.

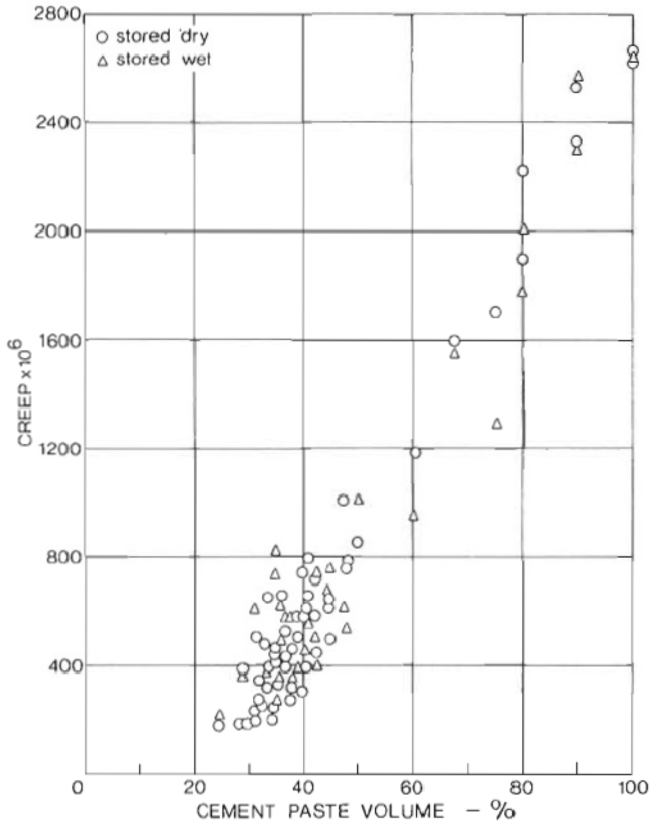

Legend: higher cement paste volume results in lower aggregate content

Figure 2.14: Creep as a function of cement paste volume (Wagner 1958)

B. Aggregate type or Physical properties of aggregate

South Africa has a variety of aggregate types, varying from aggregates found in the Karoo supergroup to those found in the Witwatersrand supergroup during mining activities. It is possible that different aggregate types may react differently on drying exposure or to the response to loading. This hypothesis will be discussed in this section

The elastic modulus is regarded as one of the most important properties of aggregates that affect creep or shrinkage. This comes from the fact that aggregate restrains the movement of water within the concrete as discussed earlier.

Alexander & Davis (1992) considered the stiffness of the embedded aggregate as one of the major factors influencing elastic modulus of concrete along with the strength of the paste phase, relative volume concentrations of aggregate and their interface characteristics. Therefore, the physical characteristics of the aggregate may affect its elastic modulus and the elastic modulus of concrete.

Aggregate types (which vary in their physical characteristics such as stiffness) may therefore affect elastic modulus (as shown in figure 2.14 below) and the subsequent creep and shrinkage. For example, the physical characteristics of Dolomite (Olifantsfontein) aggregates are different to those of Wits Quartzite (Vlakfontein) aggregates, hence they possess different elastic modulus and subsequently lead to different creep and shrinkage of concrete.

Alexander & Davis (1992) also studied the effects of seven local aggregate types in the value of concrete elastic modulus. It was found that the concretes had a large variation in elastic behaviour patterns. An indication of these findings is shown in figure 2.15 which illustrates the relationship between static elastic modulus and cube strength for different aggregate types.

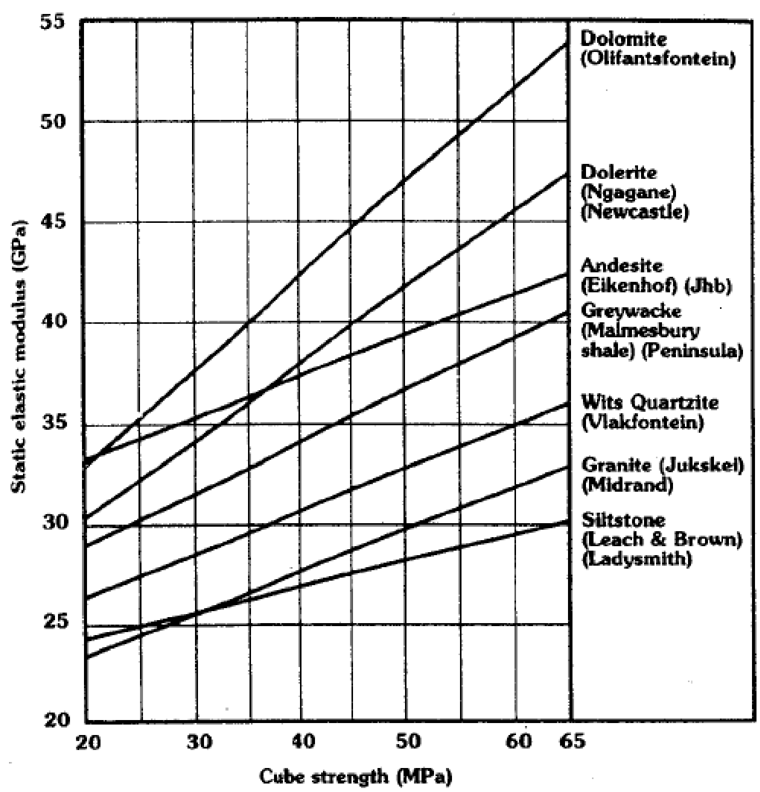

Figure 2.15: Relationship between static elastic modulus of concrete cubes and cube strength for different aggregate types (Alexander & Davis, 1992)

Ballim (1983) indicates that higher elastic modulus of the aggregate leads to greater restraint provided to shrinkage of the cement paste. Therefore, the variation in stiffness of aggregate that brings about this change should be considered for better durability. In short, stiffer aggregates result in higher elastic modulus and lower shrinkage.

The change of elastic modulus also affects the creep in concrete. In general, higher values of elastic modulus lead to lower creep strains. If the creep mechanism of delayed elastic strain is taken as an example, this relationship can be observed. In this mechanism the cement paste transfers the load to the aggregate with time and the aggregate deforms elastically over time, i.e. creeps. A stiffer aggregate (which has a higher elastic modulus) will deform less therefore creeps less than other aggregates. With less creep at the aggregate level, reduced creep is found in the concrete.

As mentioned earlier some aggregates may shrink depending on their porosity. The amount to which the aggregate shrinks determines the restraint to movement provided to the cement paste. Hobbs & Parrot (1979) provide limits to the overall shrinkage, for aggregates that shrink less than the cement paste in equation 2.12. Increased porosity in aggregates may also lead to increased creep strains.

$$\begin{aligned}
\varepsilon_{csh} &< (1-V_a)\varepsilon_{cp} + \varepsilon_{cag}V_a \;\; when \;\; E_a > E_{cp} \\
\varepsilon_{csh} &> (1-V_a)\varepsilon_{cp} + \varepsilon_{cag}V_a \;\; when \;\; E_{cp} > E_a
\end{aligned} \qquad [2.12]$$

where,

ε_{cp} = shrinkage of cement paste

ε_{cag} = shrinkage of aggregates

E_{cp} = Elastic modulus of cement paste

E_a = Elastic modulus of aggregates

The elastic modulus is not only influenced by the aggregates, as mentioned before and as it is discussed further in section 2.3.6. However the prediction models do not consider the aggregate type directly as an individual input parameter, instead recommendations are often made to national standards to adjust the elastic modulus, which is then considered to carry the effect of the aggregate type.

2.4.1.5. Curing

The effects of the curing process on creep and shrinkage are considered in two ways:

A. Curing conditions (including duration of curing)
B. Curing method

<u>A. Curing conditions</u>

It is commonly believed that longer periods of curing result in lower creep and shrinkage strains. The concrete curing environment can be varied with respect to temperature and humidity and these storage conditions control the moisture movement between the concrete and the atmosphere, i.e. shrinkage.

The temperature and the humidity of storage conditions at curing also affect the rate at which cement hydrates. The concrete society (1973) explained that the cement hydration controls the density of the gel, as the greater the degree of hydration, the greater is the density. Subsequently, a denser gel leads to lower concrete creep strains.

The duration of curing is considered in as a parameter for shrinkage prediction in all prediction models investigated in this project. With regard to creep, concrete *maturity* (i.e. age of loading, considering no temperature change) is regarded as more relevant.

Concrete maturity brings about changes in the concrete such as denser interfacial zones, but most importantly added compressive strength. For example a 28 day concrete is expected to have a higher compressive strength than a 7 day concrete. Since creep is influenced by compressive strength, the provision of age of loading as a prediction parameter of creep calculation represents this maturity trough use of higher compressive strength values for concretes loaded at a late stage.

B. Curing method

Common methods of curing in the South African construction industry are water curing and steam curing. Water curing implications to creep and shrinkage have been discussed in the previous sub-section. With regard to steam curing, the Concrete Society (1973) reports that the high temperatures experienced may alter the structure of the gel, leading to a more crystalline structure, hence to reduction of creep. Changes to shrinkage rates are therefore expected.

2.4.1.6 Elastic modulus and compressive strength

A definition of elastic modulus and an extensive discussion on the effects of the elastic modulus on creep and shrinkage has been made during the course of this chapter. Additional factors that affect the elastic modulus and therefore affect creep and shrinkage indirectly need to be identified.

This section lists the factors that influence the elastic modulus without going into great detail for the purposes of simplicity. The influence of such factors is fairly well-understood and it is readily available in the literature, therefore only a few points are highlighted here.

The factors affecting elastic modulus are:

- *Aggregate*: Elastic modulus increases with denser aggregate (i.e. less porosity), and increased volume concentration

- *Cement paste matrix:* Less porous cement matrix leads to high elastic modulus
- *Interfacial zone:* The amount of void spaces and micro-cracks in the interfacial zone strongly influences the elastic modulus. The porosity in the interfacial zone is affected by:
    - Water/cement ratio
    - Degree of hydration
    - Mineral admixtures
    - Chemical interaction between cement paste and aggregate
    - Bleeding characteristics (e.g. aggregate grading, size and geometry
- *Phase proportions:* more aggregate in concrete leads to higher elastic modulus
- *Temperature:* mixed influence, i.e. exposure to high temperatures during curing may lead to high elastic modulus, yet the opposite may be true during the life span of the structure.
- *Compressive strength:* the greater the compressive strength, the greater the elastic modulus

The compressive strength and the elastic modulus are intrinsically related. It is possible that, the factors listed above affect the compressive strength primarily and that the elastic modulus change comes as a consequence. However, significant tests are required to prove this postulation and it is not the focus of this research.

It has been observed that an increase in compressive strength leads to an increase of elastic modulus. As a result, several formulae have been developed on the relationship between these concrete properties aiming at elastic modulus prediction. This is made more relevant by the fact that it is simpler to test the compressive strength of a concrete than it is to test its elastic modulus.

Table 2.3. shows some of the developed formulae used in practice.

Table 2.3: Elastic modulus prediction using compressive strength

Source & Notes	Elastic Modulus as a function of time	Equation No.
CEB-FIP 1990* • Mean Values • Cylinder strength	$E_{cm}(t) = 21500\left(\frac{f_{cm28}}{10}\right)^{1/3}\left(\exp\left\{s\left[1-\sqrt{\left(\frac{28}{t/t_1}\right)}\right]\right\}\right)^{0.5}$	2.13
ACI 209 R-92 ** • mean strength • Cylinder strength	$E_{cm}(t) = g_{ct}\sqrt{w_d^3 \times \frac{t}{a+\beta t} \times f_{cm28}}$	2.14
SABS 0100-1 *** • Characteristic values • Cube strength	$E_{ck}(t) = (K_o + 0.2 f_{ck,28}) \times \left(0.4 + \frac{0.6 f_{ck,t}}{f_{ck,28}}\right)$	2.15
*- CEB-FIP 1990: CEB-FIP model code 1990; **- ACI 209 R-92: American Concrete Institute Committee 209 and *** - South African standard code of practice		

where:

t – time in days

$E_{cm}(t)$ - mean elastic modulus at time t

$E_{ck}(t)$ - characteristic elastic modulus at time t

f_{cm28} - mean compressive strength at the age of 28 days

$f_{ck,28}$ - characteristic compressive cube strength at 28 days

$f_{ck,t}$ - characteristic compressive cube at time t

s - variable that accounts for different cement types

K_o - constant that accounts for aggregates, given as 20 KN/mm2 as a general case

w_d - density of concrete in Kg/m3

g_{ct} - given as 0.043

a & β - constants that account to different cement types

2.4.2 Extrinsic Factors

2.4.2.1 Geometry of the concrete element (i.e. Element shape and size)

The rate of water loss from the concrete to the atmosphere is controlled by the length of the path travelled by the water. At a constant relative humidity (RH), both the shape and size of a concrete element determine the path travelled by the water, the water loss quantity and therefore the magnitude of drying shrinkage and creep. It is convenient to express the shape and size parameters by a single quantity expressed in terms of *effective or theoretical thickness* which is equal to the area of the section divided by the semi perimeter in contact with the atmosphere, $h = 2\ A_c/u$ (Eq. 2.18)

Relations between the theoretical thickness and the drying shrinkage/creep coefficients are shown in figure 2.16. In general, thicker element drying leads to more micro-cracking and proceeds slower (thus allowing more hardening due to hydration) both of which reduce the final shrinkage (Bažant, 1995).

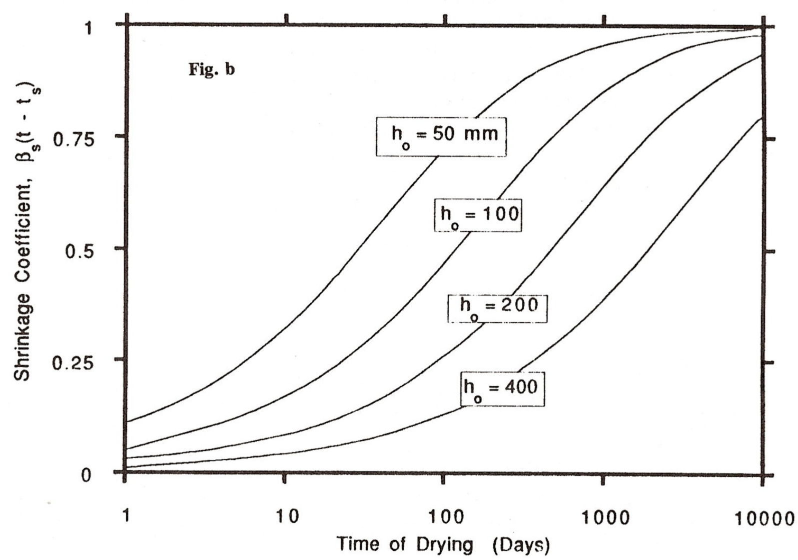

a)

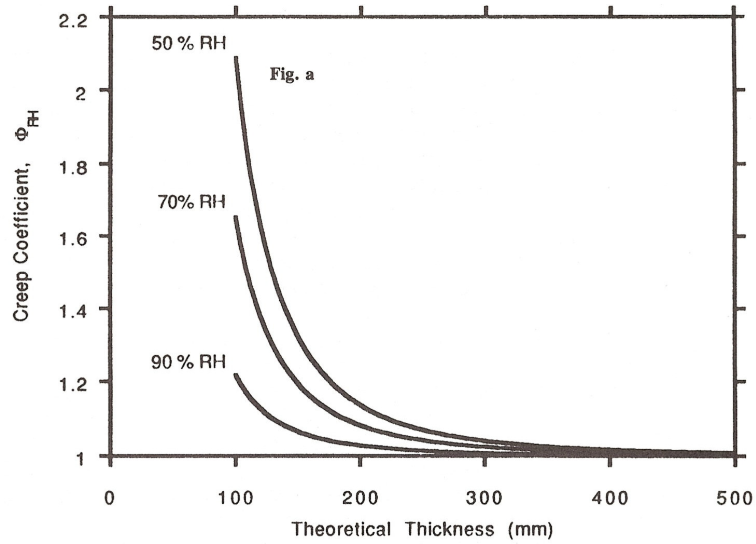

b)

Figure 2.16: a) Influence of exposure time and specimen size on drying shrinkage coefficient **b)** Influence of specimen size and relative humidity on creep coefficient (CEB FIP 1990)

2.4.2.2 Relative humidity of the environment

An increase in the relative humidity (RH) is expected to slow down the relative rate of moisture from the interior to the outer surfaces of concrete, therefore it reduces creep and shrinkage. The effects of RH on drying shrinkage and creep is shown by studies of CEB (1970) in figure 2.17.

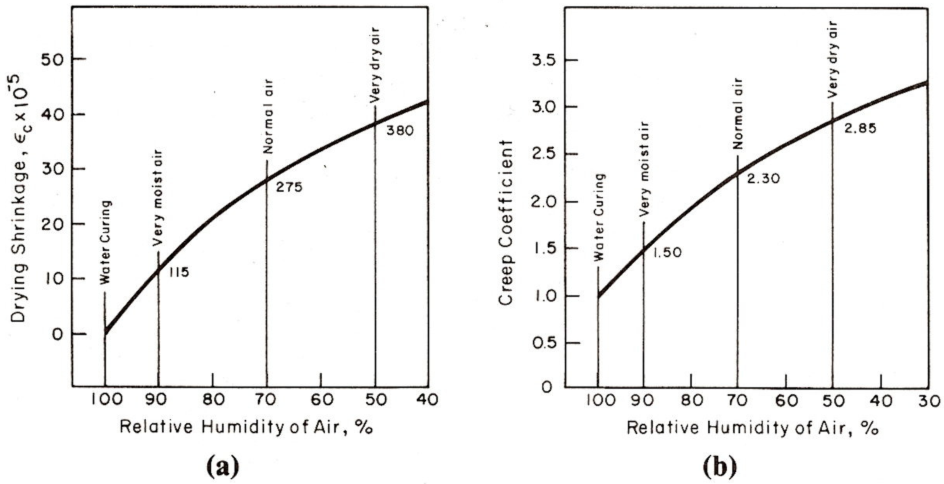

Figure 2.17: Influence of the relative humidity on **a)** drying shrinkage and **b)** creep (CEB-FIP 1970)

2.4.2.3 Stress level

For any concrete with given mixed proportions and loading conditions, the creep is found to increase linearly with applied stress up to stress/strength ratios of about 0.4 to 0.6 (different studies have indicated different limits) *(Illston & Domone, 2006)*. Figure 2.18 illustrates the relationship between stress levels and the creep for a concrete with 0.69 water/cement ratio (20 MPa nominal compressive strength), based on the works of Troxel *et al* (1958).

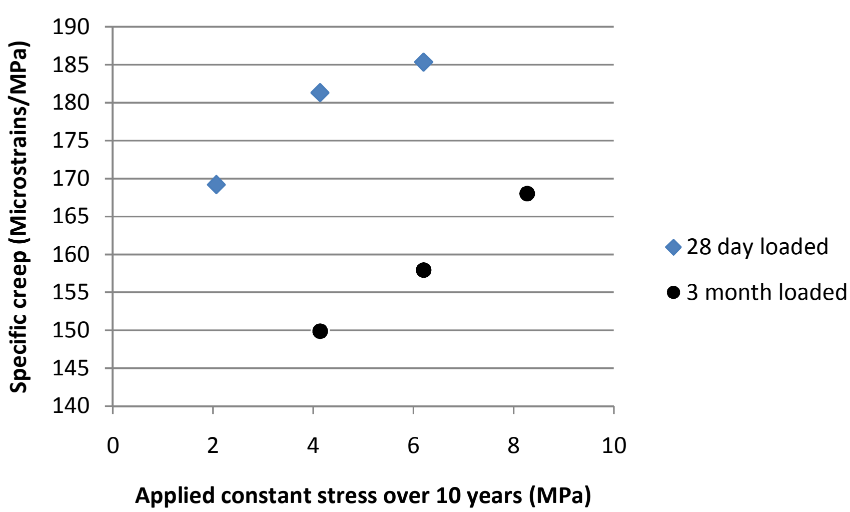

Figure 2.18: 10 year specific creep of a particular concrete at different stress levels (Adapted from Troxel *et al.* 1958)

2.4.2.4 Temperature

The temperature to which concrete is exposed can have two counteracting effects on creep. If a concrete member is exposed to high temperatures as part of the curing process before it is loaded, its strength increases and the creep strain is significantly less than that of concrete stored at a low temperature. On the other hand, exposure to high temperature during the curing period under load can increase creep.

The Concrete Society (1973) studied the effects of temperature on creep including a sudden change in temperature on a loaded specimen. The results of this study are presented in figure 2.19, showing a marked increase in creep strain upon temperature increase.

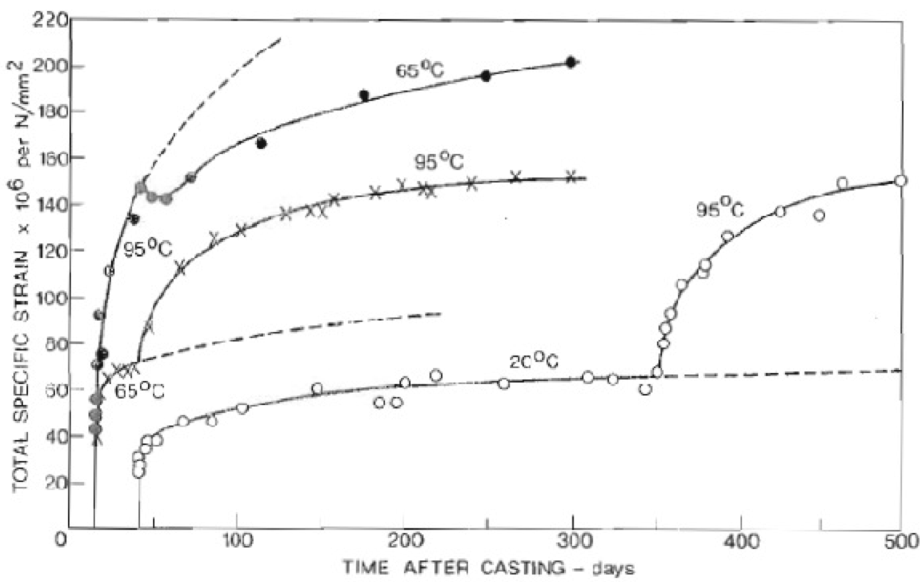

Figure 2.19: Effect of a temperature upon creep (Concrete society, 1973)

2.5 Programming approaches for creep and shrinkage

Although the mechanisms of creep and shrinkage are strongly related as discussed in section 2.3.4, separate prediction/calculation of creep and shrinkage is commonly chosen. This is a consequence of not modelling the microstructural physics within the concrete yet it is justified as a pragmatic approach to predict creep and shrinkage in the absence of a complete understanding of the microstructural processes. (van Zijl, 1999). Hence, the separate prediction approach used by the selected prediction models is regarded as acceptable and reasonable for purpose of this project.

CHAPTER 3
METHODOLOGY

3.1 Introduction and planning of the research

The purpose of this chapter is to present the methods used to perform this research as well as the plan of action that was utilized.

A plan of action or research methodology is proposed here for the determination of the most suitable creep and shrinkage prediction model to be used in concrete WRS in South Africa. Firstly, the research is divided in four phases, namely:

Phase 1: Experimental data acquisition phase
Collection of Experimental data, compilation of a national creep and shrinkage database

Phase 2: Experimental data processing phase
Selection of water retaining structures data from the database, Grouping/Classification of selected data

Phase 3: Selection of Prediction models and model processing phase
Model Selection, Analysis of the contents of the models, Programming of the models

Phase 4: Statistical analysis and comparison of prediction models to water retaining structures data

The phases will be described in detail in subsequent sections, including the research methodologies employed within each phase.

3.2 Phase 1: Experimental data acquisition

The following is a summary of the steps performed during the acquisition of experimental data for this project.

3.2.1. Collection of experimental data

Two methods were considered to obtain the required creep and shrinkage experimental data:

1. Creep and shrinkage tests by the researcher
2. Collection of data from previous experiments by different researchers

Although direct control over the experiment tests by the author may result in more reliable results, the first option was not selected for the following reasons:

- The amount of data that would be obtained by one single researcher would not be sufficient for this project
- The length of the experiments would be limited to only a few months
- Data would be limited to a few concrete materials (e.g. aggregate types)
- The acquisition of the experimental equipment (e.g. creep frames) would be time consuming.

In contrast, the second option (i.e. collection of data from previous experiments by different researchers) was selected with due realization of the fact that thorough scrutiny of data to ensure reliability is required.

To reduce the risk that the collected data was unreliable, the data sources were limited to the following:

- Local, South African industry requested experiments performed at a reputable university (with confidentiality retained).
- Academic research experiments performed at a reputable university for instance towards an approved Masters or Doctoral degree.
- Experiments performed at a reputable university by an academic research personnel member.

Reputable universities where creep and shrinkage research data could be found are the University of Cape Town (UCT) and University of Witwatersrand (WITS). Interaction with these universities to obtain this data also benefitted from previous research partnerships between Stellenbosch University and these institutions.

3.2.2 Compilation of a South African creep and shrinkage data base

It was evident during the course of this research that a South African creep and shrinkage data base was non-existent. At this stage, most studies on the response of South African concretes to load or environmental conditions were done through the use of foreign data bases such as the RILEM data base. To improve relevance to South African conditions, this research included the development of a South African data base made up of concretes typically used in South Africa.

It was noted that the development of a South African creep and shrinkage database would bring significant benefits to the construction industry through the observation of creep and shrinkage strains of concretes made of local ingredients, subject to local processing procedures and environmental conditions. For instance, the observation of creep over time, of a concrete made up of dolomite aggregates from Olifantsfontein in South Africa would finally be possible.

The database would be an asset to the country's intellectual wealth if different universities participated to supply country-wide information. Thus, a team from WITS (namely Prof Y. Ballim and Mrs. P. Gaylard) created the shrinkage part of the data base, whilst the creep database is developed in this research by the author. Both shrinkage and creep data base had significant input from the University of Cape Town (namely Prof M Alexander and Dr. H. Beushausen).

The data base is to be hosted at the South African Concrete & Cement Institute website, and it is also added to the annex CD of this document.

3.3 Phase 2: Experimental data processing

3.3.1. Selection of WRS data within the South African Data Base

Once the data base had been completed, experimental data that relate to water retaining structures was selected. To achieve this, typical design mixes (see table A1 in the appendix) that are used in the construction of water retaining structures (WRS) were used as the selection tool. Therefore, experiments that tested concrete specimens with a similar design mix, and which indeed led to concrete with properties required for WRS were selected. Note that particular strength, stiffness, water-tightness and durability performance required for WRS can be achieved with a variety of mix proportions. Thus, a range of mix compositions that could lead to suitable concrete for WRS was selected. The range is shown in table 3.1, but full detail is given in table 3.2.

Table 3.1: Ranges in concrete ingredients used to select data that relate to WRS

Ingredient	Range (kg/m^3)
Cement	150 - 450
Water	150 - 250
Stone	1000 - 1250
Sand	650 - 950
Slag	0 - 200

Table 3.2: Selected mixes that represent WRS concretes,, in kg/m^3 of concrete

	BINDER							WATER	
Experiment	CEM I	CEM II	FA	GGBS	GGCS	CFS	Total Binder	Water	Water/Binder
A1	300		0	0	0	0	300	195	0.65
A2	300		0	0	0	0	300	200	0.67
A3	300		0	0	0	0	300	200	0.67
B1	333		0	0	0	0	333	200	0.60
B2	333		0	0	0	0	333	200	0.60
B3	390		0	0	0	0	390	195	0.50
B4	333		0	0	0	0	333	200	0.60
B5	333		0	0	0	0	333	200	0.60
C1	310		0	0	0	0	310	195	0.63
C2	300		0	0	0	0	300	180	0.60
C3	311		0	0	0	0	311	207	0.67
C4	180		0	105	0	0	285	195	0.68
D1	333		0	0	0	0	333	200	0.60
D2	333		0	0	0	0	333	200	0.60
E1	333		143	0	0	0	476	200	0.42
E2	300		0	0	0	0	300	180	0.60
E3	240		0	60	0	0	300	180	0.60
F1	378		0	0	0	0	378	210	0.56
G1	360		0	0	0	0	360	180	0.50
H1	325		139	0	0	0	464	195	0.42
H2	342		146	0	0	0	488	205	0.42
H3	350		150	0	0	0	500	210	0.42
H4	435		0	0	0	0	435	185	0.43
I1		228	0	89	0	0	316.76	200	0.63
J1		270	0	40	0	0	310.3	195	0.63
K1		351	137	0	0	0	487.64	205	0.42
K2		343	133	0	0	0	476.28	200	0.42

Table 3.2: Selected mixes that represent WRS concretes (continued)

Experiment	Sand type	Sand amount (kg/m^3)	AGGREGATE Stone Type	Stone amount (kg/m^3)	Total Aggregate(kg/m^3)	Aggregate/Binder (by mass)
A1	Cape flats sand	773	greywacke	1100	1873	6.24
A2	Cape flats sand	760	greywacke	1100	1860	6.20
A3	Cape flats sand	768	greywacke	1100	1868	6.23
B1	Cape flats sand	787	sandstone	1100	1887	5.67
B2	Cape flats sand	787	sandstone	1100	1887	5.67
B3	Not available	652	greywacke or granite	1175	1827	4.68
B4	Cape flats sand	787	sandstone	1100	1887	5.67
B5	Cape flats sand	787	greywacke	1100	1887	5.67
C1	dolomite	956	dolerite	1106	2062	6.65
C2	pit sand Klipheuwel	820	greywacke	1100	1920	6.40
C3	natural sand (decomp. granite)	753	dolerite	1239	1992	6.41
C4	natural sand (decomp. granite)	803	andesite	1104	1907	6.69
D1	Cape flats sand	787	granite	1100	1887	5.67
D2	Cape flats sand	787	sandstone	1100	1887	5.67
E1	granite	655	andesite	1100	1755	3.69
E2	natural sand (decomp. granite)	803	andesite	1104	1907	6.36
E3	natural sand (decomp. granite)	803	andesite	1104	1907	6.36
F1	Wits quartzite	772	Wits quartzite	1036	1808	4.78
G1	pit sand Klipheuwel	804	greywacke	1100	1904	5.29
H1	dolomite	773	dolerite	1106	1879	4.05
H2	dolomite	721	dolerite	1106	1827	3.74
H3	dolomite	668	dolerite	1106	1774	3.55
H4	river sand Umlaas	720	tillite	1100	1820	4.18
I1	dolomite	677	dolerite	1106	1783	5.63
J1	dolomite	951	dolerite	1106	2057	6.63
K1	dolomite	754	dolerite	1106	1860	3.81
K2	dolomite	772	dolerite	1106	1878	3.94

3.3.2 Grouping of experimental data

After the experimental results had been selected according to the concrete used in water retaining structures, they were grouped for prediction of creep and shrinkage performance. This was primarily done by separating the experimental data according to the reported compressive strength and the cement type used in the design mix of the concrete tested – see Table 3.3.

Table 3.3: Groups of experimental data and their description

Experimental group	Description, i.e. cement type and compressive strength range
Group 1: CEM I 30-40 MPa	CEM type I and 30 to 40 MPa
Group 2: CEM I 41-50 MPa	CEM type I and 41 to 50 MPa
Group 3: CEM I 51-60 MPa	CEM type I and 51 to 60 MPa
Group 4: CEM II 30-40 MPa	CEM type II and 30 to 40 MPa
Group 5: CEM II 41-50 MPa	CEM type II and 41 to 50 MPa
Group 6: CEM II 51-60 MPa	CEM type II and 51 to 60 MPa

Note that concrete mixtures with compressive strength above 60 MPa, where not considered as they are not commonly used in the design of WRS. It is acknowledged that a compressive strength class of 35 MPa concrete (characteristic strength) is commonly used for WRS (BS EN1992-3). However, concretes of slightly lower and higher (average) compressive strengths were included in the evaluation, in order to increase the statistical base. Also, concrete mixtures with cement type III were not considered in this document due to insufficient information contained in the data base.

Further classification of these experiments was done prior to prediction with the models. This additional classification was done within the groups mentioned above using parameters such as time of loading, curing time, humidity, temperature and others. This is illustrated in the diagram of figure 3.1. Note that the purpose is to group sets of data (experimental results) for comparison with a single set of input parameters for prediction models. It is of course possible to use precise parameters for each experiment, as reported in the source of that particular experimental test (this is also done in this research). However, it is believed that within tight ranges, the sensitivity to particular input parameters is negligible. Most importantly, variability due to control system tolerances, such as temperature (usually ±2°C) and relative humidity (±5%), render the grouping together of data sets with individual parameters within such ranges appropriate.

The following tolerances were used during the classification of water retaining structures data:

- T – Ambient Temperature: +/- 2 °C
- RH – Ambient Relative humidity: +/- 5 %
- t_c and t_0 - Curing time and loading age: +/- 1 day
    - Minimum curing time observed: 7 days
    - Maximum curing time observed: 49 days
    - Observed curing method throughout the data is moist curing
    - Minimum loaded age observed: 14 days
    - Maximum loaded age observed: 49 days
- V/S - Volume over surface area ratio: +/- 2 mm
- h - Variable regarding geometry of the structure (explained in chapter 4. – Prediction models - under equation 4.15): +/- 2 mm
- E_{cm28} - Elastic modulus at the age of 28 days: +/- 5 GPa
    - Which resulted in data sets with f_{cm28} (i.e. compressive strength at the age of 28 days) +/- 3 MPa but same CEM type
    - Mean cylinder compressive strength used

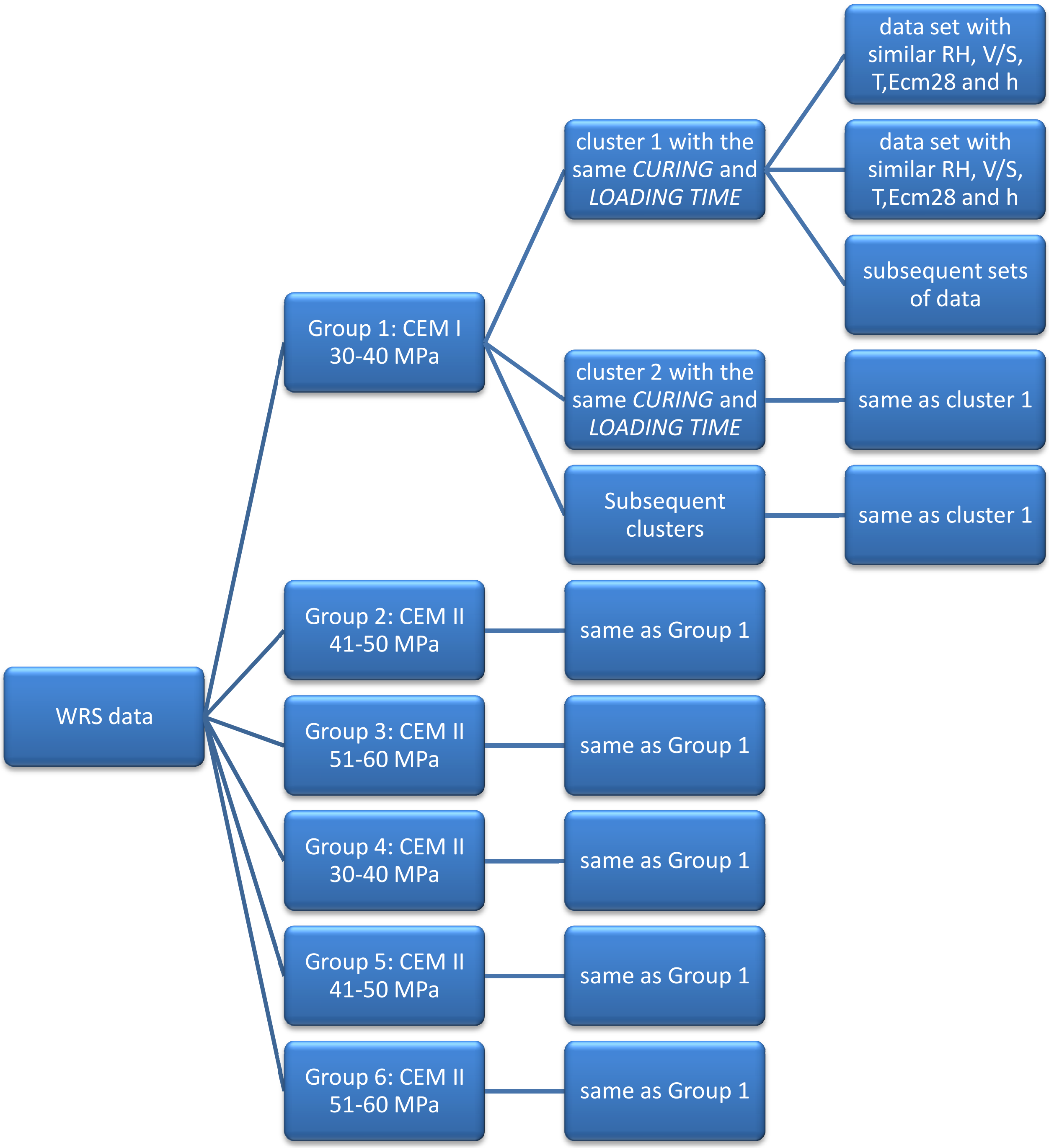

Figure 3.1: Diagram showing the classification process of the results within the experimental group to form unique data sets.

Table 3.4 summarizes the results of the categorization described above.

Table 3.4: Final sets of data arranged according to respective parameters

Group 1: CEM I 30-40 MPa									
Data set	Experiment Names	t_c (days)	t_o (days)	T (℃)	RH (%)	fcm 28 (MPa)	Ecm28 (GPa)	h (mm)	V/S (mm)
Data set A	**(A1)** DS14 Mix CA **(A2)**DS14 Mix CI **(A3)** DS14 Mix C	7	14	23	50	35	33	25.5	11.8
Data set B	**(B1)** DS 18 Mix Prima **(B2)**DS 18 Mix Malans **(B3)**DS10 Mix 0.5 OPC **(B4)** DS11 Worcester Sandstone **(B5)** DS18 Mix Greywacke	14	N.A.	23	55	35.8	27.3	50	20
Data set C	**(C1)** DS3 Mix R5 **(C2)** DS 21 Mix CAN **(C3)** DS12 Dolerite (Natal Crusher) **(C4)**DS19 Mix B65/35 0.6	28	28	23	58	36	31.25	50	21.7
Group 2: CEM I 41-50 MPa									
Data set Name	Experiment Names	t_c (days)	t_o (days)	T (℃)	RH (%)	fcm 28 (MPa)	Ecm28 (GPa)	h (mm)	V/S (mm)
Data set D	**(D1)** DS11 Granite Mix **(D2)** DS11 Villwersdorp Sandstone	14	N.A.	23	60	40.5	N.A.	50	20
Data set E	**(E1)** DS5 Mix 46 **(E2)** DS19 Mix OPC 0.6 **(E3)** DS19 Mix B 80/20 0.6	28	28	23.7	55	42.7	34.7	50	20
Data set F	**(F1)** DS7 Mix YBQ2	49	49	21	43	41	26	51	20.8

Group 3: CEM I 51-60 MPa									
Data set Name	Experiment Names	t_c (days)	t_o (days)	T (℃)	RH (%)	fcm 28 (MPa)	Ecm28 (GPa)	h (mm)	V/S (mm)
Data set G	**(G1)** DS20 NB Mix 8	7	N.A.	25	50	52	N.A.	38	17
Data set H	**(H1)** DS2 Mix 104 **(H2)** DS2 Mix 124 **(H3)** DS3 Mix 84 Rpt	29	29	22.3	65	52.3	39.7	50	20
Group 4: CEM II 30-40 MPa									
Data set Name	Experiment Names	t_c (days)	t_o (days)	T (℃)	RH (%)	fcm 28 (MPa)	Ecm28 (GPa)	h (mm)	V/S (mm)
Data set I	**(I1)** DS3 Mix 81 Rpt (36/35 N)	28	29	21	61	36	35	50	20
Group 5: CEM II 41-50 MPa									
Package Name	Experiment Names	t_c (days)	t_o (days)	T (℃)	RH (%)	fcm 28 (MPa)	Ecm28 (GPa)	h (mm)	V/S (mm)
Data set J	**(J1)** DS3 Mix 76 Repeat	29	30	21	61	42	39	50	20
Group 6: CEM II 51-60 MPa									
Package Name	Experiment Names	t_c (days)	t_o (days)	T (℃)	RH (%)	fcm 28 (MPa)	Ecm28 (GPa)	h (mm)	V/S (mm)
Data set K	**(K1)** DS2 Mix 109 **(K2)** DS3 Mix 64 Rpt	32	32	22	65	54	39	50	20

These data sets (i.e. A to K) as well as the individual experiments (i.e. A1 to K2) were later compared with strains calculated using prediction models. The remaining parameters, required to calculate creep and shrinkage strains using a prediction model were collected from the individual experiments and averaged before prediction of a data set. However, the original parameters were introduced into the models for the prediction of individual experiments.

This pragmatic approach to parameter selection ensured automation of the data set prediction whilst maintaining the accuracy of both individual experiment prediction and data set prediction.

3.4. Phase 3: Selection of prediction model and model processing

3.4.1. Selection of prediction models

The selection of the models was done according to the complexity level, region and date of origin as well as reported accuracy in the literature. Two levels of complexity were considered in this project

1. *Entry-level or Basic-level of sophistication models:* These are models that are able to provide a prediction within acceptable accuracy with reduced amount of input parameters; ideal for conceptual and tender stage design phase.

2. *Advanced-level of sophistication models:* These are models that require a higher number of parameters than the first level prediction models and are able to produce more accurate results; ideal for more accurate studies of concrete and higher confidence on the predictions.

The selection of recent models accommodates recent advances in the area of creep and shrinkage prediction. Also, the region of the world where the models were developed was considered to ensure that a wide variety of prediction approaches are evaluated. This was coupled by a study of the literature in which reported reasonable results of the selected models were found.

Table 3.5 shows the selected models with their conformity to the above mentioned criteria:

Table 3.5: Selected models

Prediction models	Short name***	Complexity level	Origin	Date of origin
Gardner and Lockman model	GL 2000	Entry	USA*	2000
South African standard code of practice	SABS 0100-1	Entry	UK* RSA**	2000
CEB-FIP model code	CEB-FIP 1990	Advanced	Europe	1990
European code of practice	EN 1992-1-1:2004	Advanced	Europe	2004
American Concrete Institute Committee 209	ACI 209R-92	Advanced	USA	2008
RILEM creep and shrinkage - model B3	B3 model	Advanced*[4]	USA	1995
Notes: * USA – United States of America; UK – United Kingdom ** RSA – currently used in the Republic of South Africa *** Short name – models are referred in this terminology throughout the document *[4] – More sophisticated than the regular advanced model				

3.4.2. Programming of the models

Each of the prediction models were subsequently programmed into an electronic format. Several software packages such as Matlab, Maple and Mathcad were considered and the features of these packages were taken into consideration before programming. At the end of this assessment Microsoft Office Excel was selected as the software tool of this project for the following reasons:

- The required experimental South African creep and shrinkage database was already in Microsoft Excel format, making it simple to transfer data from the data file into the prediction model file.
- The programme is capable to create a template file that is able to read data from the experimental data file, plot the experimental data, compute the

prediction model at various times, plot the prediction model and calculate a statistical accuracy analysis of the two plots.

- Microsoft Excel is a popular and easy-to-use programme. This ensures that a future researcher (or advanced reader) may be able understand and use the model programming in the future. In addition, this allowed the current researcher to focus the limited time of the project into correct interpretation of the model principles rather than using such time in acquainting with a new software package.

During this phase, the variable parameters such as relative humidity and temperature were left as input parameters of the spreadsheet. These parameters would vary from one set of data to the other producing different results. For example a 100x100x 200 mm concrete prism exposed to 70 % Relative humidity, 20 °C, 7 days curing, 14 days loading age will have a different input set and result from a 100x100x100 mm concrete cube exposed to 50 % Relative humidity, 25 °C, 28 days curing, 28 days loading age.

The quality of programming was subsequently verified thoroughly before the data sets and individual experiments were predicted. This was achieved through a systematic verification approach that comprised three methods:

Method 1: Visual observation of all models for a particular set of data.

Two different sets of input parameters were introduced into the models to identify a distortion trend in case of an error.

Method 2: Comparison with a worked example available in literature

The same input parameters used by a trusted example available in the literature (i.e. ACI 209.2R-08 guide example) were used in the programmed spreadsheet to calculate creep and shrinkage results at different times. The results given by the literature example were subsequently compared to the results of the programmed spreadsheet.

Method 3: Observation of model behaviour under single parameter variation

For a given set of parameters, a single parameter was changed and the observed model behaviour was compared to the expected behaviour based on physical phenomena associated with creep and shrinkage. This was repeated for different parameters.

The details and results of this systematic verification approach to the programming of the models are provided in chapter 5.

3.5 Phase 4: Statistical comparison of prediction models to water retaining structures data

Different methods have been developed to assess the accuracy of prediction models. These methods are called *statistical indicators* and they involve the use of experimental data (i.e. observed data) which is compared to the calculated data. In other words, the accuracy of the prediction models is defined by the level of conformity of the calculated data to the experimental test results.

The following statistical indicators were used in this project:

- Bažant and Panula (1990) coefficient of variation method (i.e. BP-COV method)
- CEB (1990) mean square error (i.e. CEB-MSE method)

The BP-COV method provides an elaborated method to verify the compliance of calculated values to observed values. This method includes statistical terms such as variance, mean and coefficient of variation which assure an unbiased verification of the accuracy of the models.

On the other hand, the CEB mean square error is a simpler statistical indicator as compared to the BP-COV method. This indicator was used in this project as an alternative indicator to provide objectivity and increase confidence levels of the results found in this research.

These indicators were also programmed into the Microsoft Excel Spreadsheet template mentioned before. Therefore, the quality of this programming was also verified. The results of this verification are presented in chapter 5.

3.5.1 Bažant and Panula coefficient of variation method (i.e. BP-COV method)

According to the BP-COV method, the coefficient of variation of a prediction model to the observed experimental value is given through the set of formulae provided from equation 3.1 to 3.4

$$\overline{w} = \sqrt{\frac{1}{N}\sum_{j=1}^{N} w_j^2} \qquad [3.1]$$

where

$\overline{w}$ = overall coefficient of variation relative to the mean value of creep or shrinkage

w_j = coefficient of variation of data set j, defined in equation 3.2

N = number of data sets under observation

$$w_j = \frac{s_j}{\overline{O_j}} \qquad [3.2]$$

where

s_j = the unbiased estimate of variance of a model versus a visually hand-smoothed experimental curve.

$\overline{O}_j$ = mean value of observed results given in equation 3.3.

$$\overline{O_j} = \frac{1}{n}\sum_{i=1}^{n} O_{ij} \qquad [3.3]$$

where

O_{ij} = observed values (i.e. experimental results)

n = sampling points of data set j, chosen at constant spacing in $\log(t-t_0)$ or $\log(t-t_c)$

$$s_j = \sqrt{\frac{1}{n-1}\sum_{i=1}^{n}\left(C_{ij} - O_{ij}\right)^2} \qquad [3.4]$$

where

C_{ij} = calculated values

3.5.2 CEB mean square method

The CEB-mean square error method, expresses the accuracy of a model as a measure of the magnitude of the difference between the calculated and observed values relative to the observed values. This is elucidated in the set of formulae from equations 3.5 to 3.7 below

$$F_{CEB} = \sqrt{\frac{1}{N}\sum_{J=1}^{N} F_j} \qquad [3.5]$$

with F_{CEB} = mean square error in %

and $F_j = \sqrt{\frac{1}{n-1}\sum_{i=1}^{n} f_{ij}^2}$ [3.6]

where

f_{ij} = percentage difference between calculated and observed value *i* in data set *j* , defined in 3.7.

$$f_{ij} = \frac{C_{ij} - O_{ij}}{O_{ij}} \times 100 \qquad [3.7]$$

CHAPTER 4
PREDICTION MODELS

4.1 Introduction

A creep/shrinkage prediction model is a set of equations aimed at predicting the creep/shrinkage of a structural element, while incorporating various parameters to represent physical mechanisms. These models are generally contained in a chapter of a code of practice and that is where they obtain their name from. For example, a prediction model in the EN 1992-1-1:2004 is consequently called the EN 1992-1-1:2004 prediction model. However not all models studied in this thesis have been incorporated in standards or codes of practice. Some have been proposed in scientific literature, for instance the GL 2000 prediction model.

The following is a summary of the models investigated in this project.

4.2 GL 2000

The GL 2000 model was developed by the Gardner and Lockman in 2001, and it is a modification of an earlier model, the GZ model, proposed by the Gardner and Zau in 1993. Contrary to some models analysed in this project, this model only requires the input parameters that are available to the engineer at the time of design, and therefore it was selected as basis to investigate the accuracy of these two types of models. This is thoroughly explained in section 3.4.1.

4.2.1 Shrinkage *(according to GL 2000)*

The model is formulated as follows.

$$\varepsilon_{csh}(t) = \varepsilon_{shu}\beta_{RH}\beta(t) \qquad \text{[Micro strains]} \qquad [4.1]$$

where

β_{RH} = correction term to account for humidity effects

ε_{shu} = ultimate shrinkage strains

$\beta(t)$= correction term to account for curing time and volume to surface ratio

These are defined as

$$\beta_{RH} = \left(1 - 1.18RH^{4}\right) \qquad [4.2]$$

$$\varepsilon_{shu} = \varepsilon_{shu} = 1000 \cdot K \cdot \left(\frac{30}{f_{cm28}}\right)^{1/2} \cdot 10^{-6} \qquad [4.3]$$

$$\beta(t) = \left(\frac{t - t_c}{t - t_c + 0.15 \cdot (V/S)^2}\right)^{0.5} \qquad [4.4]$$

and

RH = humidity expressed as a decimal;

t = age of concrete, days

t_c = curing time

K = 1 for Type I cement according to ASTM C150

K = 0.70 for Type II cement according to ASTM C150

K = 1.15 for Type III cement according to ASTM C150

V/S = volume-surface ratio, mm

f_{cm28} =concrete mean compressive strength at 28 days, MPa

The GL 2000 uses the following ASTM C150 cement classification:

Type I – For use when the special properties specified for any type are not required.

Type II – For general use, more especially when moderate sulphate resistance or moderate heat of hydration is desired.

Type III – For use when high early strength is desired.

4.2.2 Creep *(according to GL 2000)*

The specific creep development in time, $\varepsilon_{csp}(t)$, is defined as follows:

$$\varepsilon_{csp}(t) = \frac{\phi(t,t_0)}{E_{cm28}} \qquad \text{[Micro strains/ MPa]} \qquad [4.5]$$

where

$\phi(t,t_0)$ = creep coefficient

E_{cm28} = modulus of elasticity at 28 days, MPa

In cases where the modulus of elasticity at 28 days is not known it may be predicted through equation 4.6.

$$E_{cm}(t) = 3500 + 4300\sqrt{f_{cm28}\frac{t^{3/4}}{a + bt^{3/4}}} \qquad [4.6]$$

where

$E_{cm}(t)$ = Elastic modulus at different concrete ages, MPa

f_{cm28} = mean compressive strength at the age of 28 days (cylinder strength), MPa

$a \& b$ = constants that accounts for different cement types as follows:

Type I cement concretes, a= 2.8 and b=0.77

Type II cement concretes, a=3.4 and b=0.72

Type III cement concretes, a=1.0 and b=0.92

With cement types according to ASTM C150 standard

$\phi(t,t_0)$ is computed using equations 4.7 and 4.8.

[4.7]

$$\phi(t,t_0) = \phi_{(t_c)}\left[2\left(\frac{(t-t_0)^{0.3}}{(t-t_0)^{0.3}+14}\right) + \left(\frac{7}{t_0}\right)^{0.5}\left(\frac{t-t_0}{t-t_0+7}\right)^{0.5} + 2.5\left(1-1.086RH^2\right)\left(\frac{t-t_0}{t-t_0+0.15\left(\frac{V}{S}\right)^2}\right)^{0.5}\right]$$

with $\phi_{(t_c)}$ = correction factor to account for drying before loading

Here, t_0 is regarded as the concrete age of loading. If $t_0 = t_c \Rightarrow \phi_{(t_c)} = 1$. However, equation 4.8 applies in cases where $t_0 > t_c$.

$$\phi_{(t_c)} = \left[1 - \left(\frac{t_0 - t_c}{t_0 - t_c + 0.15\left(\frac{V}{S}\right)^2}\right)^{0.5}\right]^{0.5} \qquad [4.8]$$

4.3 CEB-FIP 1990

The total strains at time t of a concrete member is given by:

$$\begin{aligned} &\varepsilon_c(t) = \varepsilon_{ci}(t_0) + \varepsilon_{cc}(t) + \varepsilon_{csh}(t) + \varepsilon_{cT}(t) \\ &\therefore \varepsilon_c(t) = \varepsilon_{c\sigma}(t) + \varepsilon_{cn}(t) \end{aligned} \qquad [4.9]$$

where

$\varepsilon_{ci}(t_0)$ = initial strain at loading

$\varepsilon_{cc}(t)$ = creep strain at time $t > t_o$

$\varepsilon_{csh}(t)$ = shrinkage strain

$\varepsilon_{cT}(t)$ = thermal strain

$\varepsilon_{c\sigma}(t)$ = stress dependent strain ($\varepsilon_{ci}(t_0) + \varepsilon_{cc}(t)$)

$\varepsilon_{cn}(t)$ = stress independent strain ($\varepsilon_{csh}(t) + \varepsilon_{cT}(t)$)

4.3.1 Shrinkage *(according to CEB-FIP 1990)*

The shrinkage strains are given the following set of formulae presented from equation 4.10 to 4.15

$$\varepsilon_{csh}(t) = \varepsilon_{cso}\beta_s(t, t_c) \qquad \text{[Micro strains]} \qquad [4.10]$$

in which:

$$\varepsilon_{cso} = \varepsilon_s\left(f_{cm28}\right)\beta_{RH} \qquad [4.11]$$

and $\varepsilon_s\left(f_{cm28}\right)$ = notional shrinkage coefficient defined as

$$\varepsilon_s\left(f_{cm28}\right)=\left[160+10\beta_{sc}\left(9-\frac{f_{cm28}}{f_{cmo}}\right)\right]\times10^{-6} \qquad [4.12]$$

with

f_{cmo} = 10 MPa

β_{sc} = a constant to take into account the cement type as follows

For slowly hardening cements SL, β_{sc} = 4

For normal or rapid hardening cements N & R, β_{sc} =5

For rapid hardening high strength cements RS, β_{sc} =8

β_{RH} = a constant to take into account the relative humidity of the concrete member

For 40% $\leq$RH (i.e. Relative humidity) < 99%, β_{RH} = -1.55 β_{SRH}

For RH $\geq$99%, β_{RH} = + 0.25

$$\beta_{SRH} = 1-\left(\frac{RH}{RH_0}\right)^3 \text{ with } RH_0 = 100\% \qquad [4.13]$$

with, RH in percentage (%). The last variable of equation 4.10 (i.e. the time function) is defined as

$$\beta_s\left(t,t_c\right)=\left[\frac{\left(t-t_c\right)/t_1}{350\left(\frac{h}{h_0}\right)^2+\left(t-t_c\right)/t_1}\right]^{0.5} \qquad [4.14]$$

with t_1=1 day, ho= 100 mm and $h=\frac{2A_c}{u}$ [4.15]

in which,

A_c is the cross-section and u is the perimeter of the member in contact with the atmosphere, in mm^2 and mm respectively.

4.3.2 Creep *(according to CEB-FIP 1990)*

The specific creep is given as follows:

$$\varepsilon_{csp}(t) = \frac{\phi(t,t_0)}{E_{cm28}} \qquad \text{[Micro strains/ MPa]} \qquad [4.16]$$

In cases where the modulus of elasticity at 28 days is not known it can be predicted as follows:

$$E_{cm28} = 21500\left(\frac{f_{cm28}}{10}\right)^{1/3} \qquad [4.17]$$

The creep coefficient, $\phi(t,t_0)$ is calculated through the formulae presented from equation 4.18 to 4.24

$$\phi(t,t_0) = \phi_0 \beta_c(t,t_0) \qquad [4.18]$$

where

ϕ_0 = notional creep coefficient (defined in equation 4.19)

$\beta_c(t,t_0)$ = the function that takes into account the development of creep with time after loading

$$\phi_0 = \phi_{RH}\beta(f_{cm28})\beta(t_0) \qquad [4.19]$$

where,

$$\phi_{RH} = 1 + \frac{1 - RH/RH_0}{0.46\left(\frac{h}{h_0}\right)^{1/3}} \qquad [4.20]$$

$$\beta(f_{cm28}) = \frac{5.3}{\left(\frac{f_{cm28}}{f_{cm0}}\right)} \quad [4.21]$$

and $$\beta(t_0) = \frac{1}{0.1 + \left(\frac{t_o}{t_1}\right)^{0.2}} \quad [4.22]$$

The development of creep with time after loading, is taking into consideration as follows:

$$\beta_c(t, t_0) = \left[\frac{(t - t_o)/t_1}{\beta_H + (t - t_o)/t_1}\right]^{0.3} \quad [4.23]$$

with $$\beta_H = 150\left\{1 + \left(1.2\frac{RH}{RH_0}\right)^{18}\right\}\frac{h}{h_o} + 250 \le 1500 \quad [4.24]$$

The effect of elevated or reduced temperatures on the maturity of the concrete is taken into account by adjusting the concrete age according to 4.25

$$t_T = \sum_{i=1}^{n} \Delta t_i \exp\left[13.65 - \frac{4000}{273 + T(\Delta t_i)/T_0}\right] \quad [4.25]$$

where

t_T = temperature adjusted concrete age which replaces *t* in the corresponding equations, days

Δt_i = number of days where a temperature T prevails

$T(\Delta t_i)$ = temperature (ºC) during the time period Δt_i

T_0 = 1ºC

In a similar manner, the effect of the type of cement on the creep coefficient is taken into account by modifying the concrete age of loading t_o. This is done according to equation 4.26 below:

$$t_0 = t_{0,T}\left[\frac{9}{2+\left(t_{0,T}/t_{1,T}\right)^{1.2}}+1\right]^{\alpha} \geq 0.5 days$$ [4.26]

where,

$t_{0,T}$ = the concrete loading age adjusted according to equation 4.25 above, days

$t_{1,T}$ = 1 day

α = power which depends on the type of cement

For slowly hardening cements SL, α = - 1

For normal or rapid hardening cements N & R, α =0

For rapid hardening high strength cements RS, α =+ 1

4.4. EN 1992-1-1:2004

4.4.1 Shrinkage *(according to EN 1992-1-1:2004)*

The shrinkage strains are given the following set of formulae presented from equation 4.27 to 4.34

$$\varepsilon_{ct} = \varepsilon_{csh}(t) + \varepsilon_{ca}$$ [4.27]

In this case:

$\varepsilon_{csh}(t)$ = drying shrinkage and ε_{ca} = Autogenous shrinkage

4.4.2 Drying Shrinkage

The shrinkage model is as follows:

$$\varepsilon_{csh}(t) = \beta_{ds}(t,t_s)\cdot K_h \cdot \varepsilon_{cd,o}$$ [Micro strains] [4.28]

where

K_h = coefficient depending on the notional size h according to table 4.1 below

$\beta_{ds}(t,t_s)$ = function that takes into account time development and effects of geometry of the member.

Table 4.1: Coefficient K_h as a function of h

h	K_h
100	1.0
200	0.85
300	0.75
$\geq$500	0.70

The first variable in equation 4.28 is defined as

$$\beta_{ds}(t,t_s) = \frac{t-t_s}{(t-t_s)+0.04\sqrt{h^3}} \qquad [4.29]$$

The variable $\varepsilon_{cd,o}$ in equation 4.28 can be determined as follows

$$\varepsilon_{cd,o} = 0.85\left[(220+110\cdot\alpha_{ds1})\cdot\exp\left(-\alpha_{ds2}\cdot\frac{f_{cm28}}{f_{cm0}}\right)\right]\times10^{-6}\times\beta_{RH} \qquad [4.30]$$

with

α_{ds1} and α_{ds2} = constants depending on cement type

For class S cement, α_{ds1} = 3, α_{ds2} = 3

For class N cement, α_{ds1} = 4, α_{ds2} = 4

For class R cement, α_{ds1} = 6, α_{ds2} = 6

and $\beta_{RH} = 1.55\left[1-\left(\frac{RH}{RH_0}\right)^3\right]$ [4.31]

4.4.3 Autogenous Shrinkage

The autogenous shrinkage model is defined as follows:

$\varepsilon_{ca} = \beta_{as}(t) \cdot \varepsilon_{ca}(\infty)$ [Micro strains] [4.32]

where

$\varepsilon_{ca}(\infty) = 2.5(f_{ck} - 10) \times 10^{-6}$ [4.33]

and $\beta_{as}(t) = 1 - \exp(-0.2\sqrt{t})$ [4.34]

4.4.4 Creep *(according to EN 1992-1-1:2004)*

It must be noted that some of the equations presented in this section have been presented before in section 4.2.2 creep of CEB-FIP 1990, but are repeated here for convenience.

The specific creep is defined as

$\varepsilon_{csp}(t) = \dfrac{\phi(t,t_0)}{E_c}$ [Micro strains/ MPa]] [4.35]

with

$E_c = 1.05E_{cm28}$ [4.36]

The creep coefficient, $\phi(t,t_0)$, can be calculated from the formulae presented from equation 4.37 to 4.46.

$\phi(t,t_0) = \phi_0 \beta_c(t,t_0)$ [4.18 repeated as 4.37]

where

ϕ_0 = notional creep coefficient (defined in equation 4.38)

$\beta_c(t,t_0)$ = the function that takes into account the development of creep with time after loading

$\phi_0 = \phi_{RH}\beta(f_{cm28})\beta(t_0)$ [4.19 repeated as 4.38] where,

$$\phi_{RH}=\begin{cases} 1+\left(\dfrac{1-RH/100}{0.1\times\sqrt[3]{h}}\right) \quad for \;\; f_{cm28}\leq 35MPa \\ \left[1+\left(\dfrac{1-RH/100}{0.1\times\sqrt[3]{h}}\right)\times\alpha_1\right]\times\alpha_2 \quad for \;\; f_{cm28}>35MPa \end{cases}$$ [4.39a and 4.39b respectively]

The values of α_1 and α_2 are defined as follows:

$$\alpha_1=\left(\frac{35}{f_{cm28}}\right)^{0.7}$$ [4.40]

and $$\alpha_2=\left(\frac{35}{f_{cm28}}\right)^{0.2}$$ [4.41]

Note also that:

$$\beta(f_{cm28})=\frac{16.8}{\sqrt{f_{cm28}}}$$ [4.42]

and $$\beta(t_0)=\frac{1}{0.1+(t_o)^{0.2}}$$ [4.43]

The development of creep with time after loading, is taking into consideration as follows:

$$\beta_c(t,t_0)=\left[\frac{(t-t_o)}{\beta_H+t-t_o}\right]^{0.3}$$ [4.44]

with

$$\beta_H=\begin{cases} 1.5\left[1+(0.012RH)^{18}\right]h+250\leq 1500 \quad for \;\; f_{cm}\leq 35MPa \\ 1.5\left[1+(0.012RH)^{18}\right]h+250\alpha_3\leq 1500\alpha_3 \quad for \;\; f_{cm}>35MPa \end{cases}$$

[4.45a and 4.45b respectively]

and $\alpha_3 = \left(\frac{35}{f_{cm28}}\right)^{0.5}$ [4.46]

The effect of elevated or reduced temperatures within the range 0-80 ºC on the maturity of the concrete is taken into account by adjusting the concrete age according to 4.47

$$t_T = \sum_{i=1}^{n} e^{-(4000/[273+T(\Delta t_i)-13.65])} \times \Delta t_i \qquad [4.47]$$

where

t_T = temperature adjusted concrete age which replaces *t* in the corresponding equations, days

Δt_i = number of days where a temperature T prevails

$T(\Delta t_i)$ = temperature (ºC) during the time period Δt_i

In a similar manner, the effect of the type of cement on the creep coefficient is taken into account by modifying the concrete age of loading t_o. This is done according to equation 4.48 below:

$$t_0 = t_{0,T}\left[\frac{9}{2+(t_{0,T})^{1.2}}+1\right]^{\alpha} \geq 0.5 days \qquad [4.48]$$

α = power which depends on the type of cement

For slowly hardening cements SL, α = - 1

For normal or rapid hardening cements N & R, α =0

For rapid hardening high strength cements RS, α =+ 1

4.5 ACI 209 R-92

This model makes provision for moist and steam cured concretes. However, the concrete represented by the experimental data analyzed in this project have been moist cured as reported in chapter 3, therefore the formulae related to steam cured concretes are not listed below for they are not used in this project.

4.5.1 Shrinkage *(according to ACI 209 R-92)*

The shrinkage strains are given by the following set of formulae presented from equation 4.49 to 4.58

$$\varepsilon_{cs} = \frac{(t-t_c)^{\alpha 4}}{f+(t-t_c)^{\alpha 4}} \times \varepsilon_{shu} \qquad \text{[Micro strains]} \qquad [4.49]$$

where $\alpha_4 = 1$ and

For 7 days moist cured concrete, f = 35 days

For other curing periods $f = 26e^{1.42\times 10^{-2}\times(V/S)}$,days [4.50]

The ultimate shrinkage, ε_{shu} , is given by equation 4.51 below

$$\varepsilon_{shu} = 780\times 10^{-6}\times \gamma_{sh} \qquad \text{[Microstrains]} \qquad [4.51]$$

where γ_{sh} represents the product of applicable correction factors.

$$\gamma_{sh} = \gamma_{tc,sh}\times\gamma_{RH,sh}\times\gamma_{s,sh}\times\gamma_{\psi,sh}\times\gamma_{c,sh}\times\gamma_{\alpha a,sh}\times\gamma_{v/s,sh} \qquad [4.52]$$

The ultimate shrinkage corrections factors represented in equation 4.52 are:

Curing time correction factor

$$\gamma_{tc,sh} = 1.202 - 0.2337\log(t_c)$$ [4.53]

Relative humidity correction factor

$$For\begin{cases} RH = 40\%, \gamma_{RH,sh} = 1 \\ 40\% \leq RH \leq 80\%, \gamma_{RH,sh} = 1.4 - 0.0102\lambda \\ 80\% > RH \leq 100\%, \gamma_{RH,sh} = 3 - 0.030\lambda \end{cases}$$ [4.54a; 4.54b and 4.54c respectively]

Slump correction factor

$$\gamma_{s,sh} = 0.89 + 0.00161s$$ [4.55]

s = concrete slump, mm

Fine Aggregate percentage correction factor

$$\gamma_{\psi,sh} = \begin{cases} 0.3 + 0.014\psi, \ for \ \psi \leq 50\% \\ 0.9 + 0.002\psi, \ for \ \psi > 50\% \end{cases}$$ [4.56 a and 4.56 b respectively]

ψ = fine aggregate percentage

Cement content correction factor

$$\gamma_{c,sh} = 0.75 + 0.00061c$$ [4.57]

c= cement content, kg/m^3

Air content correction factor

$$\gamma_{\alpha a,sh} = 0.95 + 0.008\alpha_a$$ [4.58]

α_a = Air content in percentage of total volume

V/S correction factor

$$\gamma_{v/s,sh} = 1.2\exp(-0.00472 \times v/s)$$ [4.59]

4.5.2 Creep *(according to ACI 209 R-92)*

The compliance function that represents the total stress dependent strain caused by a unit stress is given as follows

$$J(t,t_0) = \frac{1+\phi(t,t_0)}{E_{cmto}}$$ [Microstrains/ MPa] [4.60]

where

E_{cmto} = modulus of elasticity at the time of loading given in equation 4.61 below, MPa

$$E_{cmto} = 0.043 U_w^{\ 1.5} \sqrt{\frac{t}{a+b} \times f_{cm28}}$$ [4.61]

with U_w = unit weight of concrete and constants "a" and "b" defined as in Table 4.2, kg/m^3

Table 4.2: values of constant a and b to b used in equation [4.61]

Type of cement	Moist cured concrete		Steam cured concrete	
	a	b	a	b
I (1)	4.0	0.85	1.0	0.95
III (3)	2.3	0.92	0.7	0.98

The creep coefficient, $\phi(t,t_0)$, is defined from equation 4.62 to 4 71 that follow.

$$\phi(t,t_0) = \frac{(t-t_0)^{\psi 1}}{d+(t-t_0)^{\psi 2}} \times \phi_u$$ [4.62]

where

$\psi 1$= 0.6 and d=10 days loading ages equal to 7 days for moist curing

and $\psi 1$=1.0 and $d = 26e^{1.42\times10^{-2}\times(V/S)}$ [4.63] for loading ages other than 7 days for moist cured

The ultimate creep coefficient ϕ_u is defined as follows

$$\phi_u = 2.35 \times \gamma_c \qquad [4.64]$$

where γ_c represents the product of applicable correction factors.

$$\gamma_c = \gamma_{to,c} \times \gamma_{\lambda,c} \times \gamma_{s,c} \times \gamma_{\psi,c} \times \gamma_{\alpha a,c} \times \gamma_{v/s,c} \qquad [4.65]$$

The ultimate shrinkage corrections factors represented in equation 4.65 are:

Loading age correction factor

$$\gamma_{to,c} = 1.25 t_0^{-0.118} \qquad \text{[4.66a and 4.66b respectively]}$$

Relative humidity correction factor

$$\gamma_{RH,c} = 1.27 - 0.0067 RH \qquad [4.67]$$

Slump correction factor

$$\gamma_{s,c} = 0.82 + 0.00264 s \qquad [4.68]$$

Fine aggregate percentage correction factor

$$\gamma_{\psi,c} = 0.88 + 0.0024 \psi \qquad [4.69]$$

Air content correction factor

$$\gamma_{\alpha a,c} = 0.46 + 0.09\alpha_a \geq 1 \qquad [4.70]$$

V/S correction factor

$$\gamma_{v/s,c} = \frac{2}{3}\left[1 + 1.13\exp(-0.0213 \times v/s)\right] \qquad [4.71]$$

4.6 RILEM B3 Model

4.6.1 Shrinkage *(according to RILEM B3 Model)*

The shrinkage strains are given by set of formulae presented from equation 4.72 to 4.80

$$\varepsilon_{csh}(t) = -\varepsilon_{shu} k_{RH} S(t, t_c) \quad \text{[Micro strains]} \qquad [4.72]$$

where

k_{RH} = constant to account for humidity effects

$S(t, t_c)$= shrinkage development with time

The ultimate shrinkage strain, ε_{shu}, is defined as

$$\varepsilon_{shu} = \varepsilon_{s\infty} \times \frac{E(7 + 600)}{E(t_c + \tau_{sh})} \quad \text{[Micro strains]} \qquad [4.73]$$

In which

$\varepsilon_{s\infty}$ = constant given in equation 4.78

$\frac{E(7 + 600)}{E(t_c + \tau_{sh})}$ = Ratio to account for the time dependence of the ultimate shrinkage

τ_{sh} = shrinkage half-time

$$\tau_{sh} = k_t (k_s D) \qquad [4.74]$$

where $D = 2 \times V / S$ [4.75]

$k_t = 190.8 t_c^{-0.08} \left(f_{cm28} \right)^{-0.25}$ [4.76]

and k_s = 1 for an infinite long slab

1.15 for an infinite long cylinder

1.25 for an infinite long square prism

1.30 for a sphere

1.55 for a cube

The constants $E(7+600)$ and $E(t_c + \tau_{sh})$ of equation 4.72 may be computed through the RILEM B3 model's equation to compute the Elastic modulus at different concrete ages. This is shown in equation 4.77 below.

$$E_{cm}(t) = E_{cm28} \sqrt{\frac{t}{(4 + 0.85t)}} \quad [4.77]$$

$$\varepsilon_{s\infty} = \alpha_5 \alpha_6 \left[0.091 w^{2.1} \left(f_{cm28} \right)^{-0.28} + 270 \right] \times 10^{-6} \quad [4.78]$$

w= water content, kg / m^3

α_5 = constant to account for cement type effects

For type I cement, α_5 = 1.00

For type II cement, α_5 = 0.85

For type III cement, α_5 =1.10

With cement types according to ASTM C150 standard

α_6 = constant to account for curing conditions

For steam cured specimens, α_6 = 0.75

For specimens cured in water or at 100% RH, α_6 = 1.00

For specimens sealed during curing, α_6 =1.20

The humidity effects, are taken into consideration through k_{RH}, defined as:

$$k_{RH} = \begin{cases} 1 - RH^3 & for\ RH \le 0.98 \\ -0.2 & for\ RH = 1\ (swelling\ in\ water) \end{cases}$$ [4.79a and 4.79b respectively]

Apply, linear interpolation for $0.98 \le RH \le 1$

The development of shrinkage with time, $S(t, t_c)$, is defined as follows:

$$S(t, t_c) = \tanh\left(\frac{t - t_c}{\tau_{sh}}\right)^{1/2}$$ [4.80]

4.6.2 Creep *(according to RILEM B3 Model)*

In accordance with the RILEM B3 Model, the average compliance function caused by a unit stress, incorporating instantaneous, basic and drying creep is

$$J(t, t_0) = q_1 + C_0(t, t_0) + C_d(t, t_0, t_c)$$ [Micro strains/ MPa] [4.81]

where

q_1= instantaneous strain due to unit stress defined in equation 4.82

$C_0(t, t_0)$= compliance function for basic creep defined in equation 4.84

$C_d(t, t_0, t_c)$= additional compliance function due to simultaneous drying (i.e. additional compliance function for drying creep) defined in equation 4.93

$$q_1 = \frac{0.6}{E_{cm28}}$$ [4.82]

with $E_{cm28} = 4734\sqrt{f_{cm28}}$ [4.83]

$$C_0(t, t_0) = q_2 Q(t, t_0) + q_3 \ln\left[1 + (t - t_0)^n\right] + q_4 \ln\left(\frac{t}{t_0}\right)$$ [4.84]

where

$q_2 Q(t,t_0)$= aging viscoelastic term

$q_3 \ln\left[1+(t-t_0)^n\right]$= non-aging viscoelastic term

$q_4 \ln\left(\frac{t}{t_0}\right)$= aging flow term

$Q(t,t_0)$= binomial integral term

$$q_2 = 1.2783 c^{0.5} \left(f_{cm28}\right)^{-0.9} \qquad [4.85]$$

$$Q(t,t_0) = Q_f(t_0)\left[1+\left(\frac{Q_f(t_0)}{Z(t,t_0)}\right)^{r(t_0)}\right]^{-1/r(t_0)} \qquad [4.86]$$

The following equations may be used to compute the binomial integral shown in equation 4.86.

$$Q_f(t_0) = \left[0.086(t_0)^{2/9} + 1.21(t_0)^{4/9}\right]^{-1} \qquad [4.87]$$

$$r(t_0) = 1.7(t_0)^{0.12} + 8 \qquad [4.88]$$

$$Z(t,t_0) = (t_0)^{-m} \ln\left[1+(t-t_0)^n\right] \qquad [4.89]$$

where

m=0.5 and n=0.1. These are empirical parameters with values taken as the same for all normal concretes.

$$q_3 = 0.29(w/c)^4 \times q_2 \qquad [4.90]$$

w/c = water content/cement content (i.e. water-cement ratio)

$$q_4 = 20.3\times10^{-6} \times (a/c)^{-0.7} \qquad [4.91]$$

a/c = aggregate-cement ratio by mass

$$C_d(t,t_0,t_c) = q_5\left[\exp\{-8H(t)\} - \exp\{-8H(t_0)\}\right]^{1/2} \quad for \;\; t_0 \geq t_c \qquad [4.92]$$

where

q_5 = constant given by equation 4.93

$H(t)$ *and* $H(t_0)$ are spatial averages of pore relative humidity defined by equation 4.94 and 4.95 respectively

$$q_5 = 7.57\times10^5\left(f_{cm28}\right)^{-1}\varepsilon_{shu}^{-0.6} \qquad [4.93]$$

with ε_{shu} as defined by equation 4.72 above

$$H(t) = 1-(1-RH)S(t,t_c) \qquad [4.94]$$

Given that $S(t,t_c)$ is defined by equation 4.79 above

$$H(t_0) = 1-(1-RH)S(t_0,t_c) \qquad [4.95]$$

where

$$S(t_0,t_c) = \tanh\left(\frac{t_0-t_c}{\tau_{sh}}\right)^{1/2} \qquad [4.96]$$

And τ_{sh} is given in equation 4.73

4.7 SABS 0100-1 Adjusted

4.7.1 Shrinkage *(according to SABS 0100-1)*

The original SABS 0100-1 shrinkage model predicts the 6th month and 30th year shrinkage, based on the exposed ambient relative humidity and effective section thickness. The two parameters are used to read the shrinkage value off figure 4.1.

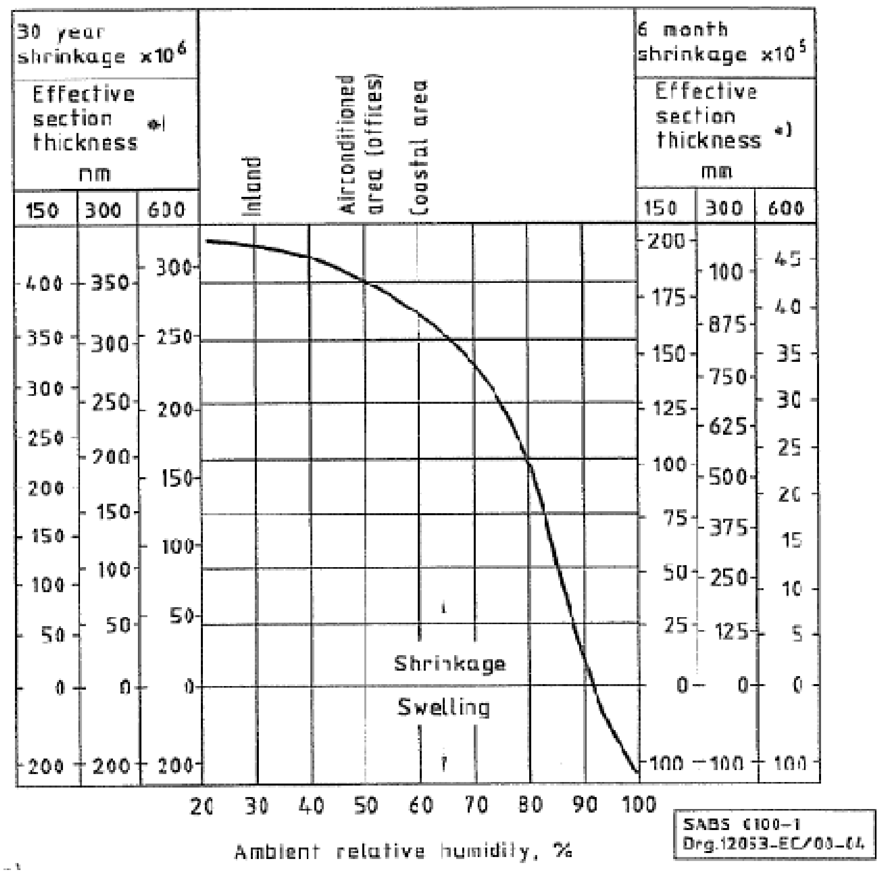

Figure 4.1: Drying shrinkage of normal-density concrete (Source: SABS 0100-1).

This approach does not provide the shrinkage values over a period of time, hence it cannot be properly compared to the experimental data which is an evolution of shrinkage with time. Modifications or Adjustments to the shrinkage model of the SABS 0100-1 to provide shrinkage evolution with time were not found in the literature, therefore this shrinkage model was not used in this project.

4.7.2 Creep *(according to SABS 0100-1 adjusted)*

The original SABS 0100-1 creep model uses a figure (see figure 4.2) to determine the creep strains as it was done in the shrinkage model; and in this model only the 30 year creep strain is obtainable. However, an adjustment to the SABS 0100-1 model to calculate the creep evolution with time has been proposed through the work of Fanourakis and Ballim (2006) and is presented in this project. The adjustment is a fitted continuous creep time curve, based on the given creep percentages reached after 1,6 and 30 months respectively. This does not solve the problem of automation (as reading off table 4.2 to determine the 30 year creep factor is still required) but it enables comparison with the acquired experimental data and performance comparison with other models. Also, the alteration does not change the model principles, it only presents the means to which the strains can be calculated over time.

The adjusted SABS 0100-1 model is formulated as follows:

$$\varepsilon_{csp}(t) = \frac{\phi_{30}}{E_{cmto}}\left[0.0258 \times (t - t_0) + 0.0286\right] \qquad [4.97]$$

where

ϕ_{30} - 30 year creep factor, obtainable from figure 4.2

and $E_{cmto} = E_{cm28}\left(0.4 + 0.6\dfrac{f_{cukt}}{f_{cuk28}}\right)$ [4.98]

with

f_{cukt} - characteristic cube compressive strength at different concrete ages

f_{cuk28} - characteristic cube compressive strength at the age of 28 days

In cases where the modulus of elasticity at 28 days is not known it can be obtained from table 4.3 or equation 4.99, and f_{cukt} may be obtained from table 4.4. Multi-linear functions (Excel interpolation) are used to digitise the information on table 4.4 during the programming phase.

Table 4.3: E_{cm28} as a function of f_{cuk28}

f_{cuk28}	20	25	30	40	50	60
E_{cm28}	25	26	28	31	34	36

$$E_{cm28} = K_0 + 0.2 f_{cuk28} \qquad [4.99]$$

Where

K_0 = a constant closely related to the modulus of the aggregate (taken as 20 KN/mm^2 for normal-density concrete).

Table 4.4: Characteristic cube compressive strength at different concrete ages

f_{cuk28}	20	25	30	35	40	45	50
3 months	23	29	34	39	44	49	54
6 months	24	30	35	40	46	51	56
12 months	25	31	36	42	48	53	58

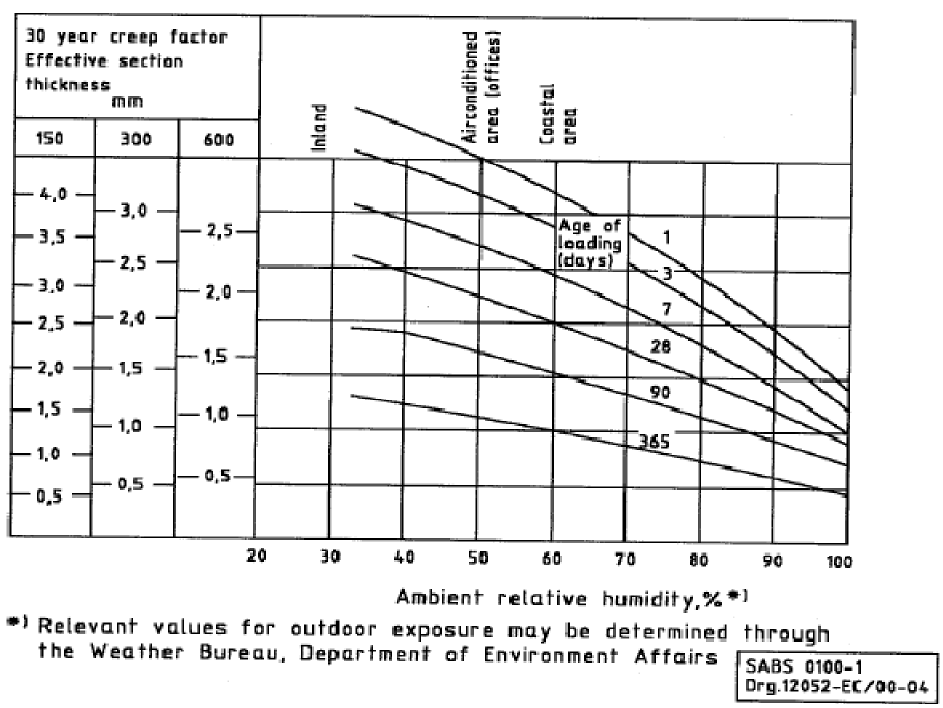

Figure 4.2: Effects of relative humidity, age of concrete at loading and section thickness upon creep factor.

4.8 Summary of all models

For each model, the presented formulae have been compiled into a general equation (wherever possible) and presented in table 4.5 (for shrinkage) and 4.6 (for creep).

Table 4.5: General equations of the shrinkage models, [Micro strains]

GL 2000	$\varepsilon_{sch}(t)=\left(\frac{t-t_c}{t-t_c+0.15(V/S)^2}\right)^{0.5}\times\left(1-1.18RH^4\right)\times 1000K\left(\frac{30}{f_{cm28}}\right)^{0.5}\times 10^{-6}$ [4.100]
CEB-FIP 1990	$\varepsilon_{csh}(t)=\left[\frac{(t-t_c)}{350\left(\frac{h^1}{100}\right)^2+(t-t_c)}\right]^{0.5}\times(-1.55)\times\left[1-\left(\frac{RH}{100}\right)^3\right]\times\left[160+90\beta_{sc}-\frac{10\beta_{sc}f_{cm28}}{10}\right]\times 10^{-6}$ [4.101] where $t_T=\sum_{i=1}^{n}\Delta t_i\exp\left[13.65-\left(4000/\{273+T(\Delta t_i)\}\right)\right]$ replaces "t" to account for temperature effect (OPTIONAL) [same as 4.26 or 4.47]

EN 1992: 2004-1-1	$$\varepsilon_{csh}(t)=\left[\frac{t-t_c}{400\left(\frac{h^{3/4}}{100}\right)^2+(t-t_c)}\right]^1\times(1.55)\times\left[1-\left(\frac{RH}{100}\right)^3\right]\times(220+110\alpha_{ds1})\times\exp\left(-\alpha_{ds2}\frac{f_{cm28}}{10}\right)\times0.85\times K_h\times10^{-6}$$ [4.102] where $t_T=\sum_{i=1}^{n}\Delta t_i\exp[13.65-(4000/\{273+T(\Delta t_i)\})]$ replaces "t" to account for temperature effect (OPTIONAL) [same as 4.26 or 4.47]
ACI 209 R -92	$$\varepsilon_{csh}(t)=\left[\frac{(t-t_c)^{\alpha4}}{f+(t-t_c)^{\alpha4}}\right]\times780\times10^{-6}\times(1.202-0.2337\log(t_c))\times\gamma_{RH,sh}\times(0.89+0.00161s)\times\gamma_{\psi,sh}\times(0.75+0.00061c)\times$$ $$(0.95+0.008\alpha_a)\times(1.2\exp(-0.00472(V/S)))$$ [4.103]
RILEM B3 model	$$\varepsilon_{csh}(t)=\alpha_5\alpha_6\left[0.091w^{2.1}(f_{cm28})^{-0.28}+270\right]\times10^{-6}\times\frac{E_{cm28}\left[\frac{7+600}{4+0.85\times(7+600)}\right]^{0.5}}{E_{cm28}\left[\frac{t_c+\left[190.8t_c^{-0.08}f_{cm28}^{-0.25}\times K_s\times2(V/S)\right]}{4+0.85\left\{t_c+\left[190.8t_c^{-0.08}f_{cm28}^{-0.25}\times K_s\times2(V/S)\right]\right\}}\right]^{0.5}}\times$$ $$K_h\times\tanh\left(\frac{t-t_c}{190.8t_c^{-0.08}f_{cm28}^{-0.25}\times K_s\times2(V/S)}\right)^{1/2}$$ [4.104]

Table 4.6: General equations of the creep models, [Micro strains / MPa]

GL 2000	$\varepsilon_{csp}(t) = \frac{1}{E_{cm28}} \times \left\{ \left[1 - \left(\frac{t_0 - t_c}{t_0 - t_c + 0.15(V/S)^2} \right)^{0.5} \right]^{0.5} \times \left[2 \times \left(\frac{(t-t_0)^{0.3}}{(t-t_0)^{0.3} + 14} \right) + \left(\frac{7}{t_0} \right)^{0.5} \left(\frac{t - t_0}{t - t_0 + 7} \right)^{0.5} + 2.5\left(1 - 1.086 RH^2\right) \times \left(\frac{t - t_0}{t - t_0 + 0.15(V/S)} \right)^{0.5} \right] \right\}$ [4.105]
CEB-FIP 1990	$\varepsilon_{csp}(t) = \frac{1}{E_{cm28}} \times \left\{ \left[\frac{t - t_0}{\left[1.5\left\{1 + (1.2 \times RH/100)^{18}\right\}h + 250\right] + t - t_0} \right]^{0.3} \times \left[1 + \frac{1 - RH/100}{0.46(h/100)^{1/3}} \right] \times \frac{5.3}{(f_{cm28}/10)^{0.5}} \times \frac{1}{\left(0.1 + t_0^{0.2}\right)} \right\}$ [4.106] where $t = \sum_{i=1}^{n} \Delta t_i \exp\left[13.65 - \left(4000/\left\{273 + T(\Delta t_i)\right\}\right)\right]$ replaces "t" to account for temperature effect (OPTIONAL) [same as 4.26 or 4.47] and $t_0 = \sum_{i=1}^{n} \Delta t_i \exp\left[13.65 - \left(4000/\left\{273 + T(\Delta t_i)\right\}\right)\right] \left(\frac{9}{2 + \left\{ \sum_{i=1}^{n} \Delta t_i \exp\left[13.65 - \left(4000/\left\{273 + T(\Delta t_i)\right\}\right)\right] \right\}^{1.2}} + 1 \right)^{\alpha} \geq 0.5$ replaces "t_o" to account for cement effects (OPTIONAL) [4.107]

EN 1992: 2004-1-1	$$\varepsilon_{csp}(t)=\frac{1}{E_{cm28}}\times\left\{\left[\frac{t-t_0}{\left[1.5\{1+(1.2\times RH/100)^{18}\}h+250\times\alpha_3\right]+t-t_0}\right]^{0.3}\times\left[1+\frac{1-RH/100}{0.46(h/100)^{1/3}}\times\alpha_1\right]\times\alpha_2\times\frac{16}{(f_{cm28}/10)^{0.5}}\times\frac{1}{(0.1+t_0^{0.2})}\right\}$$ [4.108] where $t=\sum_{i=1}^{n}\Delta t_i\exp[13.65-(4000/\{273+T(\Delta t_i)\})]$ replaces "t" to account for temperature effect (OPTIONAL) [same as 4.26 or 4.47] and $t_0=\sum_{i=1}^{n}\Delta t_i\exp[13.65-(4000/\{273+T(\Delta t_i)\})]\left(\frac{9}{2+\left\{\sum_{i=1}^{n}\Delta t_i\exp[13.65-(4000/\{273+T(\Delta t_i)\})]\right\}^{1.2}}+1\right)^{\alpha}\geq 0.5$ replaces "t_o" to account for cement effects (OPTIONAL) [same as 4.107]
ACI 209 R -92	$$J(t,t_0)=\frac{1}{0.043U_w^{1.5}\sqrt{\frac{t}{a+b}\times f_{cm28}}}\times\left\{\left(\frac{(t-t_0)^{\psi 1}}{d+(t-t_0)^{\psi 2}}\right)\times 2.35\times(1.25\times t_0^{-0.118})\times(1.27-0.0067RH)\times(0.82+0.00264s)\times (0.88+0.0024\psi)\times\psi_{\alpha a,c}\times\left(\frac{2}{3}\times[1+1.13\exp(-0.0213\times(V/S))]\right)\right\}$$ [4.109]

RILE M B3 model	$$J(t,t_0)=\frac{0.6}{E_{cm28}}+\left\{1.2783c^{0.5}(f_{cm28})^{-0.9}\times\left[0.086(t_0)^{2/9}+1.21(t_0)^{4/9}\right]^{-1}\times\left[1+\left\{\frac{\left[0.086(t_0)^{2/9}+1.21(t_0)^{4/9}\right]^{-1}}{(t_0)^{-m}\ln\left[1+(t-t_0)^n\right]}\right\}^{[1.7(t_0)^{0.12}]+8}\right]^{\frac{-1}{[1.7(t_0)^{0.12}]+8}}+0.29(w/c)^4\times1.2783c^{0.5}(f_{cm28})^{-0.9}\times\ln\left[1+(t-t_0)^n+20.3\times10^{-6}(a/c)\times\ln\left(\frac{t}{t_0}\right)\right]\right\}+7.57\times10^5(f_{cm28})^{-1}\times\alpha_5\alpha_6\left[0.091w^{2.1}(f_{cm28})^{-0.28}+270\right]\times10^{-6}\times\frac{E_{cm28}\left[\frac{7+600}{4+0.85\times(7+600)}\right]^{0.5}}{E_{cm28}\left[\frac{t_c+\left[190.8t_c^{-0.08}f_{cm28}^{-0.25}\times K_s\times2(V/S)\right]}{4+0.85\left\{t_c+\left[190.8t_c^{-0.08}f_{cm28}^{-0.25}\times K_s\times2(V/S)\right]\right\}}\right]^{0.5}}\times\left[\exp\left\{-8\left[1-(1-RH)\tanh\left(\frac{t-t_c}{190.8t_c^{-0.08}f_{cm28}\times K_s\times2(V/S)}\right)^{0.5}\right]\right\}-\exp\left\{-8\left[1-(1-RH)\tanh\left(\frac{t_0-t_c}{190.8t_c^{-0.08}f_{cm28}\times K_s\times2(V/S)}\right)^{0.5}\right]\right\}\right]$$ [4.110]
SABS 0100-1 mod	$$\varepsilon_{csp}(t)=\frac{\phi_{30}\left[0.0258\times(t-t_0)+0.0286\right]}{(K_0+0.2f_{cuk28})\left(0.4+0.6\frac{f_{cukt}}{f_{cuk28}}\right)}$$ [4.111]

CHAPTER 5
VERIFICATION OF PROGRAMMING and MODEL SCRUTINY

5.1 Verification criteria of model programming

Three different methods are used here to verify the programming of the models and to investigate the integrity of the formulae used by the models in the process.

Method 1: Visual observation of all models for particular sets of data.

Often when a prediction method is wrongly implemented it will plot different results from those which have been properly interpreted and programmed. To apply this method, two different sets of input parameters are introduced into the models to identify a distortion trend. While this method does not provide proof of direct implementation, it may indicate incorrect implementation by indicating differing behaviour.

Method 2: Comparison with a worked example available in literature

This method is implemented by using the same input parameters used by a trusted example available in the literature (i.e. ACI 209.2R-08 guide example) which computed creep and shrinkage results at different times. The results of this worked example are compared to the results of the Excel spreadsheet in which the prediction models were programmed in this research.

Method 3: Observation of model behaviour under single parameter variation

In this last method, the numerical prediction models are subjected to engineering judgement. For a given set of parameters (taken as appropriate for water retaining structures), a single parameter is changed and the observed model behaviour in the graphical representation is compared to the expected behaviour. The above is repeated for different parameters, and observations are made.

These methods take into consideration, a sensitivity analysis (method 1 and 3) as well as a more direct way of assuring quality programming (method 2).

5.1.1 Visual observation of all models for a particular set of data.

The first step of the evaluation of model programming is the observation of the collective behaviour of the models for a particular prediction. For this effect, two different sets of input parameters where chosen and are presented below.

The first set of input parameters was selected to represent concretes of standard properties and composition that are exposed to harsh conditions. This is often the case of water retaining structures constructed in dry environments (hence the low relative humidity) and constructed with a time constraint (thus the minimum curing time, and early loading age). Other factors such as temperature, compressive strength at 28 days, elastic modulus at 28 days, specimen shape and concrete composition are also taken into consideration and are presented in table 5.1. The output graphs computed by the prediction models are also shown in figures 5.1 and 5.2.

Table 5.1: Sets of input parameters

Property	Symbol	Input set 1	Input set 2	Input set of ACI 209.2R-08 Guide	Units
Exposed conditions					
Curing time	t_c	7	28	7	days
Type of curing		Moist cured	Moist cured	Moist cured	
Temperature	t^a	23	25	20	°C
Relative humidity	RH	50	80	70	%
Age of loading	t_o	14	40	14	days
Measured properties					
Compressive strength at 28 days	f_{cm28}	35	45	25	MPa

Elastic modulus at 28 days	E_{cm28}	33	35	To be calculated	GPa
Specimen shape					
Type of specimen		long square prism	long cylinder	Infinite slab	
Volume	V	780300	2000000	--	mm^3
Total surface area	S	66402	100000	--	mm^2
Cross sectional area	Ac	2601	10000	--	mm^2
Perimeter of cross sectional area	u	204	400	--	mm
Effective thickness as 2×Ac/h	h	25.5	50	--	mm
Volume/ surface area	V/S	11.751	20	100	mm
Concrete composition					
Class of cement		N	N	N	
Type of cement		I (1)	I (1)	I (1)	
water content kg/m3	w	189	187	205	kg/m^3
Slump	s	77	83	75	mm
Fine Aggregate percentage	ψ	41	40.5	40	%
Cement content	c	300	290	409	kg/m^3
Sand content		767	753	4.23 (i.e. a/c ratio)	kg/m^3
Stone content		1100	1103		kg/m^3
Aggregate	a	1867	1856		kg/m^3
Air content	α_a	5	2	2	%
Unit weight of concrete	U_w	2500	2500	2345	kg/m^3

To assist in trend detection, the shrinkage and specific creep are shown on normal and logarithmic scale. Additionally, regular time intervals up to 365 days are used, which cover the duration of the longest experimental data set used in this project.

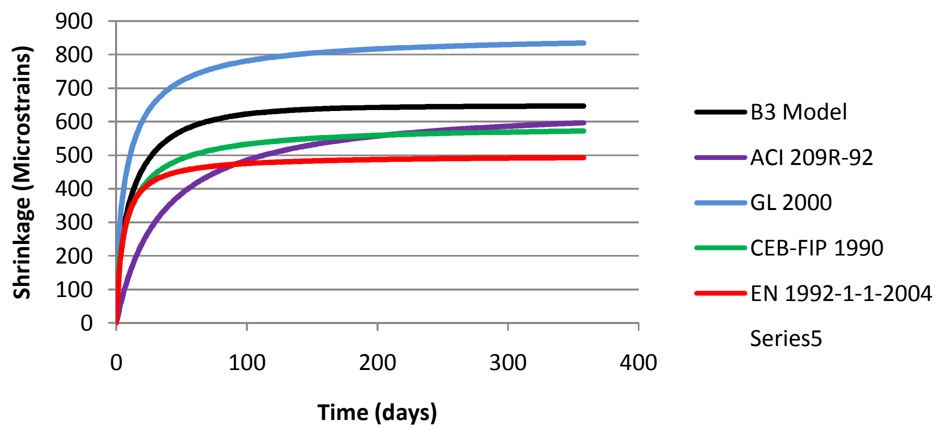

Figure 5.1.a : Calculated shrinkage strains over time for input set number 1

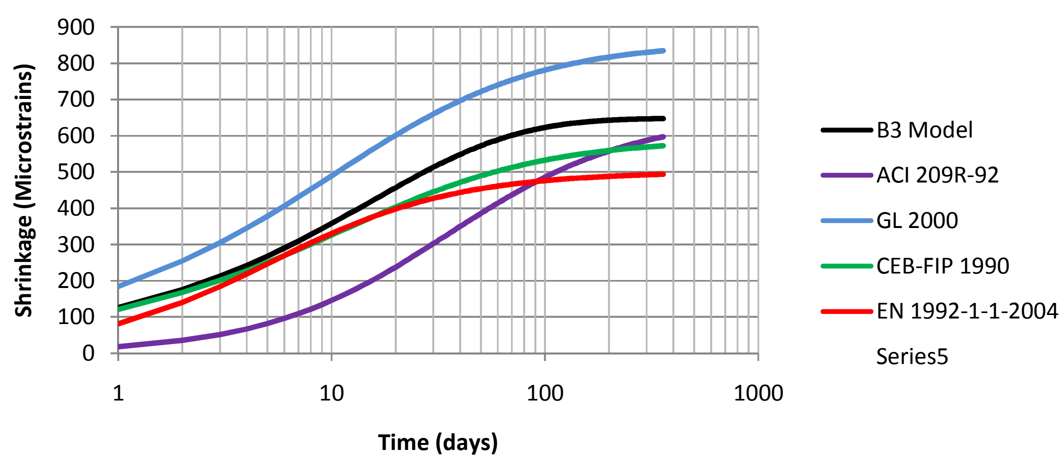

Figure 5.1.b: Calculated shrinkage strains over time (logarithmic-scale) for input set number 1

Figure 5.1 shows that the models calculate significantly different shrinkage strain evolutions, however this does not mean that the model implementations are not correct. In fact, these differences in the predicted behaviours are the reason for scrutiny in this project and chapter. Special attention is directed to the ACI 209 R-92 model that despite the early age discrepancy to the other models, computes long term strain in the same range as other models. Further attention is given to the GL 2000, whose more conservative results may have been expected due to the simplicity of the model as compared to the other models.

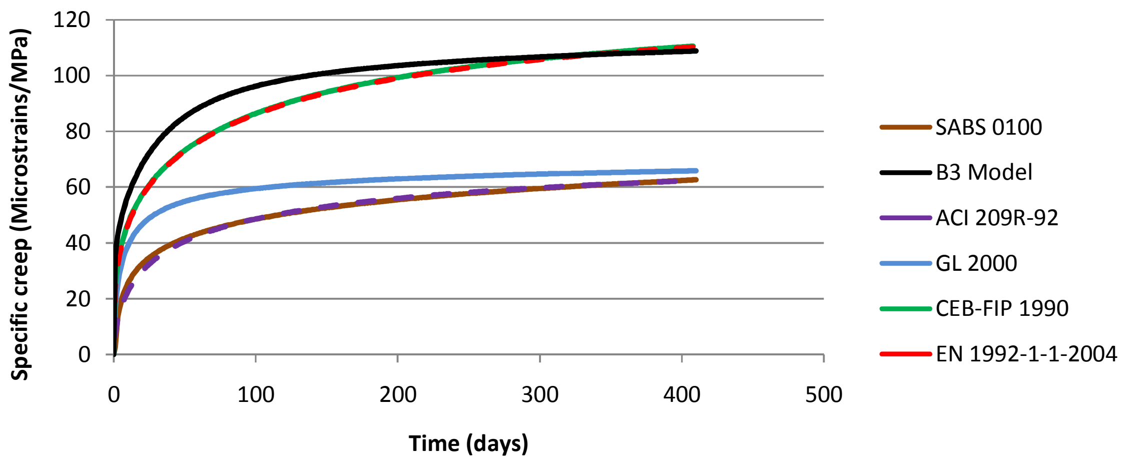

Figure 5.2.a: Calculated Specific creep strains over time for input set 1

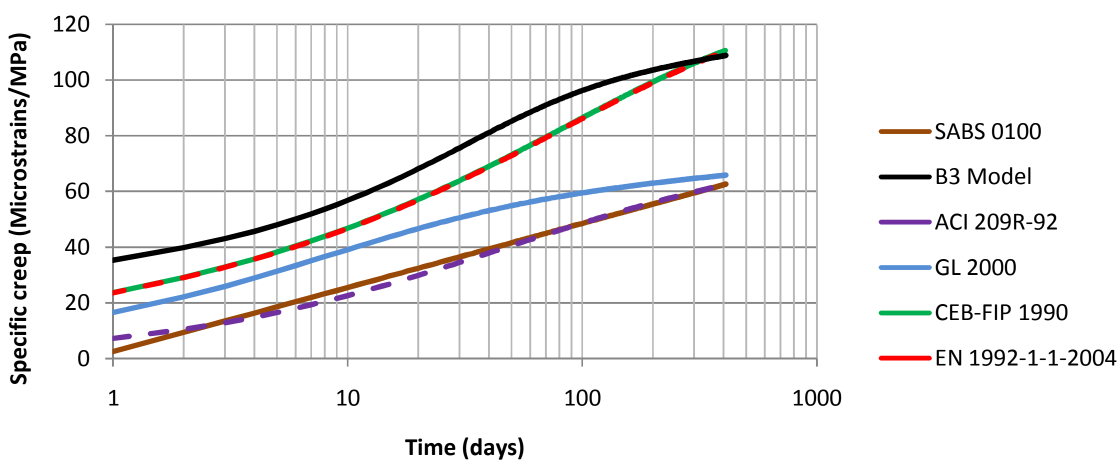

Figure 5.2.b: Calculated specific creep strains over time (logarithmic scale) for input set number 1

Figures 5.2a and 5.2b show that the calculated specific creep strains vary significantly between the models. To obtain some clarity from this evaluation, the models are observed individually in the following paragraphs.

The CEB-FIP 1990 and the EN 1992-1-1:2004 produce identical results for this set of input parameters as a result of the similar approach adopted by the models. This highlights the possibility that the individual models were correctly programmed, but increases the risk of a common mistake during the programming of both models. This uncertainty is to be clarified in the second method of evaluation in the next section.

The ACI 209R-92 model and the GL 2000 calculate lower results of specific creep strains. The ultimate specific creep of both models appears to be in the region of 65 Microstrains/MPa. These similarities between the models may be due to similar approaches in the calculation of specific creep.

The B3 Model and the SABS 0100 model do not have significant similarities to other models. Yet the B3 Model plots a similar curve to the CEB-FIP 1990 and the EN 1994-1-1:2004 whilst the SABS 0100 graph is similar to the ACI 209 R-92 graphical representation. This may indicate that the differences between the models observed in the graphical representation for this particular parameter set were caused by differences in model principle rather than errors in model implementation.

The above process is repeated for a different set of input parameters (i.e. input set 2) to study trends. If the same trends created by input set 1 are found, they may assist to identify and clear implementation errors.

The new set of input parameters shows less extreme exposure conditions. This was simulated by using a concrete that is exposed to mild conditions such as a curing time of 28 days, loading age of 40 days and high relative humidity of 80 %. The concrete composition and properties were also changed from the values introduced in the first set of input parameters to provide an entirely different evaluation. These and other input parameters are shown in table 5.1.

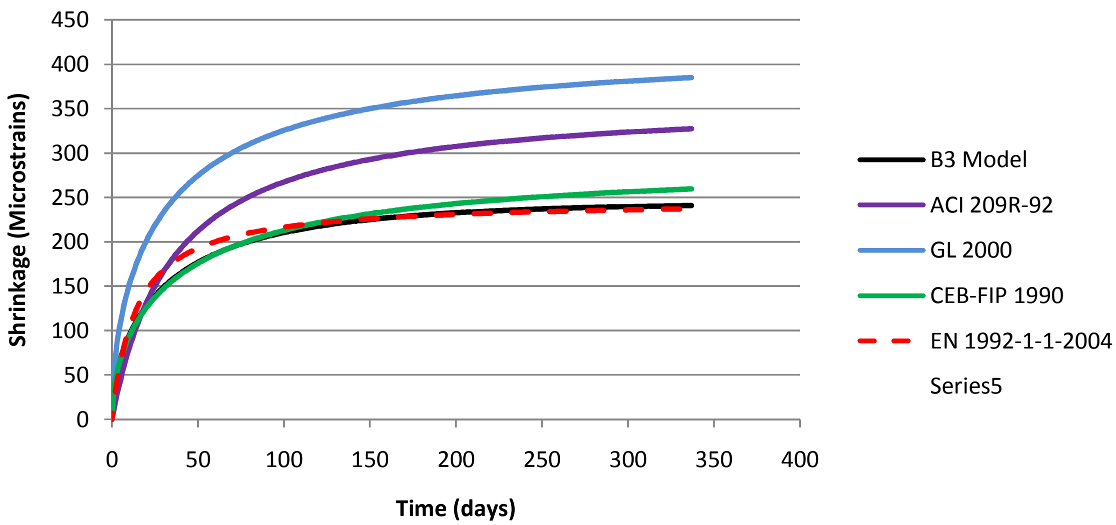

Figure 5.3.a: Calculated shrinkage strains over time for input set number 2

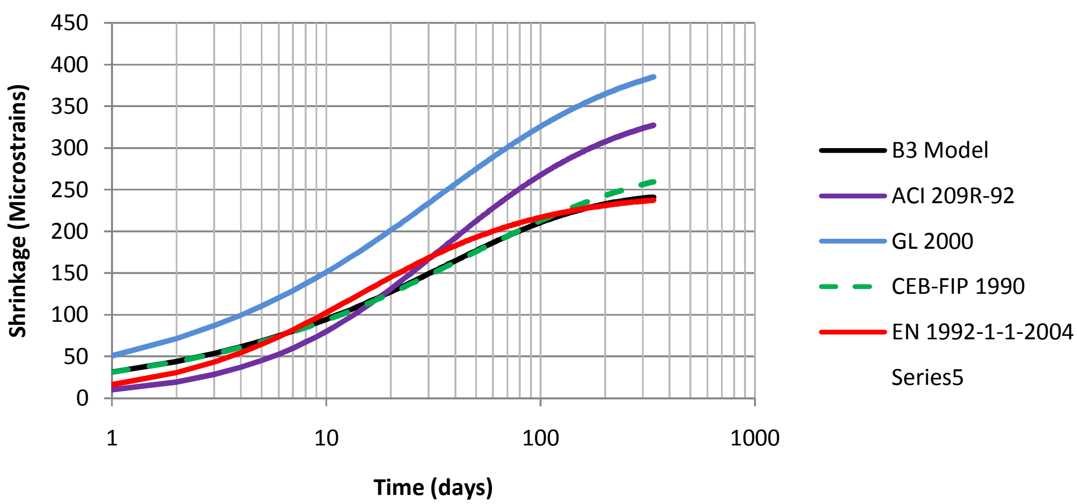

Figure 5.3.b: Calculated shrinkage strains over time for input set number 2

Also for this parameter set, the different approaches of shrinkage prediction used by the models, create a wide range of predicted shrinkage strains. However a general prediction trend can be observed in figure 5.3. This is highlighted by a difference of 150 micro strains between the highest and lowest prediction of input set 2, in a period of approximately one year which is reasonable for shrinkage prediction.

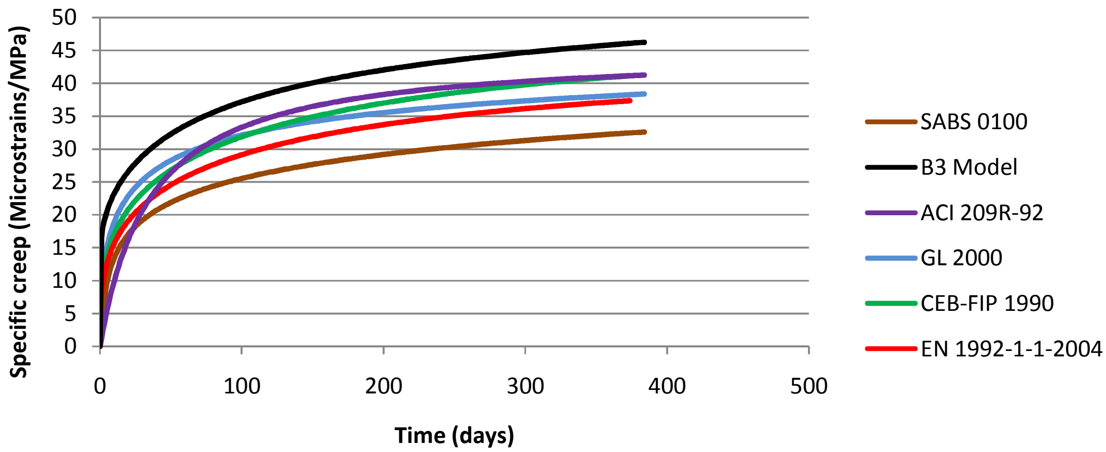

Figure 5.4.a: Calculated specific creep strains over time for input set number 2

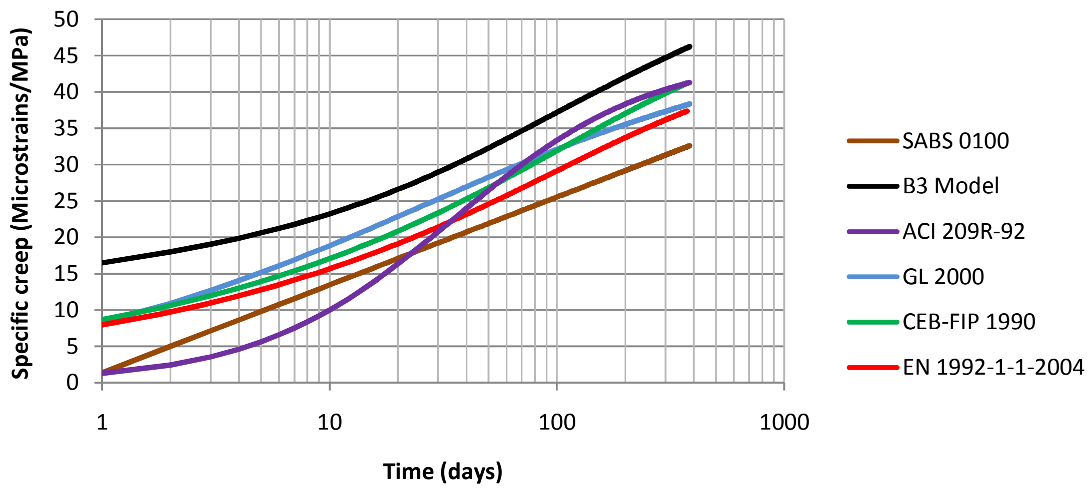

Figure 5.4.b: Calculated specific creep strains over time for input set number 2

Figure 5.4 shows that the calculated specific creep strains for the input set 2 line in a band, although significant differences do exist. As per parameter input set 1, the B3 model calculates the highest specific creep strains for the set of input parameters 2.

In summary, Method 1 produces predictions of significant difference between the models. Also, some trends of comparable predictions can be observed, however the trends are not consistent for the two data sets. Next, a published set of predictions is recalculated to verify model implementations by method 2.

5.1.2 Comparison with worked example in literature

The programming of the models is further verified by direct comparison of numerical results with published values, calculated with the same models and parameters by other researchers. This was achieved by computing (i.e. using the spreadsheet) the creep coefficients and shrinkage strains for a given set of parameters and comparing with the same coefficients and strains obtained in the example of the ACI 209.2R-08, also known as Guide for modelling and calculating shrinkage and creep in hardened concrete.

In this example, the creep coefficients and shrinkage strains of concrete are computed at 14, 28, 60, 90, 180 and 365 days after casting, for the data summarised in table 5.1.

Table 5.2 below shows the published shrinkage strains against the spreadsheet calculated shrinkage strains. The EuroCode model (EN 1992-1-1: 2004) and the British code model (BS 8110, same as SABS 10100) are not computed by the ACI guide example and therefore it is not possible to incorporate in this comparison. The shrinkage strains shown by the ACI guide for the other four models match the shrinkage strains calculated by the current implementation closely.

There are a few small discrepancies. This has been studied and found possibly due to rounding off in the ACI guide example. Indeed, the results would be identical to the decimal degree if the guide had kept all the intermediate values in their longest but more accurate form, as it is done in the programming of the models here.

Table 5.2: Shrinkage (in Micro strains) as computed by the ACI Guide and the programmed model spreadsheet

SHRINKAGE	**GL 2000**		**CEB-FIP 1990**	
Time	*ACI Guide*	*Spreadsheet*	*ACI Guide*	*Spreadsheet*
14	47	47	32	32
28	81	81	55	55
60	128	127	87	87
90	158	158	107	107
180	220	221	150	150
365	297	302	205	204
Comment	Match		Match	
SHRINKAGE	**ACI 209 R-92**		**B3 Model**	
Time	*ACI Guide*	*Spreadsheet*	*ACI Guide*	*Spreadsheet*
14	58	58	39	39
28	131	131	67	67
60	211	211	105	105
90	246	246	131	131
180	291	291	184	185
365	318	318	253	254
Comment	Match		Match	

In the ACI guide example the creep coefficients are calculated and converted to specific creep strains for all the models except for the B3 Model in which the total load related strains (i.e. including elastic strain) are presented as the result of creep calculations. For comparison purposes, the spreadsheet results are adjusted to display the total load related strains for the B3 Model as shown in table 5.3 below.

Table 5.3 shows the comparison between specific creep strains in the ACI guide example and the spreadsheet computed specific creep strains for the same four models as for shrinkage.

It can be observed from the table, that the specific creep strains (and total load related strains) computed by the ACI guide match the spreadsheet computed strains.

The small discrepancies in the strains are due to the same rounding off techniques reported in the shrinkage comparison. This was tested by replacing the rounded intermediate values in the spreadsheet which then produced the exact strains published by the ACI guide.

Table 5.3: Specific creep (in Micro strains) as computed by the ACI Guide and the programmed model spreadsheet

CREEP	**GL 2000**		**CEB-FIP 1990**	
Time	*ACI Guide*	*Spreadsheet*	*ACI Guide*	*Spreadsheet*
14	0	0	0	0
28	33	33	26	25
60	43	42	36	36
90	47	46	41	41
180	55	54	50	49
365	63	62	59	58
Comment	Match		Match	
CREEP	**ACI 209 R-92**		**B3 Model**	
Time	*ACI Guide*	*Spreadsheet*	*ACI Guide*	*Spreadsheet*
14	0	0	22	22
28	16	16	67	67
60	24	24	77	77
90	28	28	82	82
180	33	33	90	90
365	38	38	98	98
Comment	Match		Total load related strain: Match (Micro strains)	

This numerical verification is considered crucial in this evaluation process. Thus, no margin for error was allowed, except for the approximations observed and commented on above. With this in mind and the positive results obtained in this evaluation method, it has been noted that the model formulae for the sub-set of models included here were introduced correctly into the spreadsheet and the models are correctly programmed.

Although it is clear that the formulae have been properly introduced into the Excel spreadsheet, further verification is required. Indeed, it is possible that the programming only works for a particular range of exposure conditions. Therefore, the following method was developed to access whether this mathematical interpretation can replicate the expected engineering behaviour of concrete.

5.1.3 Observation of model behaviour under single parameter variation

A different approach is used to evaluate the correctness of model programming. The method used was to subject the prediction models to a base set of parameters, change one variable of this set at the time and observe the outcome in the models. In this scenario, the misinterpreted models are likely to behave different to the expected outcome. For instance if relative humidity (RH) is changed from 65% to 80%, the models are expected to calculate lower creep or shrinkage strains due to the change; however an incorrectly programmed model may not behave this way.

For the above concept, a third set of parameters shown in table 5.4 was chosen as the basis for this exercise. This set is a compromise between the harsh conditions of input set 1 and the mild conditions of input set 2, with the aim to represent another set of conditions that water retaining structures in South Africa may be exposed to.

Table 5.4: Set of input parameters number 3

Property	**Symbol**	**value**	**Units**
Exposed conditions			
Curing time	t_c	7	days
Type of curing		water cured	
Temperature	tª	25	℃
Relative humidity	RH	65	%
Age of loading	t_o	28	days
Measured properties			
Compressive strength at 28 days	f_{cm28}	45	MPa
Elastic modulus at 28 days	E_{cm28}	35	GPa
Specimen characteristics			

Type of specimen		long square prism	
Volume	V	780300	mm^3
Total surface area	S	66402	mm^2
Cross sectional area	Ac	2601	mm^2
Perimeter of cross sectional area	u	204	mm
Effective thickness as 2×Ac/h	h	25.5	mm
Volume/ surface area	V/S	11.751	
Concrete composition			
Class of cement		N	
Type of cement		I (1)	
water content kg/m3	w	187	kg/m^3
Slump	s	83	mm
Fine Aggregate percentage	ψ	40.5127	%
Cement content	c	290	kg/m^3
Sand content		753	kg/m^3
Stone content		1103	kg/m^3
Aggregate	a	1856	kg/m^3
Air content	α_a	2	%
Unit Weight	U_w	2500	kg/m^3

Whilst keeping the other parameters constant, the following parameters were subjected to change:

Relative humidity (RH): South Africa is a country subjected to a large variety of climate conditions. In regions like the KwaZulu Natal province (e.g. city of Durban) the humidity may reach elevated levels, whilst low humidity levels are observed in the North West Province (e.g. Rustenburg city).

It is also possible to have seasonal and daily variation of humidity in the same region of the country. The Western Cape raining season provides a different range of humidity levels to summer's humidity levels in which the same water retaining structure may be exposed to.

For this reason, it is important to observe whether the models in discussion can correctly adjust the calculated strains when new relative humidity values are introduced. In principle, a strain increase is expected with a decrease of relative humidity and vice-versa.

To simulate these conditions, the relative humidity is decreased from 65% to 50%, and the resulting shrinkage and specific creep strains are noted for a fixed time of 365 days after casting. The results of this variation are presented in figures 5.5 and 5.6.

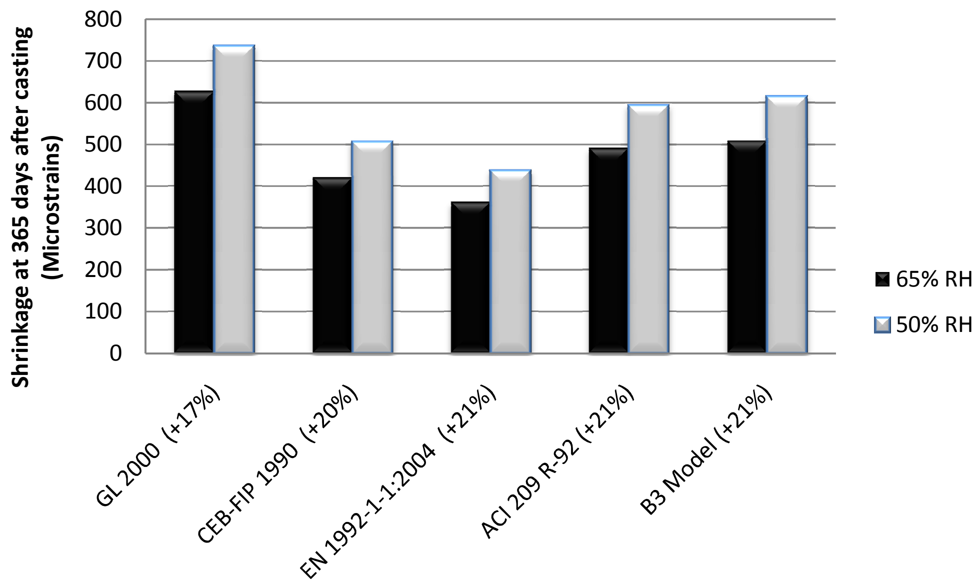

Legend: value in parenthesis indicates direction and percentage of strain change

Figure 5.5: Calculated shrinkage strains (at 365 days after casting) of input set 3 at different Relative humidity (RH)

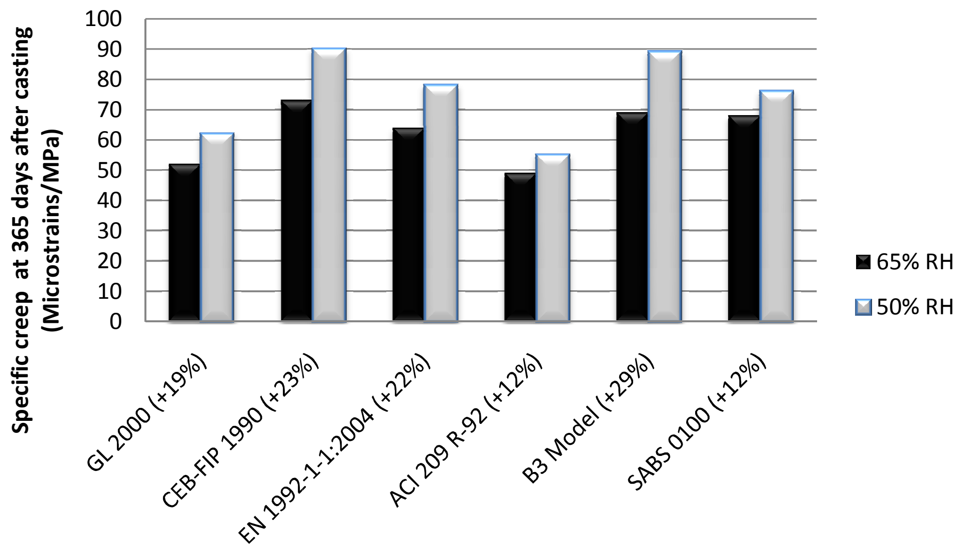

Legend: value in parenthesis indicates direction and percentage of strain change

Figure 5.6: Calculated specific creep strains (at 365 days after casting) of input set 3 at different Relative humidity (RH)

As it can be observed from figures 5.5 and 5.6, the calculated strains increases with a decrease in relative humidity, hence the models respond positively to this particular change.

Compressive strength (f_{cm28}*) and Elastic modulus (*E_{cm28}*):* In many parts of South Africa, concrete for water retaining structures are selected on the basis of compressive strength. These structures are often designed with a characteristic strength of 30 MPa, however, client specification or the need for higher safety factors may lead to the use to concretes up to approximately 60 MPa.

For this reason, the ability to calculate accurate strains across this full range of compressive strength used in the industry is important. The correlation between shrinkage and specific creep strains and the compressive strength has been observed over the years. It is expected that an increase in compressive strength lead to a decrease in overall strains as described in the literature review of this document. Furthermore, the same reasoning may be applied to the influence of elastic modulus on concrete strains.

Changing the value of compressive strength from input set 3 is not a straight-forward operation. An increase in compressive strength, ultimately leads to an increase in the elastic modulus of the concrete. Furthermore it is unlikely, that the compressive strength of a concrete increases without a change of composition. It has been reported however, that extended curing, better temperature control and delayed loading may cause a slight increase in compressive strength.

For the purposes of this exercise, the compressive strength is increased by a slight margin. Subsequently, the elastic modulus is predicted using the equation $E_{cm28} = 21500\sqrt[3]{\frac{f_{cm28}}{10}}$ (CEB-FIP, 1990) yet the composition and shape of the structure remained unchanged. The strains are then expected to reduce as a result of these changes. Table 5.5 shows the changes made from the original input set.

Table 5.5: Compressive strength and elastic modulus changes to input set 3

Property changed	Original (Input set 3)	Changed
Compressive strength	45 MPa	55 MPa
Elastic modulus	35 GPa	37 GPa

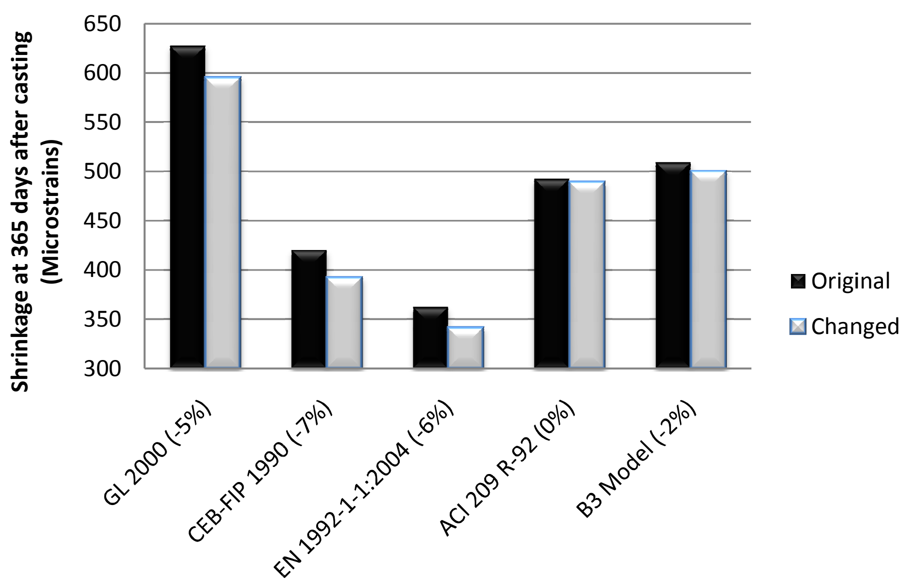

Legend: value in parenthesis indicates direction and percentage of strain change

Figure 5.7: Calculated shrinkage strains (at 365 days after casting) of input set 3 at different compressive strengths and Elastic modulus

In figure 5.7, no change is found for the ACI 209 R-92 model. This is the case because the model is based on concrete composition correction factors affecting the ultimate shrinkage. In other words, the model implies that a change in compressive strength has to be achieved through change in composition of the concrete, and since the composition is left unchanged (for simplicity reasons), no change can be observed in the model.

The small change in the B3 model has a similar reasoning as to the constant behaviour of the ACI 209R-92. The B3 shrinkage model is more dependent on water composition than on the compressive strength as can be verified by the formula $\varepsilon_{s\infty} = \alpha_1 \alpha_2 \left[0.019 w^{2.1} (f_{cm28})^{-0.28} + 270\right] \times 10^{-6}$ for ultimate shrinkage strain calculation. The exponents acting on water content (i.e. *w*) and compressive strength (i.e. f_{cm28}) show that a change in *w* is likely to modify the outcome of the equation more than a change in f_{cm28}. In practice these changes occur simultaneously, but in this exercise the water content (*w*) is left unchanged hence the small change in shrinkage strains.

With regard to the other models, significant reduction of strains can be observed with the increase in compressive strength and elastic modulus. Based on these results, it is possible to note that the models respond correctly to the changes.

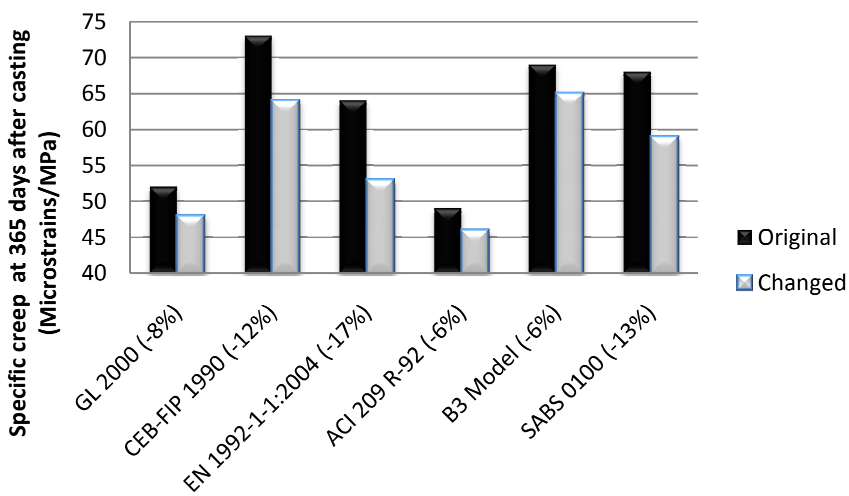

Legend: value in parenthesis indicates direction and percentage of strain change

Figure 5.8: Calculated specific creep strains (at 365 days after casting) of input set 3 at different compressive strengths and Elastic modulus

It can be seen from figure 5.8 that the calculated specific creep strains decreases when the compressive strength and elastic modulus are increased. This is the expected model behaviour, thus the models respond positively to the changes made.

Specimen characteristics: The same concrete can be used in different structural elements of the water retaining structures. However, different shapes of structural elements, may ultimately determine the extent to which it shrinks or creeps.

In practice, these numerical models are used to predict the creep and shrinkage strains of real structures such as slabs, columns and beams. In a laboratory environment, specimens of different sizes may be used to represent the real structure. Consequently, a laboratory sized specimen could be used in the development of input set 3, the base line input set for this exercise.

In the same manner that the models are expected to calculate different strains between a slab and a beam, they are expected to calculate unequal strains between two different sized specimens. It is well understood and reported that shrinkage and creep are size and shape-dependent. Carrying this concept, the specimen characteristics specified in input set 3 are changed accordingly and model responses are noted.

The changes made to specimen shape of input set 3, are presented in table 5.6, while the response observed in the models is shown figures 5.9 and 5.10.

Table 5.6: Specimen shape changes to input set 3

Specimen shape				
Property	**Symbol**	**Original**	**Changed**	**Units**
Type of specimen		long square prism	long square prism	
Volume	V	780300	780300	mm^3
Total surface area	S	66402	52866	mm^2
Cross sectional area	Ac	2601	5625	mm^2
Perimeter of cross sectional	u	204	300	mm

area				
Effective thickness as 2×Ac/h	h	25.5	37.5	mm
Volume/ surface area	V/S	11.751	14.75	
Comment on changes	*Changes provide a bulkier specimen*			

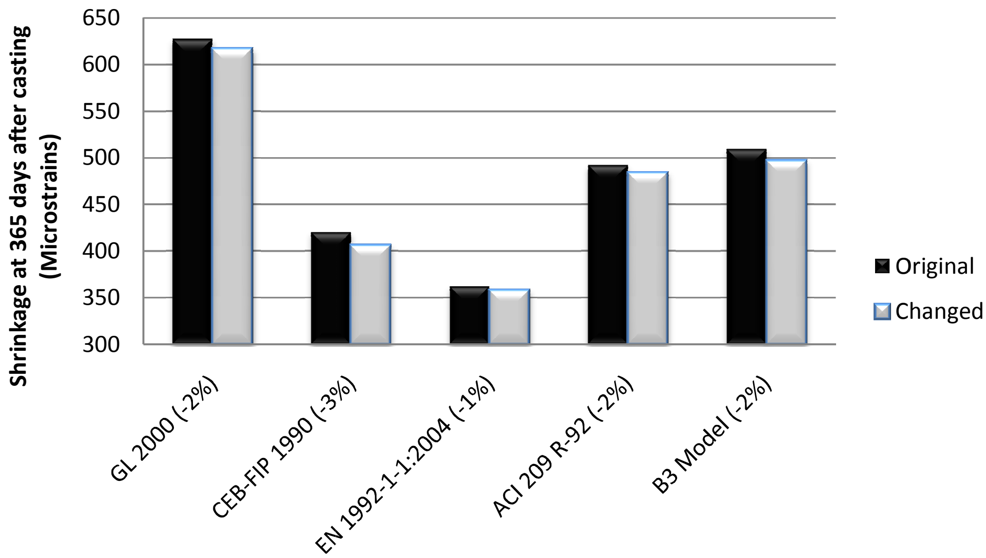

Legend: value in parenthesis indicates direction and percentage of strain change

Figure 5.9: Calculated shrinkage strains (at 365 days after casting) of input set 3 with different specimen shape.

The calculated shrinkage strains reduce when the specimen is made bulkier as shown by figure 5.9. This is the expected behaviour and it shows that the shrinkage models are in agreement with the physical behaviour of concrete.

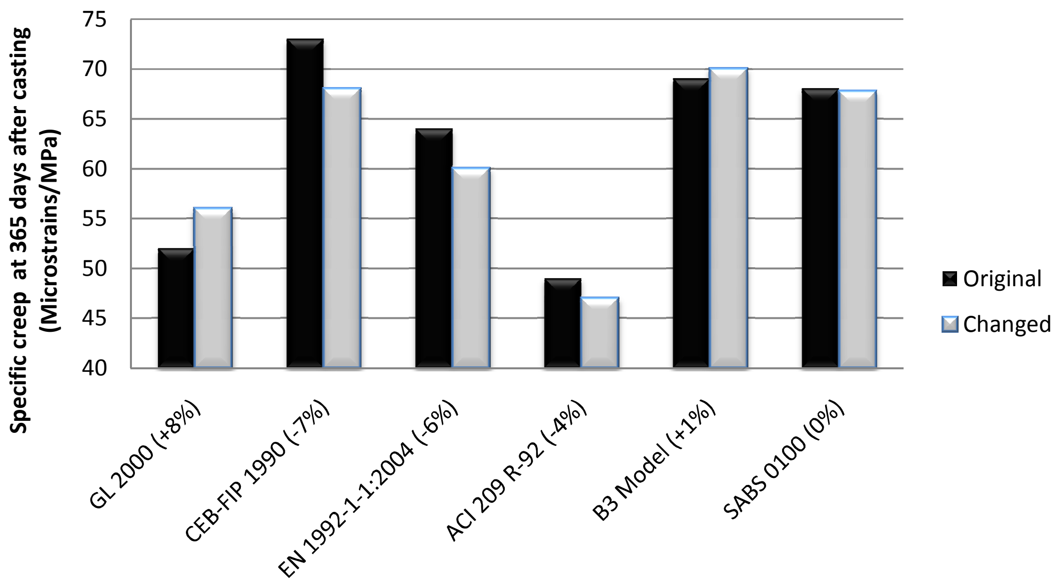

Legend: value in parenthesis indicates direction and percentage of strain change

Figure 5.10: Calculated specific creep strains (at 365 days after casting) of input set 3 with different specimen shapes.

A different set of results can be observed from figure 5.10. The CEB-FIP 1990, EN 1992-1-1: 2004 and the ACI 209 R-92 models respond to the parameter change as expected.

The SABS 0100's figure C.2 of annex C makes provision for changes in effective thickness of a member between 150mm, 300mm, and 600mm, however no provision is made for small specimen changes such as these of this exercise. Subsequently, the respective creep coefficient remains the same and the respective specific creep also remains unchanged. This is a simpler model relatively to the others and this was expected.

With regard to the GL 2000, the model's inability to respond correctly to a change in specimen characteristics (i.e. V/S change) is due to a faulty principle in the model itself. This is shown in derivation 5.1 below by calculating the limit of the creep coefficient as V/S tends to infinity. It is important to remember that a specimen with a larger V/S to the other is a bulkier specimen, therefore taking this limit as V/S tends to infinite, implies testing a bulkier specimen and vice-versa.

Derivation 5.1.

With $\phi(t,t_0)=\sqrt{1-\sqrt{\dfrac{t_0-t_c}{t_0-t_c+0.15\left(\dfrac{V}{S}\right)^2}}}\times\left[f(t,t_0)+f(h)\times\sqrt{\dfrac{t-t_0}{t-t_0+0.15\left(\dfrac{V}{S}\right)^2}}\right]$

$$\lim_{\frac{V}{S}\to\infty}\phi(t,t_0)=\sqrt{1-\sqrt{\frac{t_0-t_c}{\infty}}}\times\left[f(t,t_0)+f(h)\times\sqrt{\frac{t-t_0}{\infty}}\right]=1\times[f(t,t_0)+f(h)\times 0]=f(t,t_0)$$

and

$$\lim_{\frac{V}{S}\to 0}\phi(t,t_0)=\sqrt{1-\sqrt{\frac{t_0-t_c}{t_0-t_c}}}\times\left[f(t,t_0)+f(h)\times\sqrt{\frac{t-t_0}{t-t_0}}\right]=0\times[f(t,t_0)+f(h)\times 1]=0$$

The model implies that as specimen becomes slender (i.e. as V/S becomes smaller), the specific creep becomes smaller (see $\lim_{\frac{V}{S}\to 0}\phi(t,t_0)$), which is not in agreement with the physical behaviour of concrete.

Derivation 5.1 shows that the inability of the model to respond correctly to a change in specimen characteristics is not caused by misinterpretation or bad implementation of the model formulae. It is caused by a model principle that is not correct.

The principle behind the response of the B3 model to a change of specimen characteristics (i.e. V/S change) is only partially correct. This is studied by calculating the limit of the compliance function as V/S tends to infinity. This brings the drying creep to zero which is correct. The limit of the compliance function as V/S tends to zero does bring the drying coefficient to zero which is not correct. This is visually shown in figure 5.11.

Derivation 5.2.

The full derivation 5.2 is provided in the appendix (too long for this section):

With $J(t,t_0)=q_1+C_0(t,t_0)+C_d(t,t_{0,}t_c)=q_1+C_0(t,t_0)+q_5\times\sqrt{e^{-8H(t)}-e^{-8H(t0)}}$

$$\lim_{\frac{V}{S}\to\infty} J(t,t_0) = \lim_{\frac{V}{S}\to\infty}\left[q_1 + C_0(t,t_0) + q_5 \times \sqrt{e^{-8H(t)} - e^{-8H(t0)}} \right] = q_1 + C_0(t,t_0) + 0 = q_1 + C_0(t,t_0)$$

And,

$$\lim_{\frac{V}{S}\to 0} J(t,t_0) = \lim_{\frac{V}{S}\to 0}\left[q_1 + C_0(t,t_0) + q_5 \times \sqrt{e^{-8H(t)} - e^{-8H(t0)}} \right] = q_1 + C_0(t,t_0) + 0 = q_1 + C_0(t,t_0)$$

Hence the model implies that as V/S increases (i.e. as the specimen becomes bulkier), the drying creep becomes zero and the total strains reduce to $q_1 + C_0(t,t_0)$. This is in agreement with physical behaviour of concrete. However, it is also shown that in the B3 model, as V/S decreases (i.e. the specimen becomes slender), the drying creep also becomes zero and the total strains reduce to $q_1 + C_0(t,t_0)$ which is not in agreement with the physical behaviour of concrete.

For the model to respond appropriately to changes across the realistic range of V/S, it is necessary that the drying creep decreases continuously with increased V/S and vice-versa. However, this is not the case. To clarify the matter, figure 5.11 (which shows the specific drying creep as a function of V/S) was computed for a fixed time of 365 days after casting. All other parameters are kept constant.

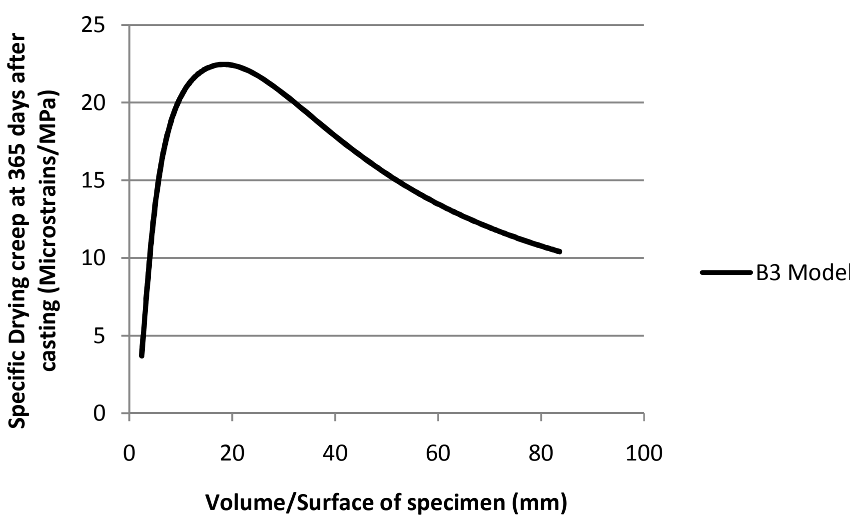

Figure 5.11: B3 Model calculated specific drying creep strains (at 365 days after casting) for different specimen V/S with all other parameters of input set 3 kept constant

From figure 5.11 it is possible to observe that the effect of V/S in the specific drying creep (consequently specific creep) of the B3 Model is mixed. It indeed, allows the possibility for a specimen with a V/S equal to 50 (e.g.) to have the same specific creep to a specimen with a V/S equal to 10 (e.g.) which is not physically sound. It must also be noted that according to the model, a specimen with V/S equal to 14.75 may have a larger specific drying creep than a slender specimen with V/S equal to 11.75, which is also not correct. The latter example, is the example used in this exercise.

Beyond the V/S equal to 20 region (i.e. where maximum occurs), the B3 model responds positively to specimen characteristic changes and the drying creep approaches zero as V/S tends to infinity which is correct.

The above explanation shows that the inability of the model to respond correctly to a change in specimen characteristics for this particular set of input parameters is not caused by misinterpretation or bad implementation of the model formulae. It is caused by a model principle that is not correct across the full range of realistic V/S parameter values.

To show this further, another change of specimen characteristics is made. This is done with the intention to observe the behaviour of the model on the right hand side of the curve shown in figure 5.11. The changes and responses are shown in table 5.7.

Table 5.7: Changes to specimen characteristics to be implemented in B3 model and respective response

Changes Specimen shape				
Property	**Symbol**	**Original**	**Changed**	**Units**
Type of specimen		long square prism	long square prism	
Volume	V	1000000	1000000	mm^3
Total surface area	S	25000	15000	mm^2

Volume/ surface area	V/S	40	50	
Comment on changes	*Changes provide a bulkier specimen*			
Response (i.e. Results)				
Property	**Symbol**	**Original**	**Changed**	**Units**
Specific creep at the age of 365 days after casting	$C_d(t, t_0, t_c)$	66	63	Micro strains /MPa

The lower specific creep predicted by the B3 model (i.e. 4.5%) for a bulkier specimen (i.e. larger V/S), follows the trend of figure 5.11 after the maximum. This is physically correct, and it indicates that the implementation of the model into the spreadsheet is properly done.

Curing time: Time constrains are a reality in the construction industry. In the construction of water retaining structures, contractors may be subjected to time limitations. To address this issue, curing time may be reduced in some instances, which affects the quality of the concrete.

Certainly, a change in curing time does not occur in isolation. It may affect the strength of the concrete as discussed before and prompt other changes in the construction schedule such as change of loading age. For example, a reduction of curing time of a slab, may allow the contractor to load the slab earlier as a platform (for materials and equipment) of the next casting phase, thus reducing the overall time of construction.

The possibility of curing time changes is real during the construction phase. For that reason it is important that the models are capable of noticing the change and adjust the calculated strains.

The purpose of this exercise is to change one parameter at a time from the baseline input set. Therefore, the time of curing is changed in isolation despite the above described implications. This is permissible, as the desired outcome of this exercise is only to observe model responses. However, for design purposes the designer is required to obtain all the necessary information caused by the change of curing period before proceeding with the design.

The input set 3, specified a curing time of 7 days. This is the case because in the construction industry this is often the minimum threshold value. Reducing this value further would be unrealistic, therefore the time of curing is increased from 7 days to 14 days and the response is observed. Note, that a decrease in overall strains is expected in response to this change.

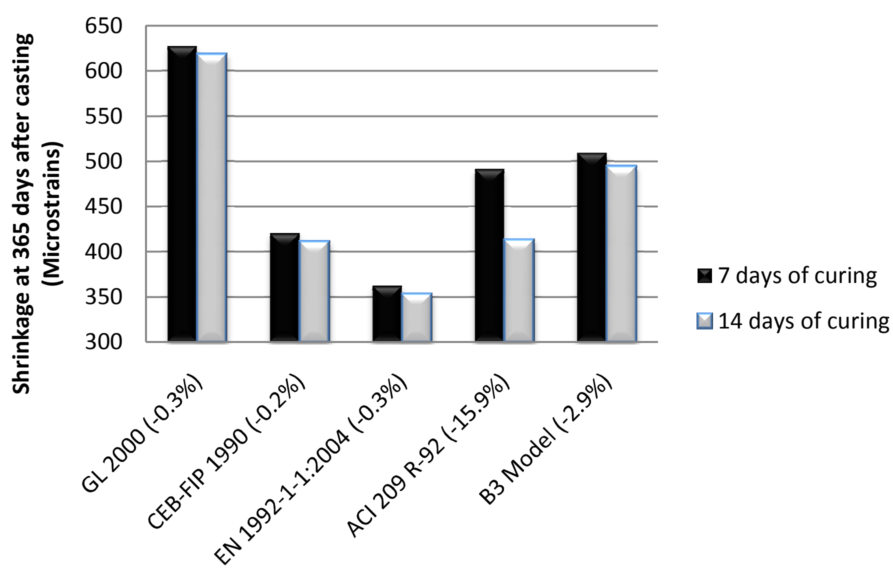

Legend: value in parenthesis indicates direction and percentage of strain change

Figure 5.12: Calculated shrinkage strains (at 365 days after casting) of input set 3 at different periods of curing.

For the implemented change, a reduction in calculated shrinkage strain results can be observed in figure 5.12, for all numerical models. Despite the small change in most models, this is in accordance with the expected model behaviour and it is noted that the models respond positively to the change.

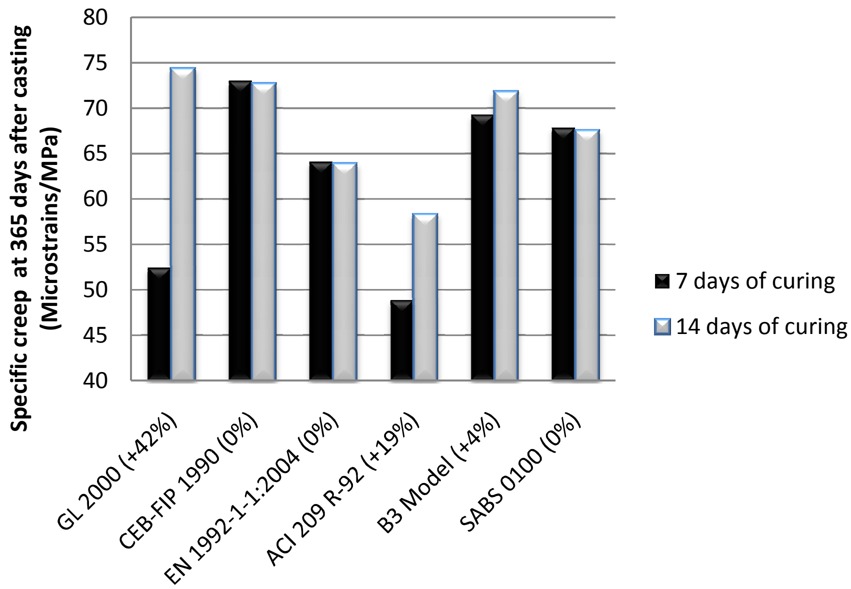

Legend: value in parenthesis indicates direction and percentage of strain change

Figure 5.13: Calculated specific creep strains (at 365 days after casting) of input set 3 at different periods of curing.

None of the models displays the expected behaviour therefore each model is investigated further (see figure 5.13). This was done to identify the true cause of this behaviour, as faulty model principles could, once again be the source of behaviour noncompliance.

The CEB-FIP 1990, EN 1992-1-1:2004 and the SABS 0100 show no specific creep response to the change in curing time, because the models do not consider the curing time parameter in the calculation of specific creep. Consequently, a change in this parameter does not have any effect on the specific creep.

The GL 2000 increment on the calculated specific creep is due to a faulty principle in the model. This is shown mathematically through derivation 5.3 that follows.

Derivation 5.3

As determined before the creep coefficient of the GL2000 is given by the formula:

$$\phi(t,t_0)=\sqrt{1-\sqrt{\frac{t_0-t_c}{t_0-t_c+0.15\left(\frac{V}{S}\right)^2}}}\times\left[f(t,t_0)+f(h)\times f\left(t,t_0,\frac{V}{S}\right)\right]$$

As t_c increases, the difference between t_o and t_c decreases. Therefore, the effect of an increase of t_c into the creep coefficient ($\phi(t,t_0)$) can be represented as through the limit of $\phi(t,t_0)$ as t_o-t_c tends to zero.

$$\lim_{(to-tc)\to 0}\phi(t,t_0)=\sqrt{1-0}\times[f_1(t,t_0)+f(h)\times f_2(t,t_0)]=[f_1(t,t_0)+f(h)\times f_2(t,t_0)]$$

Hence, as t_c increases, the creep coefficient tends to the shown expression.

On the other hand, as t_c decreases, the difference between t_0 and t_c increases. Therefore, the effect of a decrease of t_c into the creep coefficient can be represented as through the limit of ϕ_{28} as t_0-t_c tends to t_0.

$$\lim_{(to-tc)\to to}\phi(t,t_0)=\sqrt{1-\sqrt{\frac{t_0}{t_0+0.15\left(\frac{V}{S}\right)^2}}}\times\left[f(t,t_0)+f(h)\times f\left(t,t_0,\frac{V}{S}\right)\right]$$

For very large t_o,

$t_0>>0.15\left(\frac{V}{S}\right)^2$ then $\frac{t_0}{t_0+0.15\left(\frac{V}{S}\right)^2}=1$, and $\lim_{(to-tc)\to to}\phi(t,t_0)=0$

For a $t_0\approx 0.15\left(\frac{V}{S}\right)^2$ then $\frac{t_0}{t_0+0.15\left(\frac{V}{S}\right)^2}=\frac{1}{2}$, and $\lim_{(to-tc)\to to} \phi(t,t_0) = 0.54 \times \left[f(t,t_0) + f(h) + f\left(t, t_{0,} \frac{V}{S} \right) \right]$

Therefore in the GL 2000 model, as t_c decreases the creep coefficient tends to zero or 54% of the maximum obtainable creep coefficient. This in turn implies that the specific creep decreases, with an increment of curing time, which is not in line with the physical behaviour of concrete.

The derivation shows that the inability of the model to respond correctly to a change in curing time is not caused by misinterpretation or bad implementation of the model formulae. It is caused by a model principle that is not correct.

With regard to the ACI 209R-92 model, a similar problem is encountered. The approach in which the model considers the curing time causes the unexpected increase in specific creep strains.

The model considers specific creep through the formula:

$\phi(t,t_0) = \frac{(t-t_0)^{\psi 1}}{d + (t-t_0)^{\psi 1}} \times v_u$, in which:

d=10 days and ψ_1 = 0.6 for a curing time of 7 days in moist environment

or $d = 26\left[\exp 1.42 \times 10^{-2} (v/s)\right]$ and ψ_1=1 for curing times larger than 7 days in moist environment.

This principle is graphically represented in figure 5.14. To achieve this, the time function $\frac{(t-t_0)^{\psi 1}}{d + (t-t_0)^{\psi 1}}$ of the formula is computed in isolation for different curing times whilst all other parameters of input set 3 are kept constant.

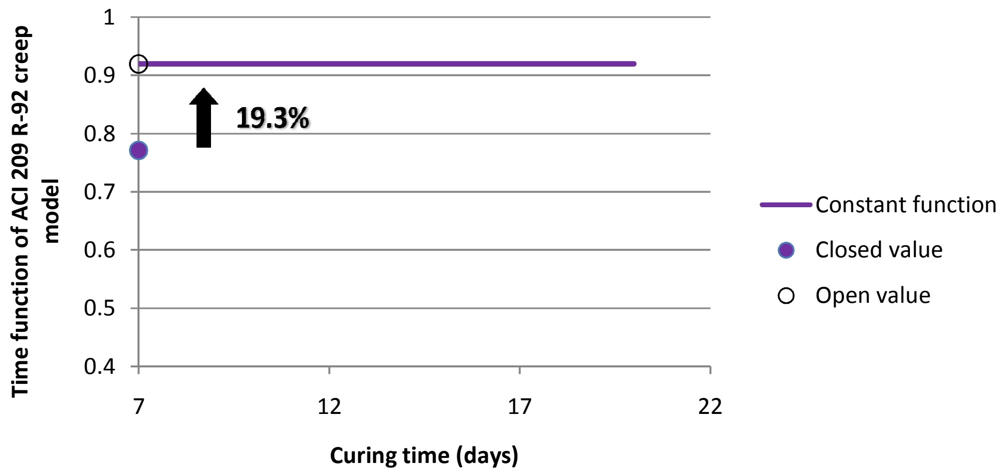

Figure 5.14: Calculated time evolution function coefficient of input set 3 at different periods of curing.

Figure 5.14, shows that the changes of variables "d" and "ψ_1" cause the value of $\frac{(t-t_0)^{\psi 1}}{d+(t-t_0)^{\psi 1}}$ to increase, and consequently cause the specific creep to increase by the same amount (i.e. 19.3% in this case). This indicates that the model has been correctly implemented into the spreadsheet and that the observed response of the model is due to the model approach to curing time.

The B3 Model had a 4% increase in specific creep which is also a negative response to the increase in curing time. Investigations into the model formulae revealed that this response is also due to a model defective approach.

Graphical representation was selected as the most suitable method to elucidate the above statement. Whilst keeping all the other parameters of input set 3 constant, the time of curing is changed incrementally from 7 days to 14 days. According to the B3 model, the period of curing t_c only affects the drying creep of concrete. Therefore, the formulae of the B3 model are used to compute figure 5.15 below which shows the specific drying creep as a function of curing time.

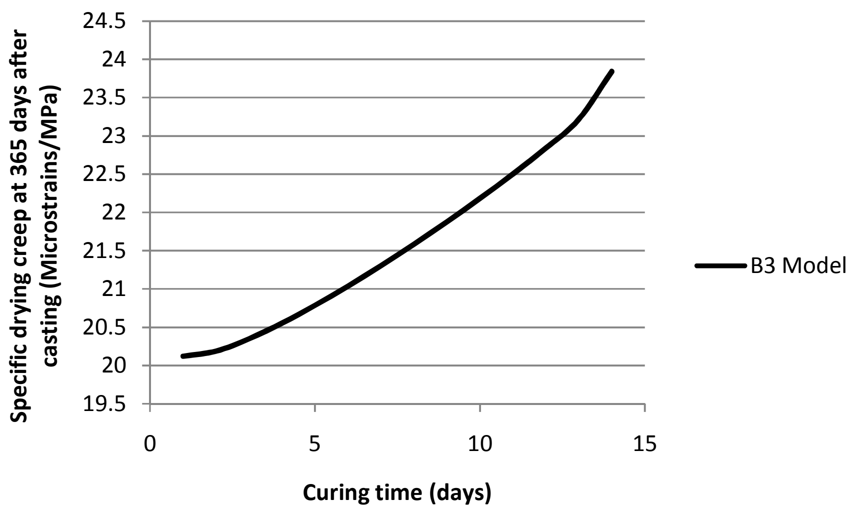

Figure 5.15: B3 Model calculated specific drying creep strains (at 365 days after casting) for different periods of curing with all other parameters of input set 3 kept constant

The figure shows that an increase in time of curing results in an increase in the calculated specific drying creep (according to the B3 model). Subsequently the creep strains are also increased with the increase of curing time which is not in agreement with the physical behaviour of concrete.

The above shows that the interpretation and implementation of the model formulae are not the cause for the negative response of the model. Instead, this is caused by the faulty effect of the time of curing into the creep phenomena described by the model.

Loading age: The last parameter changed in this evaluation method is the loading age. It came in line with the reality that time limitations in the construction industry may induce this change as discussed before.

It is possible that under some circumstances, a contractor may change the loading age without changing the curing period. Hence this change in isolation was justifiable for this exercise.

Input set 3, specified a curing time of 7 days and a loading age of 14 days, because in the construction industry these are often taken as minimum threshold values. In this exercise the loading age is increased from 14 days to 28 days and the response to calculated specific creep strains is observed. In principle, the creep strains are expected to reduce because the time of load exposure is reduced by this change.

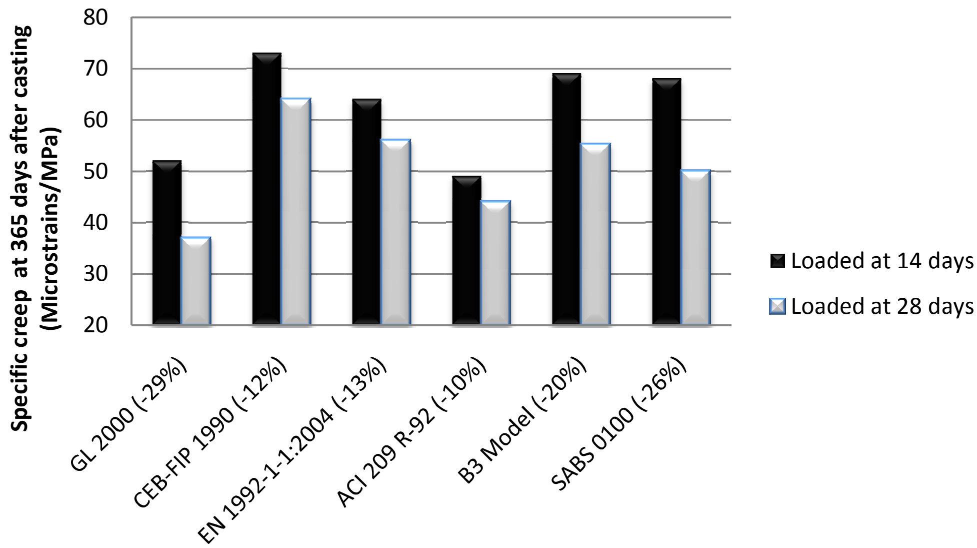

Legend: value in parenthesis indicates direction and percentage of strain change

Figure 5.16: Calculated specific creep strains (at 365 days after casting) of input set 3 at different ages of loading

Figure 5.16, shows a decrease of specific creep strains in all numerical models when the age of loading is delayed. This is in agreement with the expected model behaviour and physical behaviour of concrete. Hence, it indicates a positive response to the change and good implementation of model principles.

5.2. Verification of the programming of statistical indicators

The accuracy of the prediction models to the experimental data was measured through the implementation of statistical indicators. The indicators used are the Bažant and Panula (1978) coefficient of variation (BP-COV) method (1978) and the CEB (1990) mean square error method (1990). For convenience, these were also programmed in Microsoft Excel, in the same spreadsheet template that the numerical models have been programmed.

The formulae which make up these methods have been described before, yet it is necessary to verify whether these are also properly programmed. Therefore, the observed values (i.e. experimental data, O_{ij}) and the calculated values (i.e. calculated using prediction models, C_{ij}) are manipulated to create extreme scenarios in which the statistical methods responses are studied.

The above mentioned scenarios are hereby listed:

Scenario 1: Setting the experimental and calculated data to the same value

When the experimental and calculated data are set to have the same values, the statistical indicators are expected to display a zero error. This is the case, as the scenario implies that the calculated values are a faultless prediction of the observed values. The BP-COV method and the CEB mean square error method computed a zero error when this change was implemented in the spreadsheet.

Scenario 2: Setting the calculated data to zero whilst the experimental data remains the same.

When the calculated data is set to zero, while the experimental data is left unchanged, the statistical indicators are expected to have a mixed response. The CEB mean error method is expected to compute an error of 100% whilst the BP-COV method should compute a positive value which varies with the data. This is explained in derivation 5.4

Derivation 5.4

In the CEB mean error method:

$$F_{ij} = \sqrt{\frac{1}{n-1}\sum_{i=1}^{n}\left(\frac{C_{ij}-O_{ij}}{O_{ij}}\times 100\right)^2}$$

$$\lim_{Cij\to 0} F_{ij} = \sqrt{\frac{1}{n-1}\sum_{i=1}^{n}\left(\frac{-O_{ij}}{O_{ij}}\times 100\right)^2} = \sqrt{\frac{1}{n-1}\sum_{i=1}^{n}(-100)^2} = \sqrt{\frac{n-1}{n-1}\times(-100)^2} = 100$$

In the BP-COV method

$$COV = \frac{\sqrt{\frac{1}{n-1}\sum_{i=1}^{n}\left(O_{ij}-C_{ij}\right)^2}}{\frac{1}{n}\sum_{i=1}^{n}O_{ij}}$$

$$\lim_{Cij\to 0} COV = \frac{\sqrt{\frac{1}{n-1}\sum_{i=1}^{n}\left(O_{ij}\right)^2}}{\frac{1}{n}\sum_{i=1}^{n}O_{ij}} = \sqrt{\frac{n^2}{n-1}}\times\sqrt{\frac{\sum_{i=1}^{n}\left(O_{ij}\right)^2}{\left(\sum_{i=1}^{n}O_{ij}\right)^2}}$$

When the calculated data (i.e. C_{ij}) is set to zero, the CEB mean square error method computes an error percentage of 100%, which is the anticipated result. To assess whether the BP-COV method responds according to the calculated limit as C_{ij} tends to zero, a more elaborate approach is required.

Whilst keeping the C_{ij} values at zero, the BP-COV method is used to calculate the coefficient of variation (i.e. COV) between C_{ij} and experimental values (i.e. O_{ij}). Subsequently, the limit of COV as C_{ij} tends to zero ($\lim_{Cij\to 0} COV$) established in derivation 5.4 is calculated for the same experimental values (O_{ij}) as above. The resulting value for the $\lim_{Cij\to 0} COV$ and the calculated COV using the BP COV method under this scenario are equal which was the forecasted result.

This procedure was repeated for different sets of O_{ij} and the same result was found.

Scenario 3: Setting the experimental data to zero whilst the calculated data remains the same

When the experimental (i.e. observed) values are set to zero, while the calculated data is left unchanged, the statistical indicators are expected to output a calculation error message. The reason for that is expressed in the formulae above (see derivation 5.4), in which the observed value (i.e. O_{ij}) is a denominator. Setting this variable to zero, implies a division by zero. Hence an error is expected in this computation.

Indeed, the statistical indicators indicates an error in the calculation of the error percentages under this scenario, which is the expected result.

In the three scenarios created to evaluate the implementation of these statistical indicators, the results are appropriate. This indicates that the statistical methods are introduced correctly into the Excel spreadsheet.

5.3. Assessment on integrity of programming of prediction models and statistical indicators

The overall assessment at this stage is that the analytical models have been properly interpreted and programmed. Unquestionably, unexpected responses of these models to particular variable changes were observed, however after investigation it was noted that human-error on the implementation of this models is not the cause.

Furthermore, the statistical indicators used to evaluate the accuracy of the analytical models were also subjected to scrutiny. After careful study of these indicators, it was observed that these are also accurately programmed and are capable of perform their function.

CHAPTER 6
ANALYSIS OF PREDICTION MODELS

6.1 Introduction

The purpose of this chapter is to discuss the advantages as well as the disadvantages of the prediction models. The applicability of these models to WRS is also under discussion.

The main disadvantage of all models is that they are calibrated to large historic sets of experimental data with reasonable accuracy, which may not be replicated once a different set of data is used. This may be due to the different characteristics of concrete used amongst the experimental data as concrete technology evolves but also because the characteristics of concrete vary according to the region of the world. Therefore as Ballim (2006) explains significant errors can be incurred if models developed in other countries are adopted into local design specifications without consideration of the climatic and material differences which may affect the prediction.

Despite the above disadvantage these design models enable the engineer to anticipate the approximate shrinkage or creep that a structure may experience at any desirable time. For WRS, this is a powerful tool for durability and sound structural performance as discussed in chapter 1.

6.2 Assessment criteria and assessment of models

The criteria used to assess these models are:

- Complexity of the model: divided into entry and advanced level
- Minimum mechanisms incorporated (i.e. input parameters required)
    - Description of concrete by mechanical properties such as compressive strength or elastic modulus or by use of mix design proportions
    - Ambient relative humidity

  - Cement type
  - Age at loading
  - Duration of drying or curing time
  - Duration of loading
  - Specimen size
- Possibility of substitution of elastic modulus and compressive strength by tested values
- Use of mathematical expressions that are not highly sensitive to small changes in input parameters
- Use of simple mathematical expressions
- Creep expressions to accommodate for drying before loading

Table 6.1 summarises the input parameters and characteristics of the models.

Table 6.1: Input parameters and characteristics of the models

	GL 2000		CEB-FIP 1990		EN 1992-1-1:2004		ACI 209 R-92		B3 Model		SABS 0100
Minimum input requirements	Shrinkage (SHR)	Creep (CR)	SHR	CR	SHR	CR	SHR	CR	SHR	CR	CR
Ambient relative humidity	✓	✓	✓	✓	✓	✓	✓	✓	✓	✓	✓
Cement type	✓	✓	✓	✓	✓	✓	✗	✓	✓	✓	✗
Duration of drying or curing time	✓	✓	✓	✗	✓	✗	✓	✓	✓	✓	✗
Specimen size	✓	✓	✓	✓	✓	✓	✓	✓	✓	✓	✗ *5
Compressive strength	✓	✓	✓	✓	✓	✓	✗ **	✓	✓	✓	✓
Elastic modulus	N/A	✓	N/A	✓	N/A	✓	N/A	✓	✓	✓	✓
Age of loading	N/A	✓	N/A	✓	N/A	✓	N/A	✓	N/A	✓	✓
Other input parameters	✗	✗	✗	✓	✗	✓	✓	✓	✓	✓	✓
Temperature	✗	✗	✗	✓	✗	✓	✗	✗	✗	✗	✗
Slump	✗	✗	✗	✗	✗	✗	✓	✓	✗	✗	✗
Fine Aggregate content	✗	✗	✗	✗	✗	✗	✓	✓	✗	✗	✗
Aggregate content	✗	✗	✗	✗	✗	✗	✗	✗	✓	✓	✗
Aggregate type	✗	✗	✗	✗	✗	✗	✗	✗	✗	✗	✓
Air content	✗	✗	✗	✗	✗	✗	✓	✓	✗	✗	✗
Cement content	✗	✗	✗	✗	✗	✗	✓	✗	✓	✓	✗

Water content	✗	✗	✗	✗	✗	✗	✗	✗	✓	✓	✗
Curing type	✗	✗	✗	✗	✗	✗	✓	✓	✓	✓	✗
Characteristics of the models											
Possibility of substitution of elastic modulus and compressive strength by tested values	✓	✓	✓	✓	✓	✓	✗	✓	✓	✓	✓
Low sensitivity of mathematical expressions to small input parameter changes	✗ *	✗ *	✓	✓	✓	✓	✗ ***	✗ ***	✓	✓	✗ [*6]
Mathematical expressions simply to use	✓	✓	✓	✓	✓	✓	✓	✓	✗	✗	✓
Drying before loading enabled for creep prediction	N/A[*7]	✓	N/A	✗	N/A	✗	N/A	✓	N/A	✓	✗
Complexity of the model	Entry-level		Advanced-level		Advanced-level		Advanced-level		Advanced-level[*4]		Entry-level

Legend:

* - model is highly sensitive to a change in ambient relative humidity;

**- although the compressive strength is not used, mix proportions are utilized to describe the concrete; therefore it is a valid approach;

*** - highly sensitive to curing period

*[4] - more sophisticated than the advanced level

*[5] - there is provision for effective section thickness of structural element of 150, 300 and 600 mm. No provision made for small specimens or other structural elements.

*[6] - highly sensitive to changes of specific creep

*[7] - N/A refers to not applicable while "×" means not incorporated

6.3 GL 2000

6.3.1 Advantages of GL 2000 model

This is a basic model with simple mathematical equations. This enables the engineer to identify modelling errors with ease and compute limit or derivation analysis to the model more comfortably than other models.

The GL 2000 contains all the minimum required parameters, which is a significant characteristic of the model considering that it is an entry-level model. This gives confidence to a designer that intends to use this model

It also enables the substitution of tested values for compressive strength and elastic modulus, which enables designers to calculate the creep and shrinkage phenomena more accurately.

The simplicity of the model and the minimum input parameter requirements facilitate minimum computation time and make this model suitable to be used in a design office during preliminary stages of design.

6.3.2 Disadvantages of GL 2000 model

The mathematical expressions are highly sensitive to relative ambient humidity. This may induce errors in the prediction, when the exact value of this input parameter is not known. It also increases the risk of human error during computation stages.

Derivation 5.1 in chapter 5 showed that the GL 2000 may respond incorrectly to a change in V/S (i.e. specimen size). Additionally, the model is likely to respond incorrectly to a chance in curing time as indicated by derivation 5.3.

The simplicity of the models is also a liability as it often results in overly conservative values of creep and shrinkage. This may restrain its use for long term strain calculation due to economic reasons, as excessively conservative design is costly.

6.4 CEB-FIP 1990

6.4.1 Advantages of CEB-FIP 1990 model

The mathematical equations of this model are reasonably simple. Furthermore, the shrinkage model contains all the minimum requirements established in the assessment criteria. This indicates that the principles behind the model are sound.

As per the GL 2000, this model also enables the substitution of tested values for compressive strength and elastic modulus; and apart from exposed temperature, the model only requires the minimum input parameters established before. This empowers the engineer and makes the model suitable for use in a design environment.

The low sensitivity of the model to small changes of input parameters reduces the impact of human error and avoids large errors when some parameters are not completely known at design stage.

The ability to consider temperature effects on creep is unique to this model and the EN 1992-1-1:2004; it is therefore an advantage to these models as temperature effects may not be disregarded as discussed in chapter 2.

6.4.2 Disadvantages of CEB-FIP 1990 model

The CEB-FIP 1990 does not consider the initial drying period in the creep calculations, which in turn means that drying before loading is not considered in creep calculations. This shortcoming is aggravated because in WRS construction drying is likely to occur before loading for the majority of structural elements.

Type of curing is also not considered. With its advanced complexity level, the model is expected to consider this parameter, as it may affect creep and shrinkage calculation.

WRS are not constructed in controlled temperature environments therefore the designer is unable to provide a precise temperature and duration in which this temperature prevails as the model specifies.

6.5 EN 1992-1-1:2004

6.5.1 Advantages of EN 1992-1-1:2004 model

The similarities between the CEB FIP 1990 and EN 1992-1-1:2004 models are evident in this section and the section that follows. The same input parameters are required and the approaches used are similar, therefore the positive characteristics of these models are also similar.

- The mathematical equations are reasonably simple.
- The shrinkage model contains all the minimum requirements established in the assessment criteria.
- The model enables substitution of tested values for compressive strength and elastic modulus.
- Apart from exposed temperature, the model only requires the minimum input parameters established before.
- The model has low sensitivity to small changes of input parameters.
- Temperature effects to creep prediction are considered.

- Correction factors are provided for high strength concretes.

6.5.2 Disadvantages of EN 1992-1-1:2004 model

As per the CEB-FIP 1990 model, the EN 1992-1-1:2004 does not consider drying before loading in creep calculations and type of curing. Also, the temperature and duration in which the temperature prevails may not be known at design phase.

6.6 ACI 209 R- 92

6.6.1 Advantages of ACI 209 R- 92 model

The mathematical equations of this model are simple and based on correction factors to the ultimate strain. This enables designers with minimal background knowledge to use it safely.

The use of mix proportions approach to describe the concrete is useful when the mix design has been finalized. Therefore it is a useful model to verify the prediction made by another model during the design phase where the exact concrete mix proportions are not known.

Although the mix proportion approach is also in use for creep model, mechanical properties of the concrete are also used in creep calculation. The substitution of tested values for compressive strength and elastic modulus is also allowed which ensures better prediction. Moreover, the creep model contains all the minimum input requirements established in the assessment criteria, which indicate sound model principles.

Curing types, moist and steam curing are considered. This enables the engineer to consider the type of curing in the design stage or when verification of calculated strains by other model is processed.

6.6.2 Disadvantages of ACI 209 R- 92 model

The shrinkage model does not consider cement type as one of the input parameters; despite the fact of recognizing cement content as one of these parameters. This contradiction may add detrimentally to the accuracy of the model and designer confidence level on the model.

The mix design approach to describe the concrete may be useful as mentioned in the previous section. However, it restricts the use of the model to a stage when these proportions are known. It also disables the possibility of improving its accuracy by substitution of tested properties of the concrete as it is observed in the shrinkage model.

Temperature effects are not considered, despite the advanced level of complexity of the ACI 209 R-92 model. The influence of temperature to creep and shrinkage has been discussed in chapter 2 and should not be disregarded.

The model is highly sensitive to the curing period of the concrete. In fact, the mathematical expressions of the model change for curing periods different to 7 days. The high sensitivity to curing period changes is aggravated by the fact that the model may respond in opposite direction to the expected change as shown in figure 5.14 of chapter 5.

6.7 RILEM B3 Model

6.7.1 Advantages of RILEM B3 model

The B3 model is a detailed and sophisticated model that is able to include all the basic input requirements stated in the assessment criteria and other parameters that are relevant as well. These additional parameters are the water, cement and aggregate content. The mix proportions and the usual mechanical properties of the concrete are able to describe the concrete thoroughly.

Unique features of this model when compared to others in this project are its ability to distinguish the basic creep from the drying creep and the use of a compliance function which reduces the risk of errors due to inaccurate values of the elastic modulus.

The model has low sensitivity to small changes of input parameter and it enables the substitution of tested values of compressive strength and elastic modulus which improves its accuracy. It also accounts for drying before loading which is often the case in WRS construction.

Curing methods are extensively covered under the B3 model. It accounts for steam or water curing and sealed structural elements in the form of correction factors to the ultimate shrinkage coefficient, which is a practical way of dealing with this parameter. From all models under scrutiny in this project, only the B3 model and the ACI 209 R-92 take curing methods into consideration.

6.7.2 Disadvantages of RILEM B3 model

The most apparent disadvantage of this model is its complexity. The mathematical expressions are complex and the combination of these expressions creates a matrix of equations of considerable size. This increases computational time significantly, if the designer is processing these computations by hand and increases the risk of computational or programming mistakes due to the number of equations involved.

The effects of temperature to creep and shrinkage are not considered despite this increased level of complexity. Also the effects of cement content and aggregate content are only considered for the creep phenomena and not in shrinkage calculation.

The model requires specific concrete mix proportions which may not be available at the time of design. This may limit its use to a later stage as a confirmation model, yet considering the complexity of the model the designer may want to use the model as the main method.

Although the specimen geometry is considered, in terms of volume/surface area ratio, an additional requirement in the form of the shape of the structure is required. A list is provided with values for respective shapes. This is not a general method, as some structural elements may have shapes that differ significantly from the shapes provided on the list (e.g. column heads inside on the inside of a reservoir).

Furthermore, the model may respond incorrectly to specimen size (V/S) or curing time chances as indicated in derivation 5.2 and figure 5.15 respectively.

6.8 SABS 0100

6.8.1 Advantages of SABS 0100 creep model

The main advantage of the SABS 0100 creep model is its simplicity. It allows quick computations without the use of many input parameters within acceptable accuracy. These simple mathematical expressions make the model suitable to be used in a design office during the preliminary stages of design.

Also of relevant importance is the provision for aggregate type which is unique for this model. The model uses work done by Alexander (1985) which enables the calculation of elastic modulus at the age of 28 days according to aggregate type through the equation $E_{cm28} = K_0 + 0.2 f_{cm28}$ (Equation 6.1), in which K_o represents the aggregate type.

It is also possible to substitute the value of elastic modulus and compressive strength by tested values which improves its accuracy.

6.8.2 Disadvantages of SABS 0100 creep model

The main disadvantage of the SABS 0100 model is its table built-in approach to model the specific creep. As a result of this approach, the 30 year creep coefficient needs to be regarded as an input parameter. This causes automation limitations, a non programmable model and high sensitivity to changes of the 30 year creep coefficient to the overall specific creep.

The overly simple approach implies that some of the basic input requirements established in the assessment criteria (i.e. cement type and curing time) which are of importance to creep calculation are not considered. Consequently drying before loading, which is a reality in WRS construction, is also not considered.

The provision for effective section thickness of structural element of 150, 300 and 600 mm does not cover small specimens used during laboratory testing or structural elements of significantly different sizes. This prevents calibration to standard tests and limits the designer to the provided table.

CHAPTER 7
RESULTS

7.1. Introduction

In this chapter, the measured strains of all data sets are compared with the corresponding calculated strains of the creep and shrinkage models. The individual experimental results within the data sets are also compared with their respective calculated strains.

The comparison takes place in the form of statistical evaluation of the prediction models to the experimentally measured strains (table 7.1 to 7.18) as well as a visual observation through illustrations from figure 7.1 to figure 7.20. For scientific reasons, greater importance is given to the statistic evaluation over the visual observations; however conclusions can be drawn in terms of under/over prediction of the models through the illustrations.

The accuracy of model predictions to individual experiments is shown in Appendix A. In this chapter the results presented are those of sets of data which contain a number of these experiments grouped together as explained before in Chapter 3.

7.2 Shrinkage results

7.2.1. Data set A

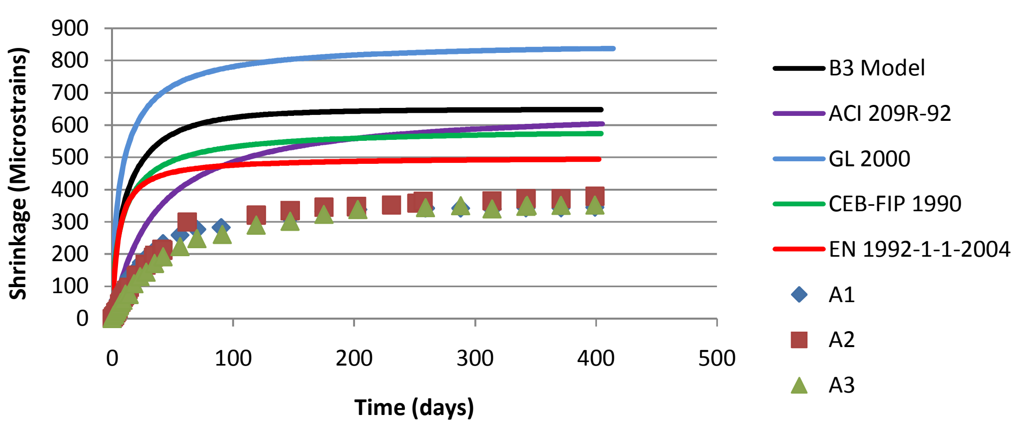

Figure 7.1 a) Measured and calculated shrinkage strains over time – data set A

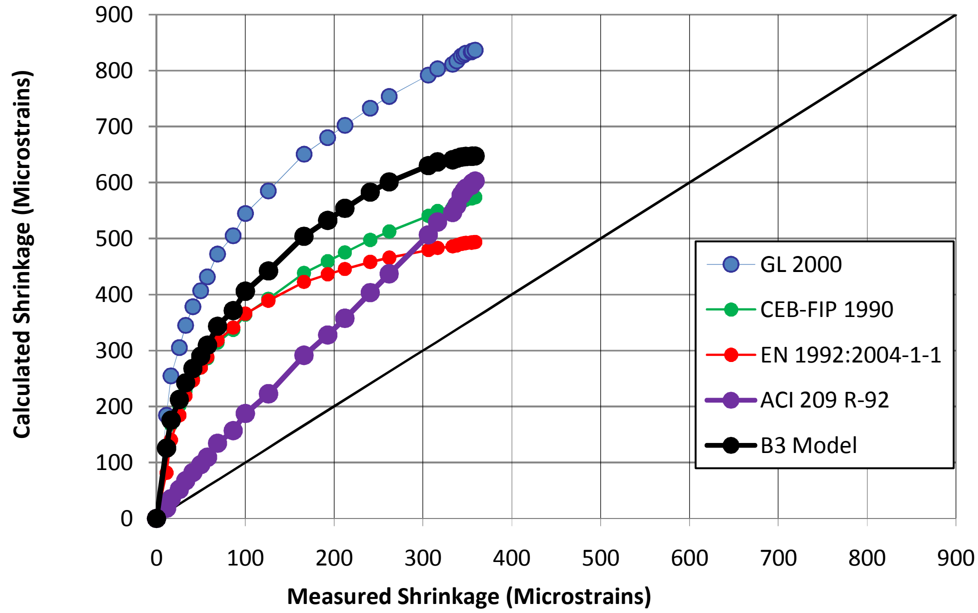

Figure 7.1 b) Calculated vs. Measured shrinkage - data set A

Table 7.1: Properties of tested concrete, statistical results and visual observation for shrinkage prediction of data set A.

Data set Name	Experiment Names	t_c (days)	T (°C)	RH (%)	$f_{cm\,28}$ (MPa)	H (mm)	V/S (mm)
Data set A	A1,A2,A3	7	23	50	35	25.5	11.8

Models	GL 2000	CEB-FIP 1990	EN 1992 -1-1: 2004	ACI 209 R-92	B3 Model
BP-COV* (%)	258	138.6	121.4	**88.2**	172.7
CEB MSE** (%)	629.8	391.7	334.1	**80.3**	421.7
Observation	All models over predict the measured shrinkage				

Legend: * - COV: Bažant and Panula coefficient of variation;

** - CEB MSE: CEB Mean square error

***- highlighted cell indicates lowest error.

7.2.2. Data set B

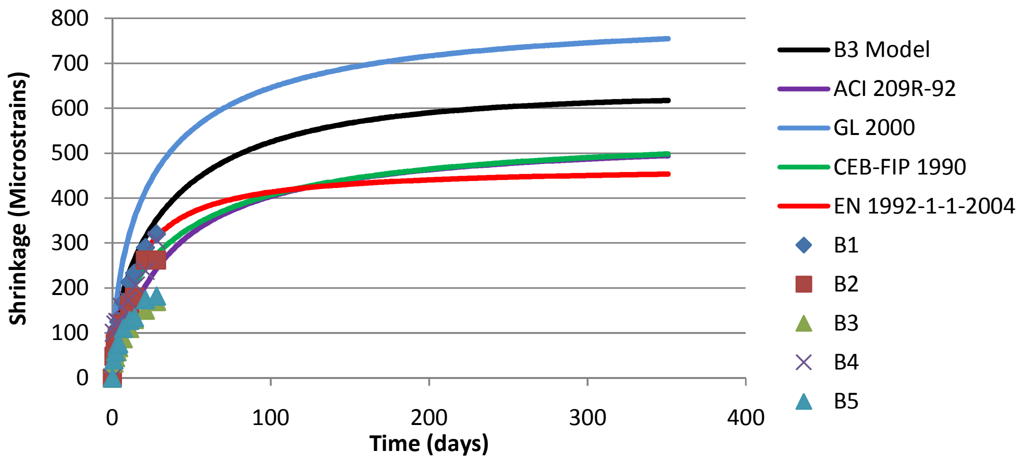

Figure 7.2 a) Measured and calculated shrinkage strains over time – data set B

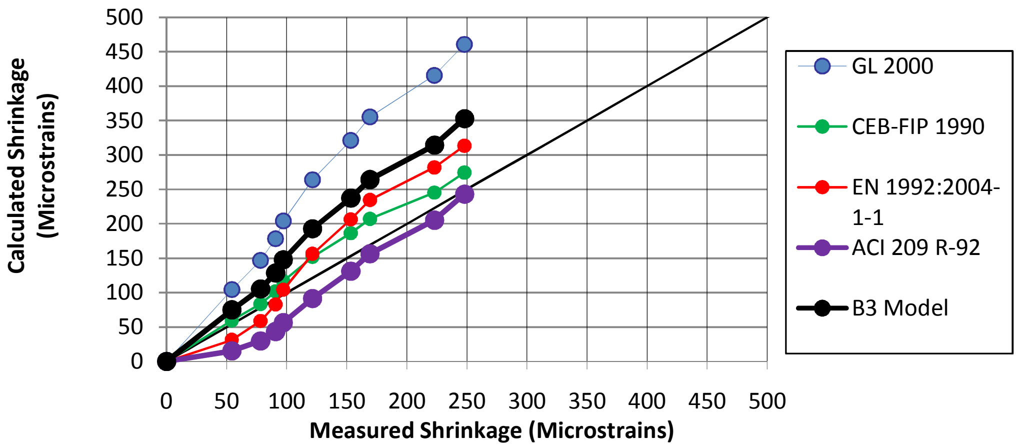

Figure 7.2 b) Calculated vs. Measured shrinkage - data set B

Table 7.2: Properties of tested concrete, statistical results and visual observation for shrinkage prediction of data set B.

Data set Name	Experiment Names	t_c (days)	T (℃)	RH (%)	$f_{cm\ 28}$ (MPa)	H (mm)	V/S (mm)
Data set B	B1,B2,B3,B4,B5	14	23	55	35.8	50	20

Models	GL 2000	CEB-FIP 1990	EN 1992 -1-1:2004	ACI 209 R-92	B3 Model
BP-COV (%)	118.2	**19.3**	35.3	26.5	57.6
CEB-MSE (%)	100.3	**16.5**	28.9	40.1	47.3
Observation	Over predicts	Over predicts	Over predicts	Under predicts	Over Predicts

7.2.3 Data set C

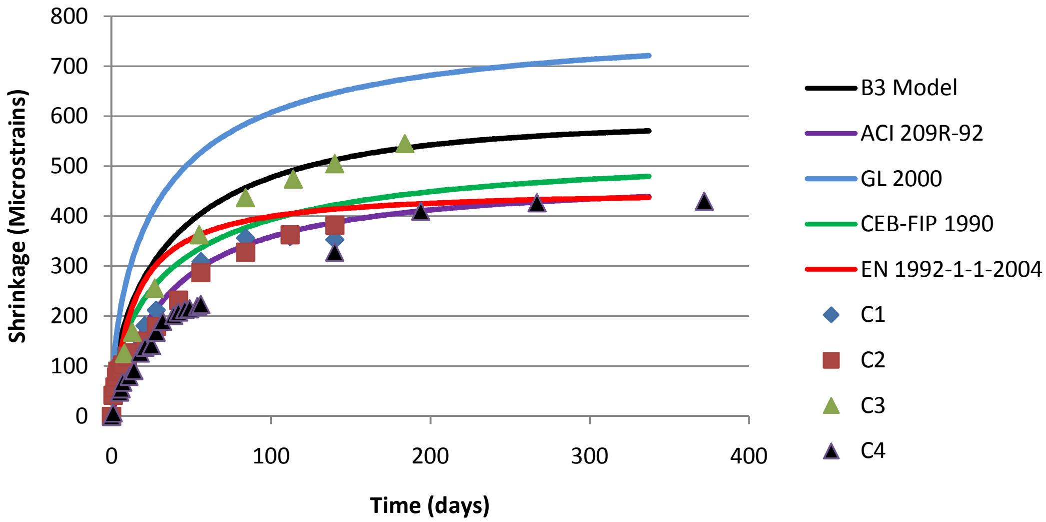

Figure 7.3 a) Measured and calculated shrinkage strains over time – data set C

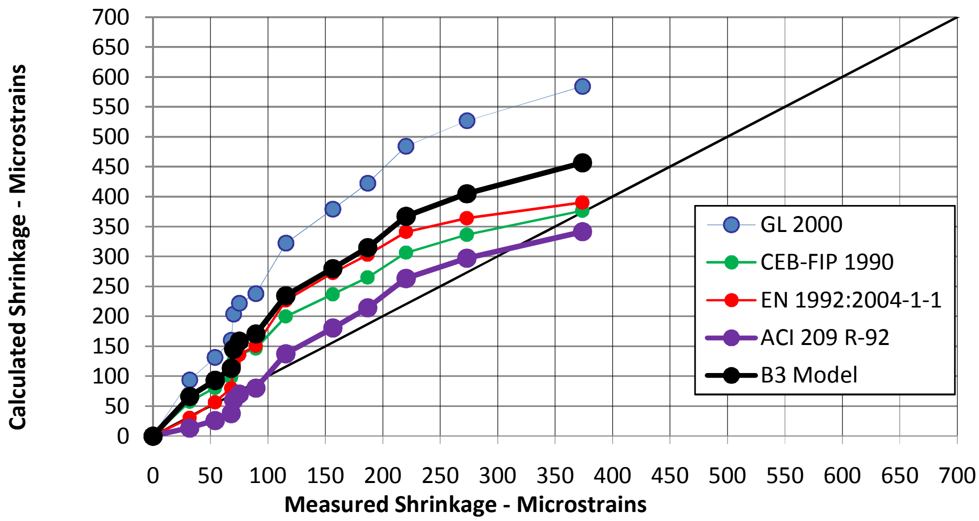

Figure 7.3 b) Calculated vs. Measured shrinkage - data set C

Table 7.3: Properties of tested concrete, statistical results and visual observation for shrinkage prediction of data set C.

Data set Name	Experiment Names	t_c (days)	T (℃)	RH (%)	$f_{cm\ 28}$ (MPa)	H (mm)	V/S (mm)
Data set C	C1,C2,C3,C4	28	23	58	36	50	21.7

Models	GL 2000	CEB-FIP 1990	EN 1992 - 1-1:2004	ACI 209 R-92	B3 Model
BP-COV (%)	126.4	38.8	49.8	**16.1**	66.5
CEB-MSE (%)	145.9	55.0	55.0	**27.4**	80.0
Observation	Over predicts	Over predicts	Over predicts	Mixed Behaviour*	Over Predicts

Legend: *- Mixed behaviour: indicates that the model fluctuates around the 45° line, and it is often an good prediction

7.2.4 Data set D

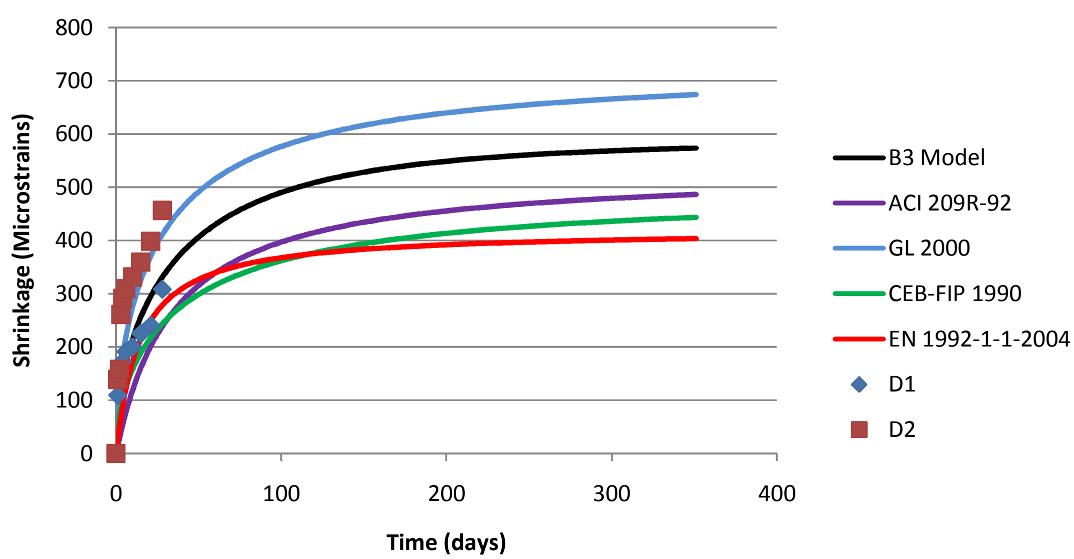

Figure 7.4 a) Measured and calculated shrinkage strains over time – data set D

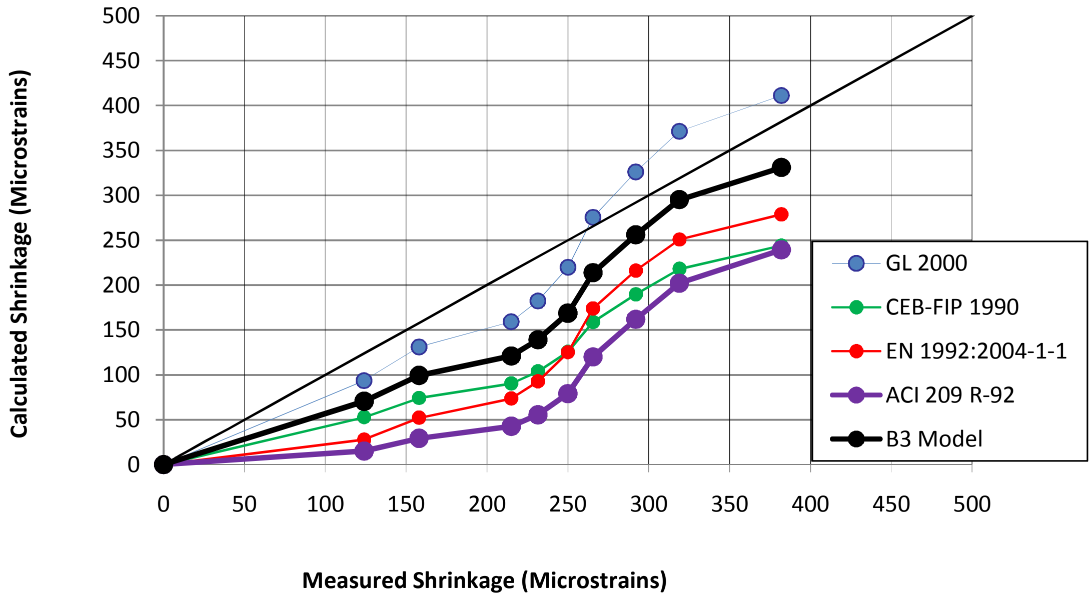

Figure 7.4 b) Calculated vs. Measured shrinkage - data set D

Table 7.4: Properties of tested concrete, statistical results and visual observation for shrinkage prediction of data set D.

Data set Name	Experiment Names	t_c (days)	T (°C)	RH (%)	$f_{cm\ 28}$ (MPa)	H (mm)	V/S (mm)
Data set D	D1,D2	14	23	60	40.5	50	20

Models	GL 2000	CEB-FIP 1990	EN 1992 - 1-1:2004	ACI 209 R-92	B3 Model
BP-COV (%)	**17.0**	49.6	48.3	65.1	28.9
CEB-MSE (%)	**17.2**	47.4	51.7	65.8	30.9
Observation	Mixed Behaviour	Under predicts	Under predicts	Under predicts	Under Predicts

7.2.5 Data set E

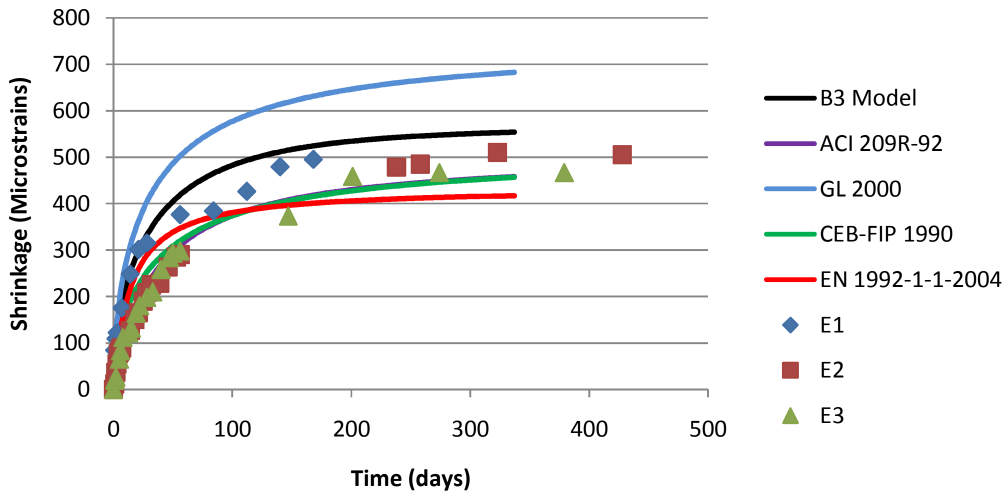

Figure 7.5 a) Measured and calculated shrinkage strains over time – data set E

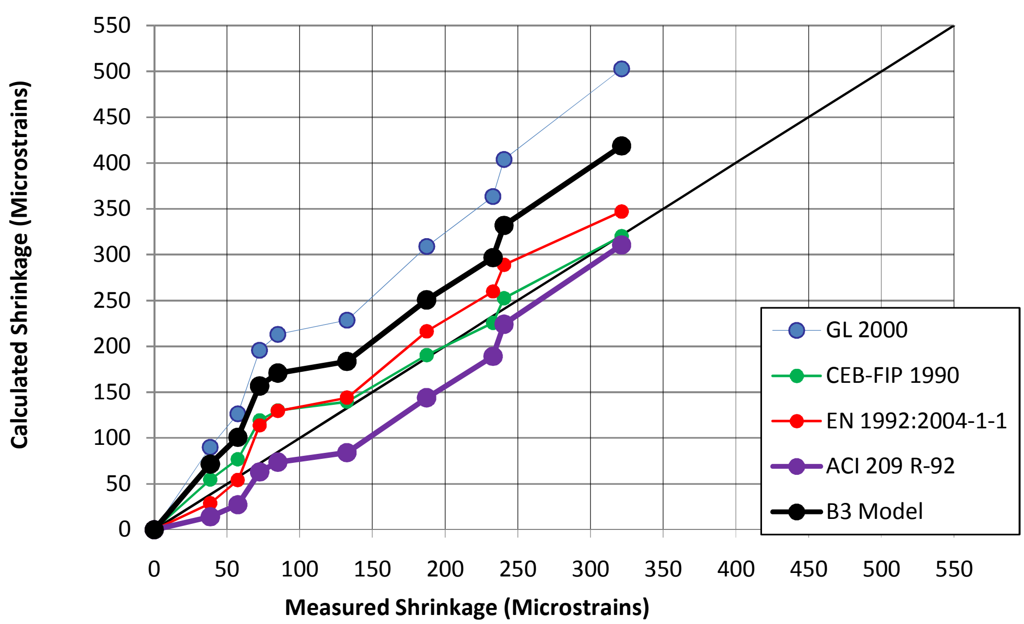

Figure 7.5 b) Calculated vs. Measured shrinkage - data set E

Table 7.5: Properties of tested concrete, statistical results and visual observation for shrinkage prediction of data set E.

Data set Name	Experiment Names	t_c (days)	T (℃)	RH (%)	$f_{cm\ 28}$ (MPa)	H (mm)	V/S (mm)
Data set E	E1,E2,E3	28	23.7	55	42.7	50	20

Models	GL 2000	CEB-FIP 1990	EN 1992 -1-1:2004	ACI 209 R-92	B3 Model
COV (%)	90.5	**17.0**	22.1	24.7	51.8
CEB-MSE (%)	104.6	31.4	**27.8**	35.4	66.3
Observation	Over Predicts	Mixed Behaviour	Over predicts	Over predicts	Over Predicts

7.2.6. Data set F

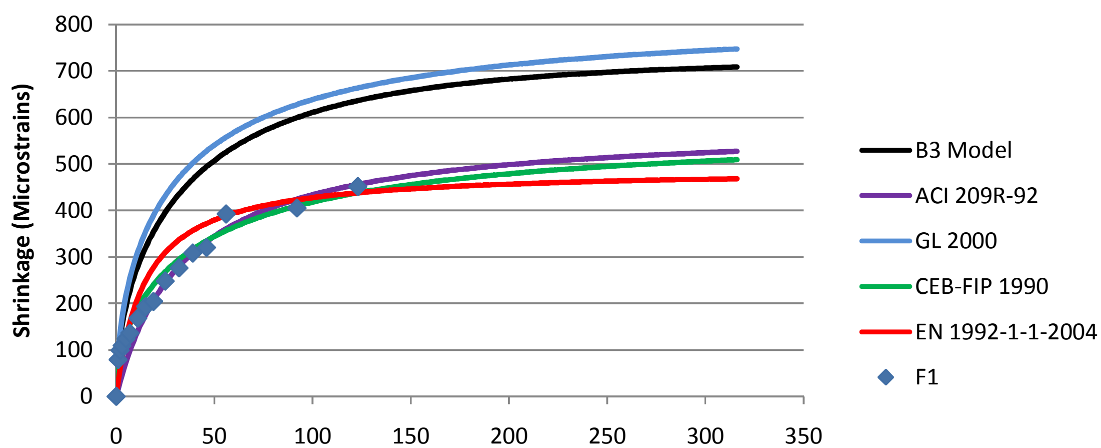

Figure 7.6 a) Measured and calculated shrinkage strains over time – data set F

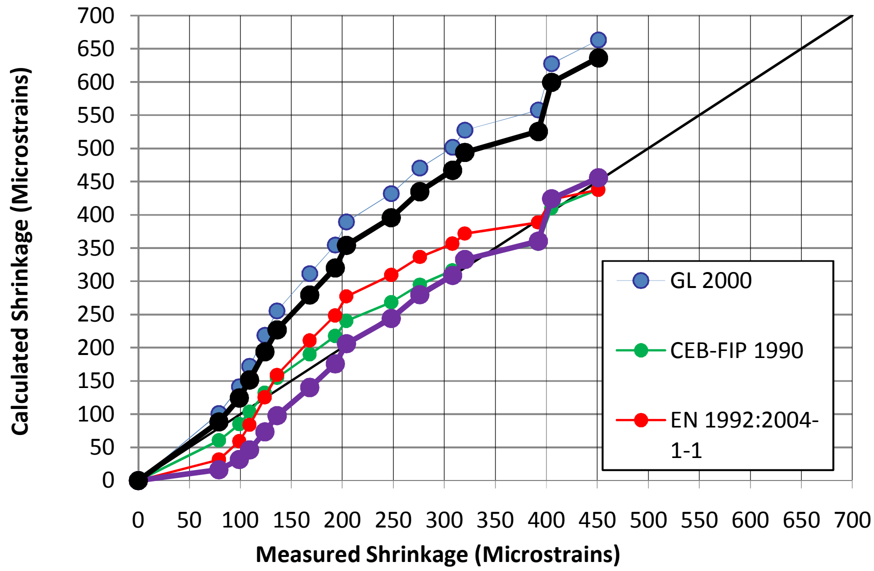

Figure 7.6 b) Calculated vs. Measured shrinkage - data set F

Table 7.6: Properties of tested concrete, statistical results and visual observation for shrinkage prediction of data set F.

Data set Name	Experiment Names	t_c (days)	T (°C)	RH (%)	$f_{cm\ 28}$ (MPa)	H (mm)	V/S (mm)
Data set F	F1	49	21	43	41	51	20.8

Models	GL 2000	CEB-FIP 1990	EN 1992-1-1: 2004	ACI 209 R-92	B3 Model
BP-COV (%)	73.0	**9.0**	19.7	16.3	59.8
CEB-MSE (%)	67.2	**11.2**	26.4	33.8	52.7
Observation	Over Predicts	Mixed Behaviour	Mixed Behaviour	Under predicts	Over Predicts

7.2.7. Data set G

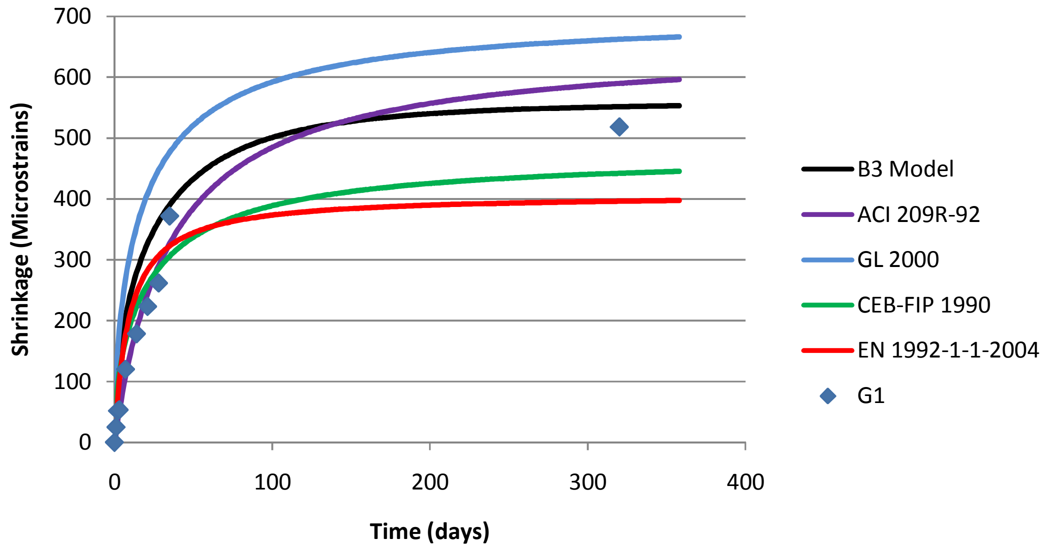

Figure 7.7 a) Measured and calculated shrinkage strains over time – data set G

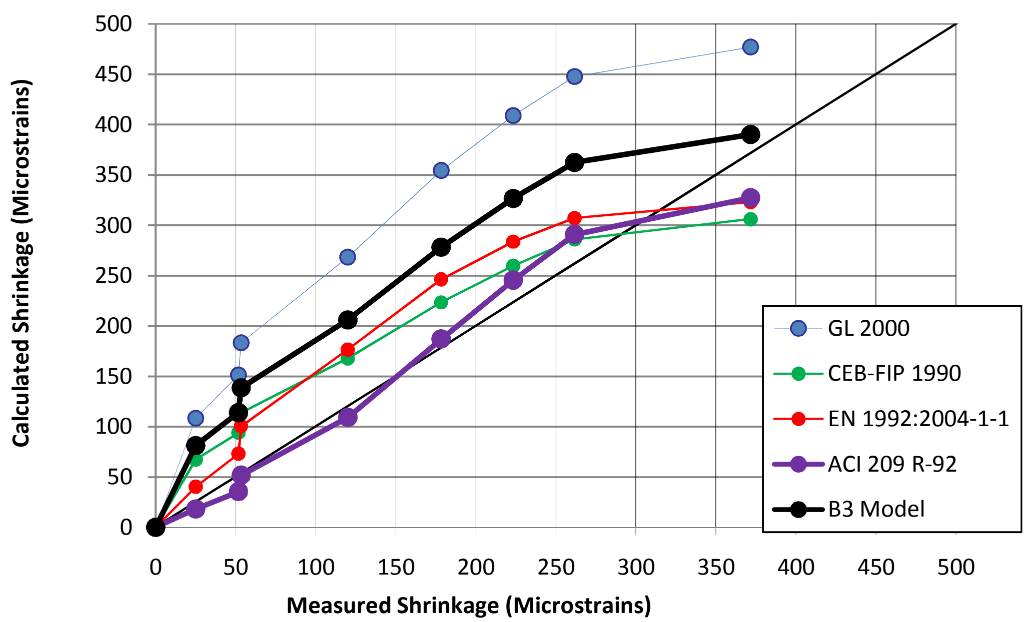

Figure 7.7 b) Calculated vs. Measured shrinkage - data set G

Table 7.7: Properties of tested concrete, statistical results and visual observation for shrinkage prediction of data set G.

Data set Name	Experiment Names	t_c (days)	T (℃)	RH (%)	$f_{cm\ 28}$ (MPa)	H (mm)	V/S (mm)
Data set G	G1	7	25	50	52	38	17
Models	GL 2000	CEB-FIP 1990	EN 1992- 1-1 : 2004	ACI 209 R-92	B3 Model		
BP-COV (%)	72.4	25.7	29.9	**15.3**	37.8		
CEB-MSE (%)	157.3	71.4	43.1	**15.6**	101.2		
Observation	Over Predicts	Over predicts	Over predicts	Mixed behaviour	Over Predicts		

7.2.8. Data set H

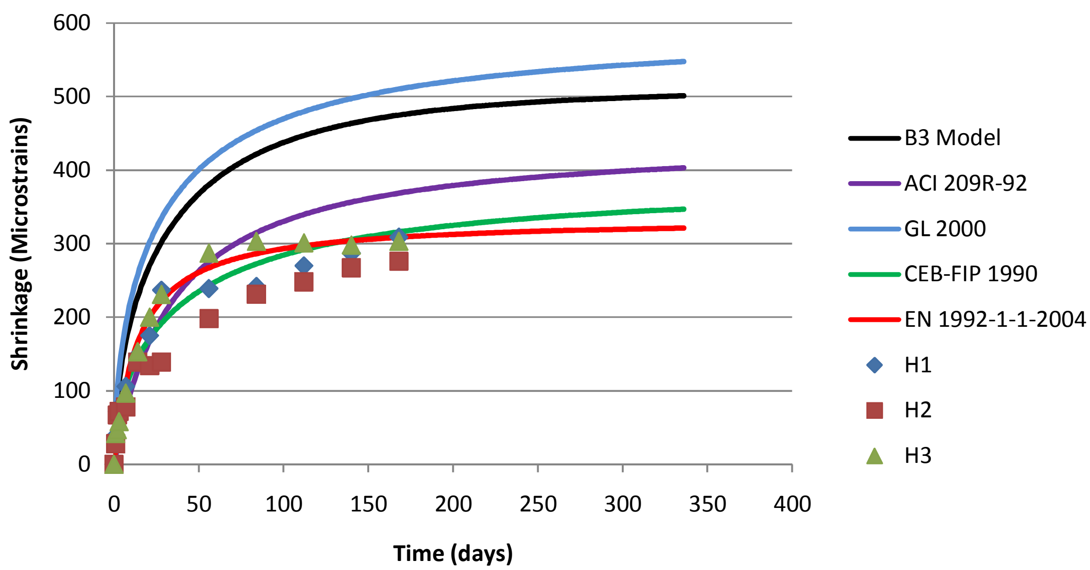

Figure 7.8 a) Measured and calculated shrinkage strains over time – data set H

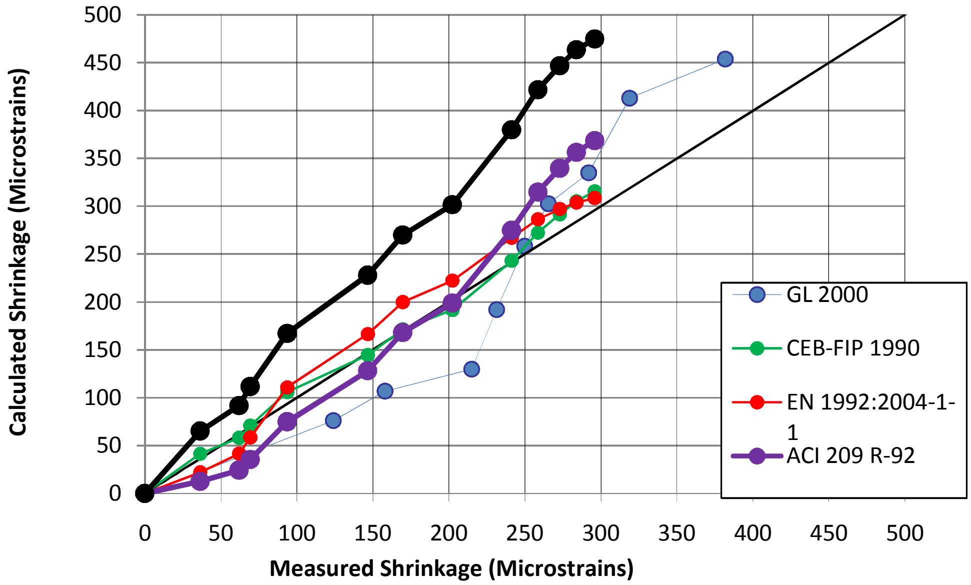

Figure 7.8 b) Calculated vs. Measured shrinkage - data set H

Table 7.8: Properties of tested concrete, statistical results and visual observation for shrinkage prediction of data set H.

Data set Name	Experiment Names	t_c (days)	T (℃)	RH (%)	$f_{cm\ 28}$ (MPa)	H (mm)	V/S (mm)
Data set H	H1,H2,H3	29	22.3	65	52.3	50	20

Models	GL 2000	CEB-FIP 1990	EN 1992-1-1: 2004	ACI 209 R-92	B3 Model
BP-COV (%)	92.0	**6.9**	13.7	26.1	74.1
CEB-MSE (%)	81.4	**7.2**	18.7	33.5	62.2
Observation	Mixed behaviour	Mixed behaviour	Over predicts	Mixed behaviour	Over Predicts

7.2.9 Data set I

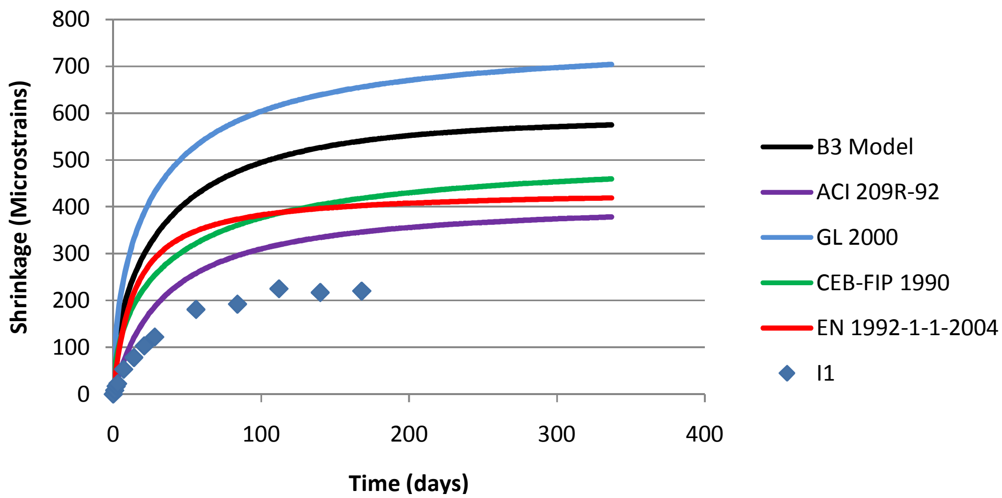

Figure 7.9 a) Measured and calculated shrinkage strains over time – data set I

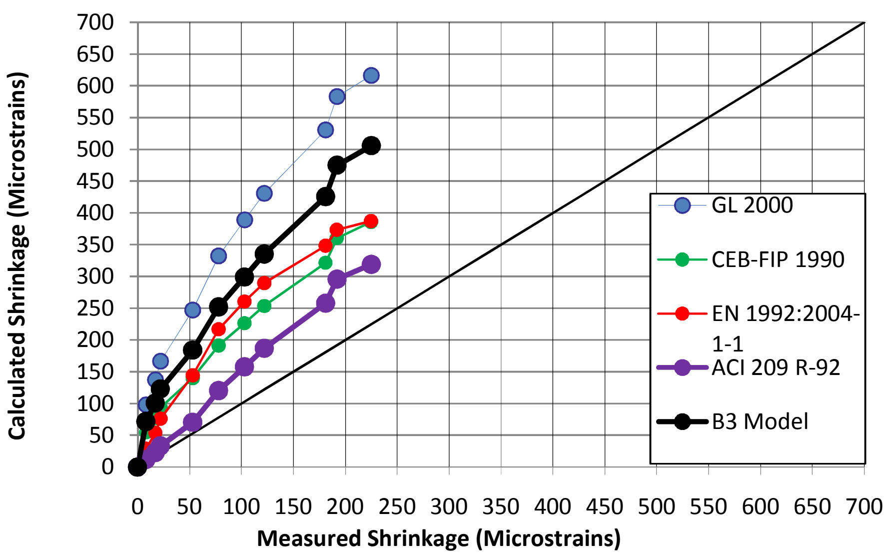

Figure 7.9 b) Calculated vs. Measured shrinkage - data set I

Table 7.9: Properties of tested concrete, statistical results and visual observation for shrinkage prediction of data set I.

Data set Name	Experiment Names	t_c (days)	T (°C)	RH (%)	$f_{cm\ 28}$ (MPa)	H (mm)	V/S (mm)
Data set I	I1	28	21	61	36	50	20

Models	GL 2000	CEB-FIP 1990	EN 1992 1-1: 2004	ACI 209 R-92	B3 Model
BP-COV (%)	287.4	124.8	134.6	**66.9**	204.0
CEB-MSE (%)	479.5	238.3	162.5	**48.7**	336.7
Observation	All models over predict the measured shrinkage				

7.2.10. Data set J

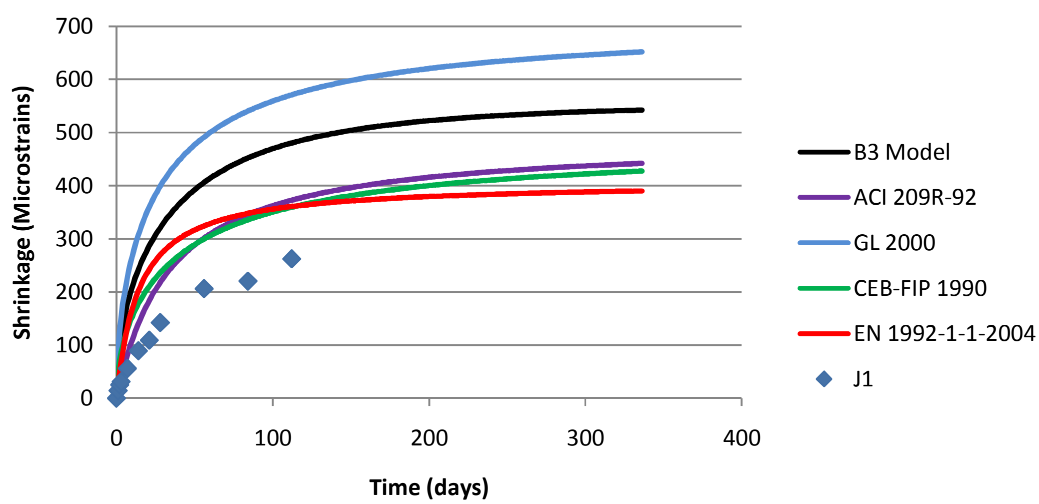

Figure 7.10 a) Measured and calculated shrinkage strains over time – data set J

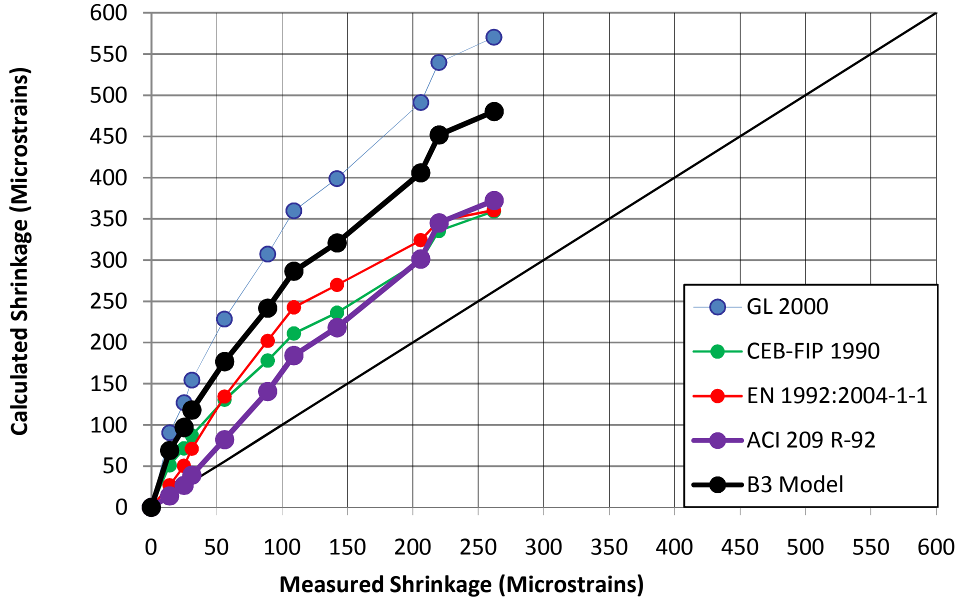

Figure 7.10 b) Calculated vs. Measured shrinkage - data set J

Table 7.10: Properties of tested concrete, statistical results and visual observation for shrinkage prediction of data set J.

<table>
<tr><th>Data set Name</th><th colspan="2">Experiment Names</th><th>t_c (days)</th><th>T (℃)</th><th>RH (%)</th><th>$f_{cm\ 28}$ (MPa)</th><th>H (mm)</th><th>V/S (mm)</th></tr>
<tr><td>Data set J</td><td colspan="2">J1</td><td>29</td><td>21</td><td>61</td><td>42</td><td>50</td><td>20</td></tr>
<tr><td>Models</td><td>GL 2000</td><td colspan="2">CEB-FIP 1990</td><td colspan="2">EN 1992 - 1-1:2004</td><td colspan="2">ACI 209 R-92</td><td>B3 Model</td></tr>
<tr><td>BP-COV (%)</td><td>204.5</td><td colspan="2">75.8</td><td colspan="2">84.5</td><td colspan="2">69.1</td><td>145.4</td></tr>
<tr><td>CEB-MSE (%)</td><td>281.9</td><td colspan="2">125.5</td><td colspan="2">94.1</td><td colspan="2">47.4</td><td>199.8</td></tr>
<tr><td>Observation</td><td colspan="8">All models over predict the measured shrinkage</td></tr>
</table>

7.2.11 Data set K

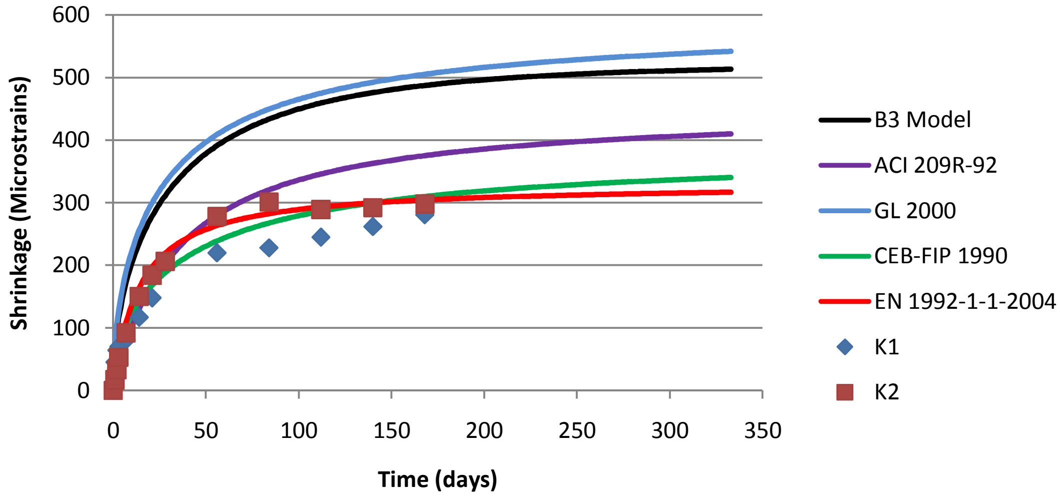

Figure 7.11 a) Measured and calculated shrinkage strains over time – data set K

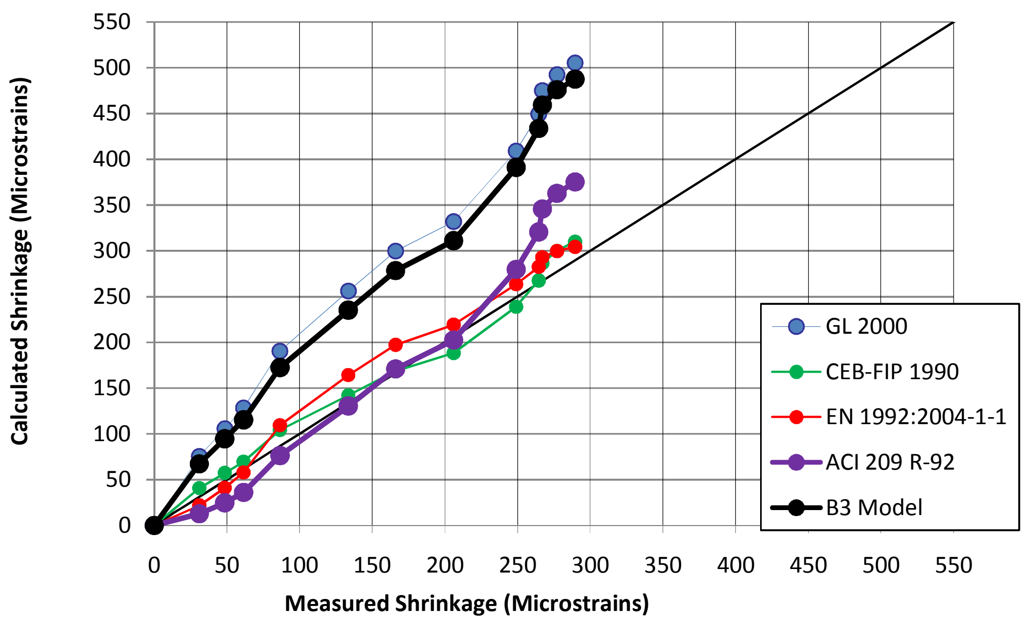

Figure 7.11 b) Calculated vs. Measured shrinkage - data set K

Table 7.11: Properties of tested concrete, statistical results and visual observation for shrinkage prediction of data set K.

Data set Name	Experiment Names	t_c (days)	T (℃)	RH (%)	$f_{cm\ 28}$ (MPa)	H (mm)	V/S (mm)
Data set K	K1,K2	32	22	65	54	50	20

Models	GL 2000	CEB-FIP 1990	EN 1992 - 1-1: 2004	ACI 209 R-92	B3 Model
BP-COV (%)	93.8	**8.6**	13.0	27.8	83.3
CEB-MSE (%)	93.9	**13.5**	15.9	30.3	79.4
Observation	Over Predicts	Mixed behaviour	Over predicts	Mixed behaviour	Over Predicts

7.3. Creep Results

7.3.1. Data set A

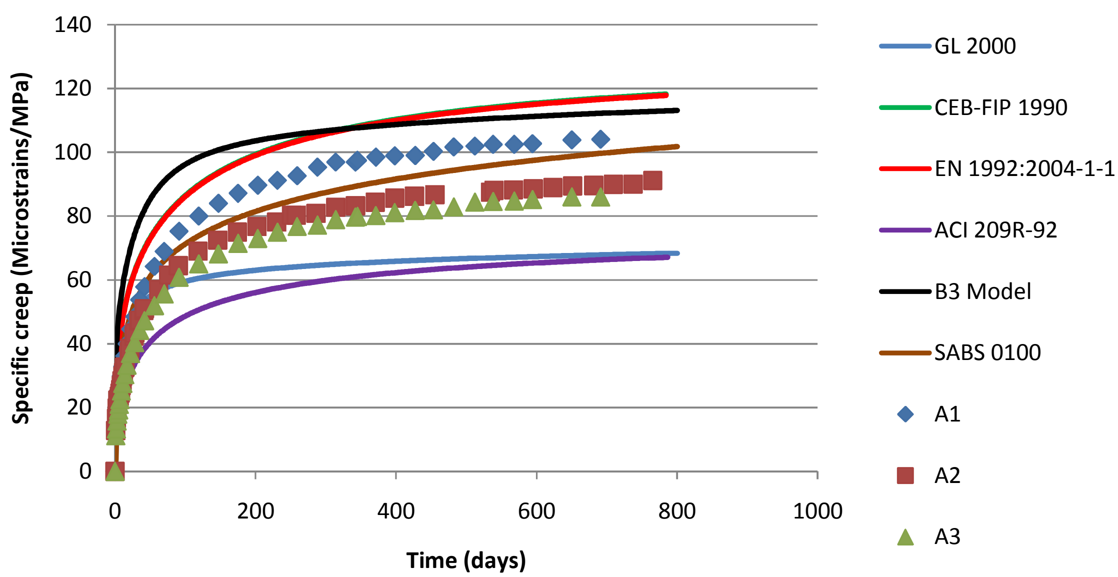

Figure 7.12 a) Measured and calculated specific creep strains over time – data set A

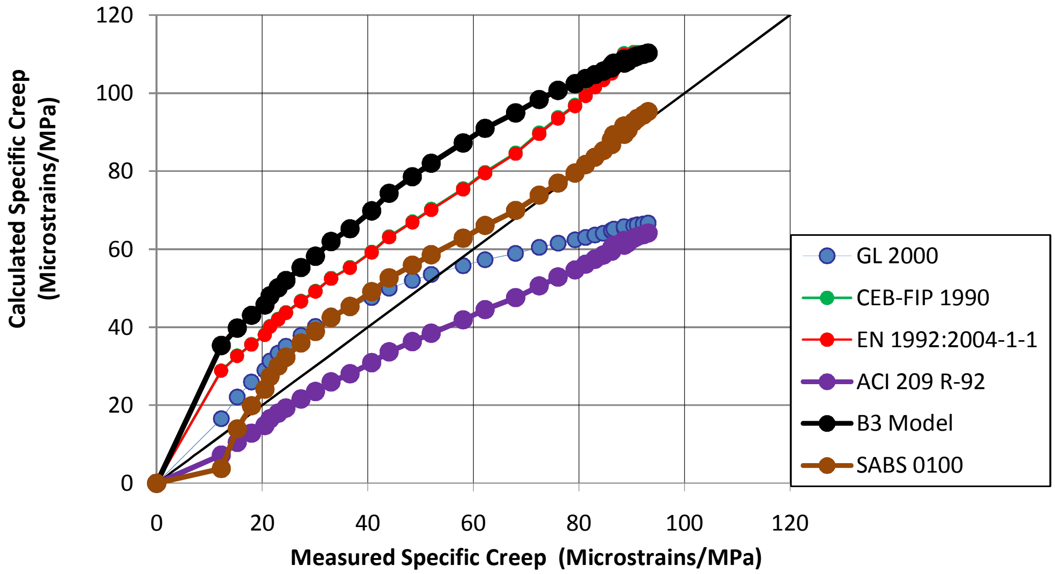

Figure 7.12 b) Calculated vs. Measured specific creep - data set A

Table 7.12: Properties of tested concrete, statistical results and visual observation for creep prediction of data set A.

Data set Name	Experiment Names	t_c (days)	t_o (days)	T (℃)	RH (%)	$f_{cm\ 28}$ (MPa)	E_{cm28} (GPa)	H (mm)	V/S (mm)
Data set A	A1,A2,A3	7	14	23	50	35	33	25.5	11.8

Models	GL 2000	CEB-FIP 1990	EN 1992 - 1-1: 2004	ACI 209 R-92	B3 Model	SABS 0100
BP-COV (%)	26.2	38.7	38.3	34.2	54.7	**12.2**
CEB-MSE (%)	28.5	57.9	57.4	28.2	82.1	**20.4**
Observation	Mixed Behaviour	Over Predicts	Over Predicts	Under Predicts	Over Predicts	Over Predicts

7.3.2. Data set C

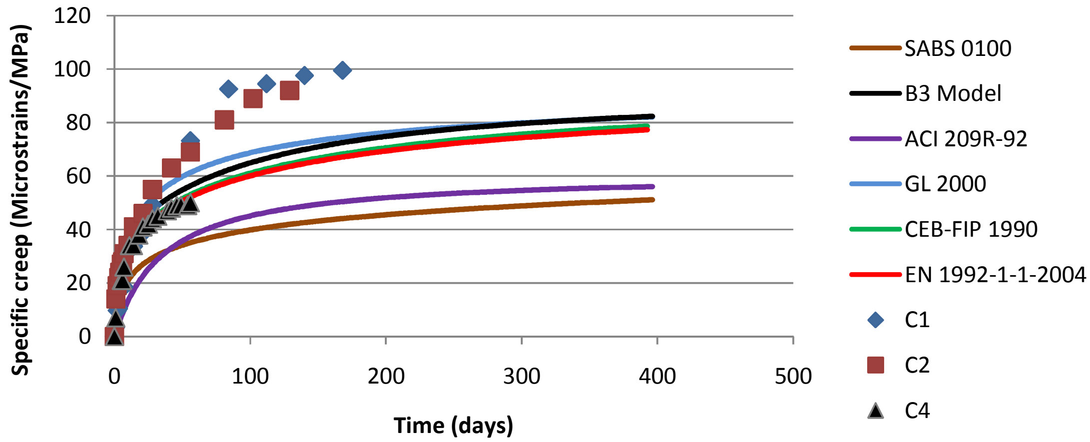

Figure 7.13 a) Measured and calculated specific creep strains over time – data set C

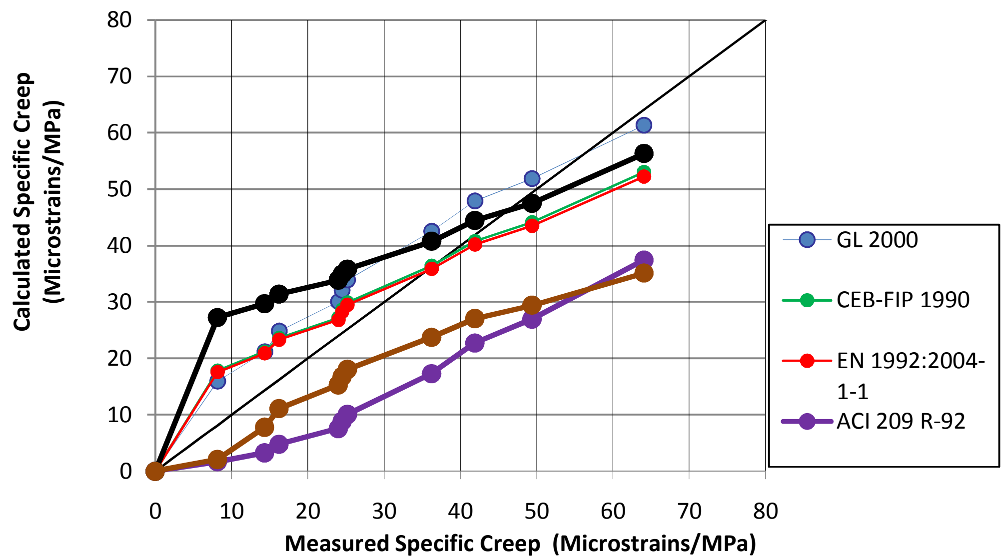

Figure 7.13 b) Calculated vs. Measured specific creep - data set C

Table 7.13: Properties of tested concrete, statistical results and visual observation for creep prediction of data set C.

Data set Name	Experiment Names	t_c (days)	t_o (days)	T (℃)	RH (%)	$f_{cm\ 28}$ (MPa)	E_{cm28} (GPa)	H (mm)	V/S (mm)
Data set C	C1,C2,C4	28	28	23	58	36	31.25	50	21.7

Models	GL 2000	CEB-FIP 1990	EN 1992 - 1-1: 2004	ACI 209 R-92	B3 Model	SABS 0100
BP-COV (%)	24.0	**22.7**	22.9	62.4	40.3	50.0
CEB-MSE (%)	**41.8**	44.3	42.8	61.8	89.7	42.3
Observation	Mixed Behaviour	Mixed Behaviour	Mixed Behaviour	Under Predicts	Mixed Behaviour	Under Predicts

7.3.3 Data set E

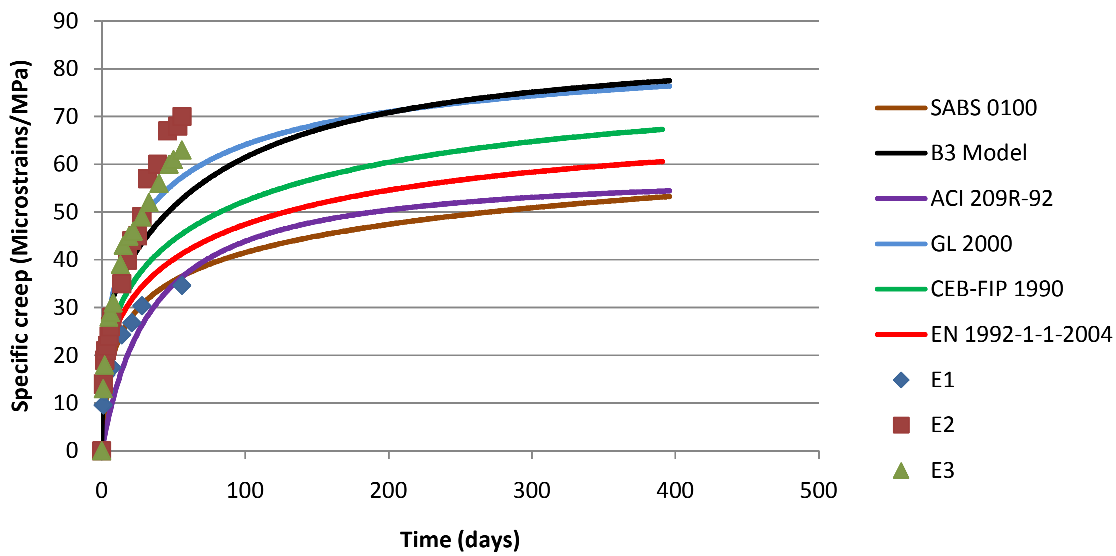

Figure 7.14 a) Measured and calculated specific creep strains over time – data set E

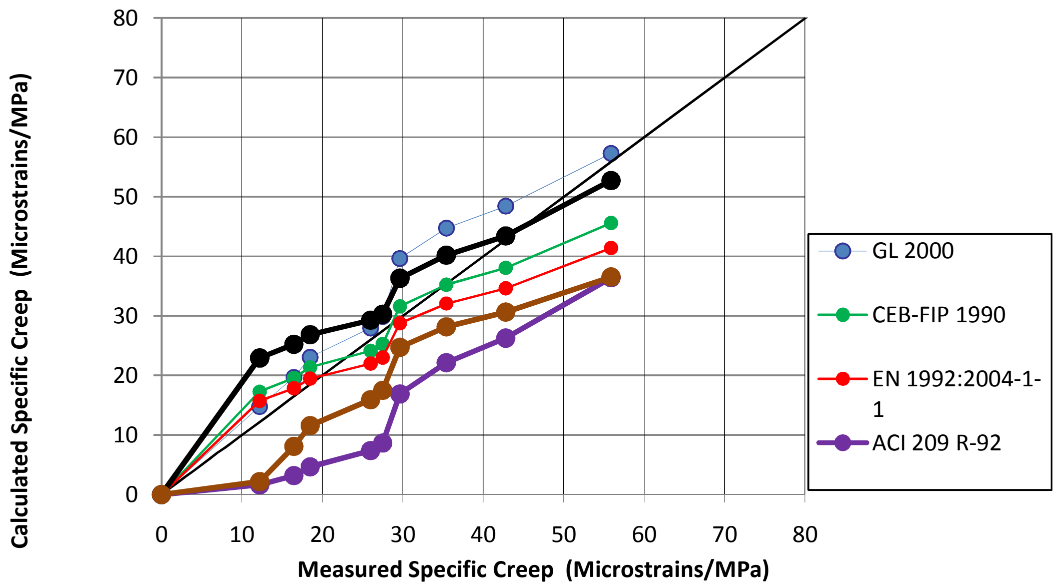

Figure 7.14 b) Calculated vs. Measured specific creep - data set E

Table 7.14: Properties of tested concrete, statistical results and visual observation for creep prediction of data set E.

Data set Name	Experiment Names	t_c (days)	t_o (days)	T (°C)	RH (%)	$f_{cm\ 28}$ (MPa)	E_{cm28} (GPa)	H (mm)	V/S (mm)
Data set E	E1,E2,E3	28	28	23.7	55	42.7	34.7	50	20

Models	GL 2000	CEB-FIP 1990	EN 1992 - 1-1: 2004	ACI 209 R-92	B3 Model	SABS 0100
BP-COV (%)	22.5	**17.0**	22.4	58.6	25.1	39.0
CEB-MSE (%)	22.5	17.9	**16.1**	62.2	38.6	40.7
Observation	Mixed Behaviour	Mixed Behaviour	Mixed Behaviour	Under Predicts	Mixed Behaviour	Under Predicts

7.3.4 Data set H

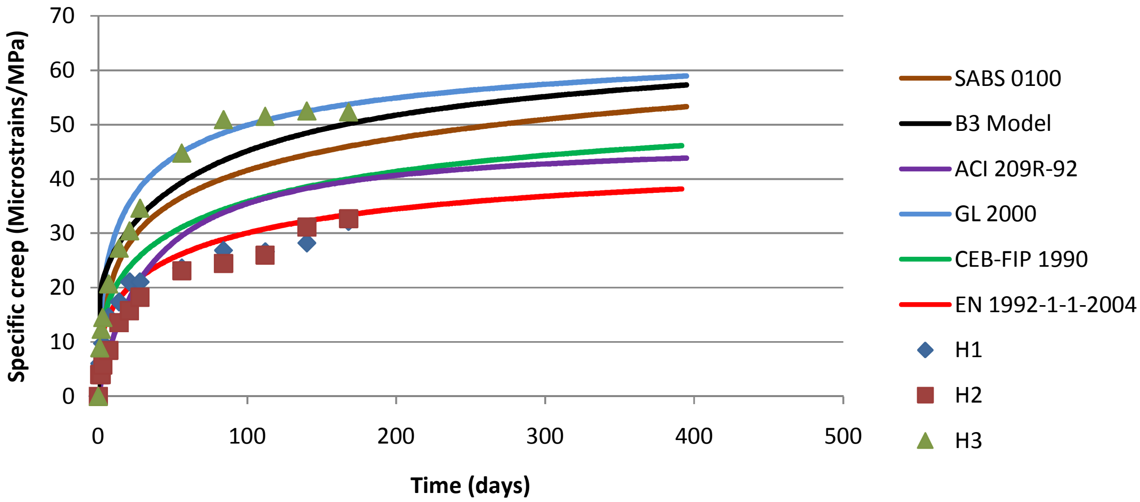

Figure 7.15 a) Measured and calculated specific creep strains over time – data set H

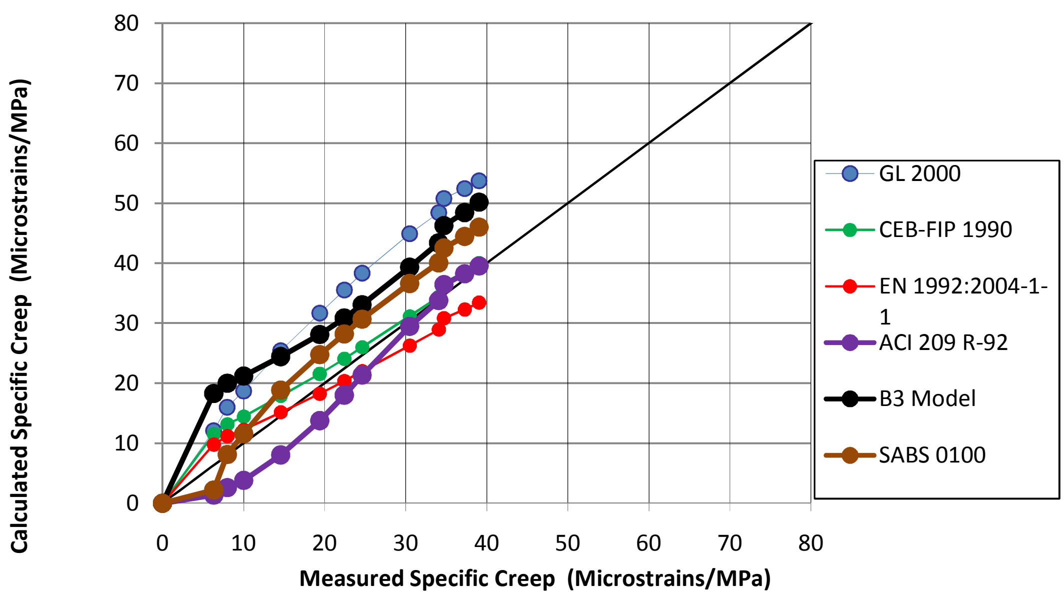

Figure 7.15 b) Calculated vs. Measured specific creep - data set H

Table 7.15: Properties of tested concrete, statistical results and visual observation for creep prediction of data set H.

Data set Name	Experiment Names	t_c (days)	t_o (days)	T (°C)	RH (%)	$f_{cm\ 28}$ (MPa)	E_{cm28} (GPa)	H (mm)	V/S (mm)
Data set H	H1,H2,H3	29	29	22.3	65	52.3	39.7	50	20

Models	GL 2000	CEB-FIP 1990	EN 1992 - 1-1: 2004	ACI 209 R-92	B3 Model	SABS 0100
BP-COV (%)	61.1	**14.8**	17.0	21.1	50.4	26.6
CEB-MSE (%)	65.4	33.8	**22.8**	38.8	83.9	27.9
Observation	Over Predicts	Over Predicts	Under Predicts	Under Predicts	Over Predicts	Over Predicts

7.3.5 Data set I

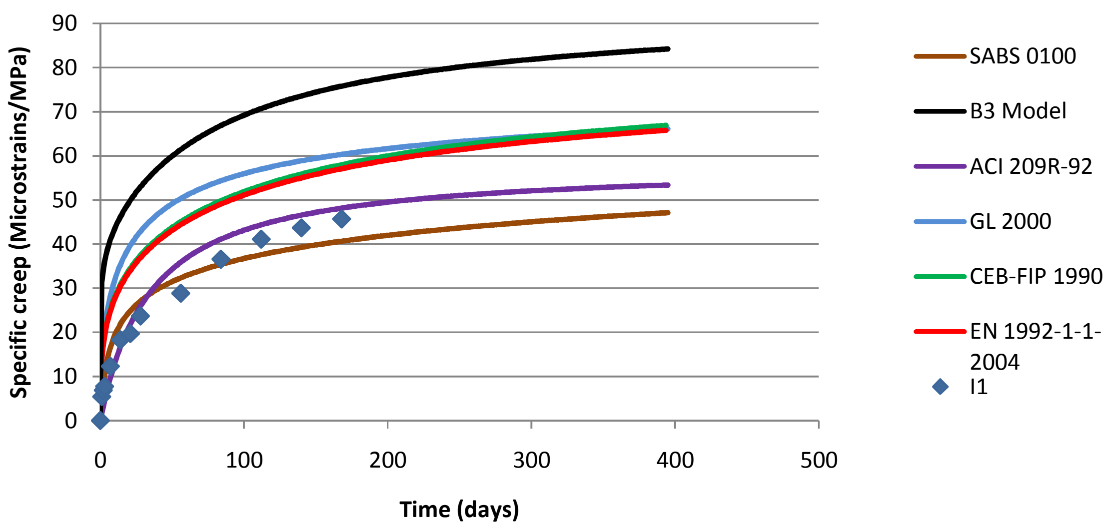

Figure 7.16 a) Measured and calculated specific creep strains over time – data set I

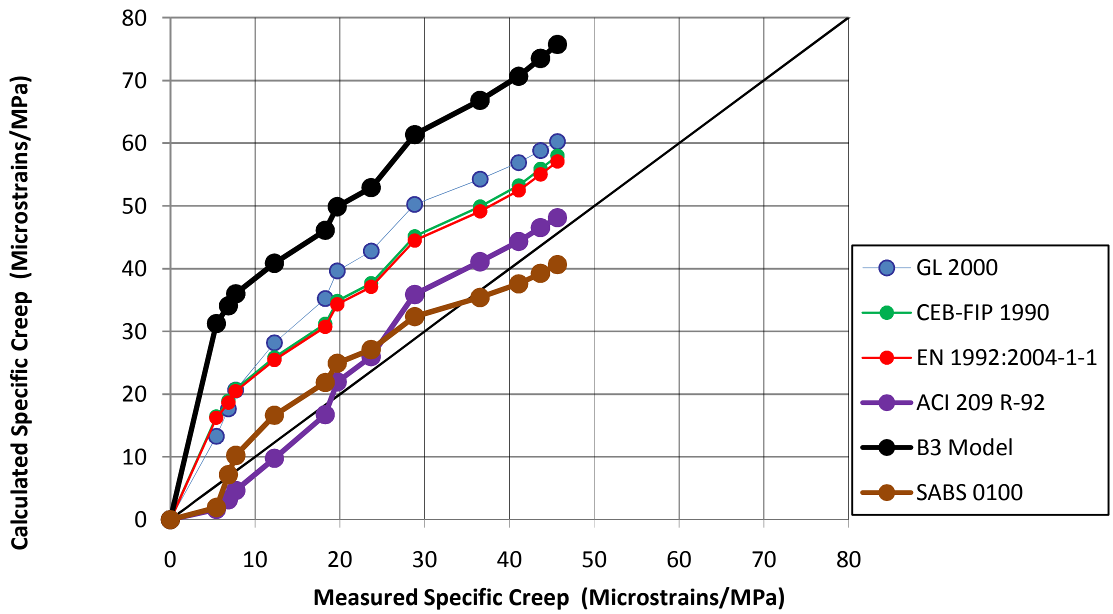

Figure 7.16 b) Calculated vs. Measured specific creep - data set I

Table 7.16: Properties of tested concrete, statistical results and visual observation for creep prediction of data set I

Data set Name	Experiment Names	t_c (days)	t_o (days)	T (°C)	RH (%)	$f_{cm\ 28}$ (MPa)	E_{cm28} (GPa)	H (mm)	V/S (mm)
Data set I	I1	28	29	21	61	36	35	50	20

Models	GL 2000	CEB-FIP 1990	EN 1992 - 1-1: 2004	ACI 209 R-92	B3 Model	SABS 0100
BP-COV (%)	79.0	65.2	62.5	17.7	142.1	**17.5**
CEB-MSE (%)	103.2	106.1	103.3	30.2	236.3	**26.3**
Observation	Over Predicts	Over Predicts	Over Predicts	Mixed Behaviour	Over Predicts	Mixed Behaviour

7.3.6 Data set J

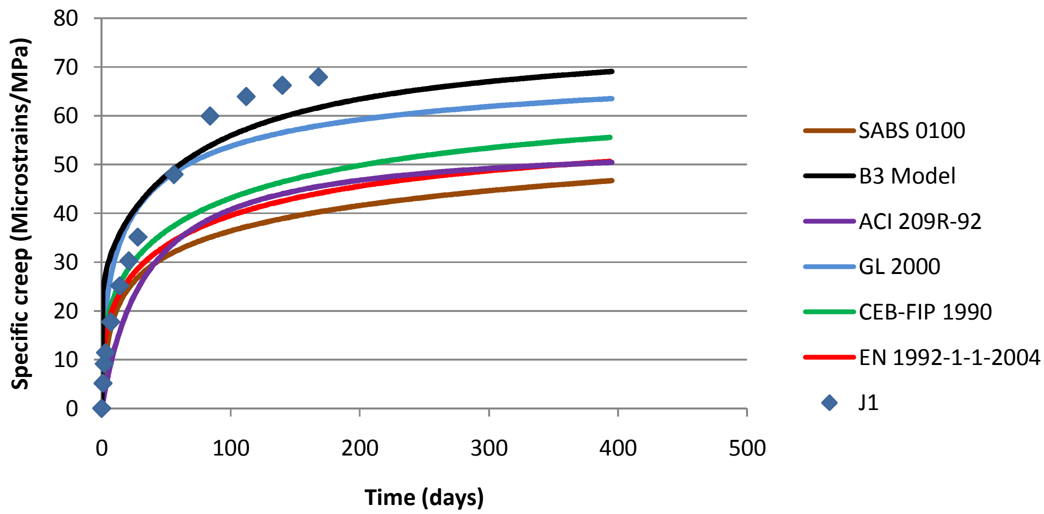

Figure 7.17 a) Measured and calculated specific creep strains over time – data set J

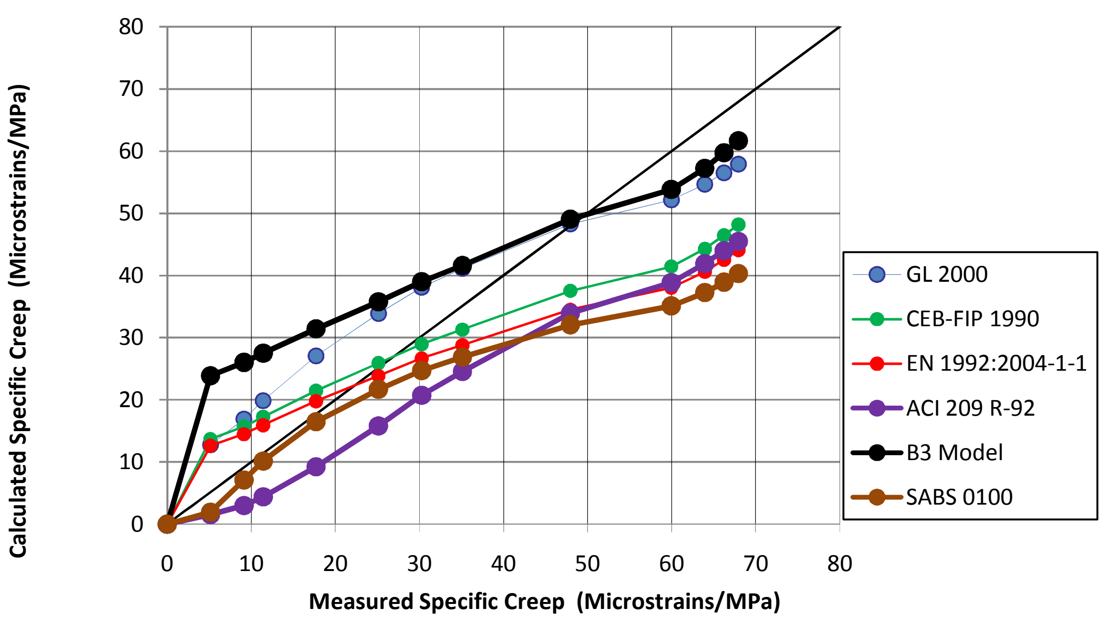

Figure 7.17 b) Calculated vs. Measured specific creep - data set J

Table 7.17: Properties of tested concrete, statistical results and visual observation for creep prediction of data set J

Data set Name	Experiment Names	t_c (days)	t_o (days)	T (°C)	RH (%)	$f_{cm\,28}$ (MPa)	E_{cm28} (GPa)	H (mm)	V/S (mm)
Data set J	J1	29	30	21	61	42	39	50	20

Models	GL 2000	CEB-FIP 1990	EN 1992 - 1-1: 2004	ACI 209 R-92	B3 Model	SABS 0100
BP-COV (%)	**25.6**	36.3	42.6	44.3	36.7	48.2
CEB-MSE (%)	58.2	57.9	52.2	45.0	127.9	**33.7**
Observation	All models over predict creep at early stages and under predict it in the long term					

7.3.7 Data set K

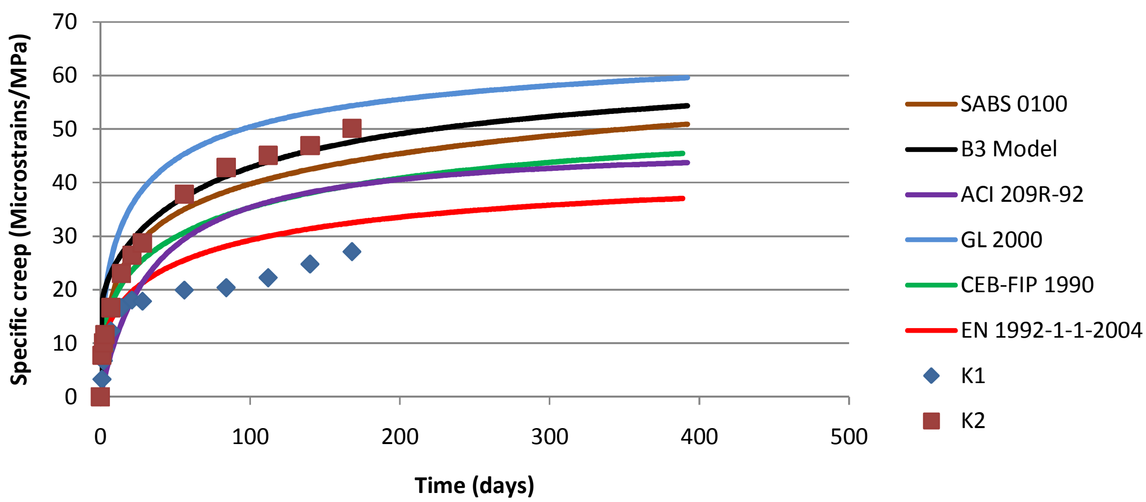

Figure 7.18 a) Measured and calculated specific creep strains over time – data set K

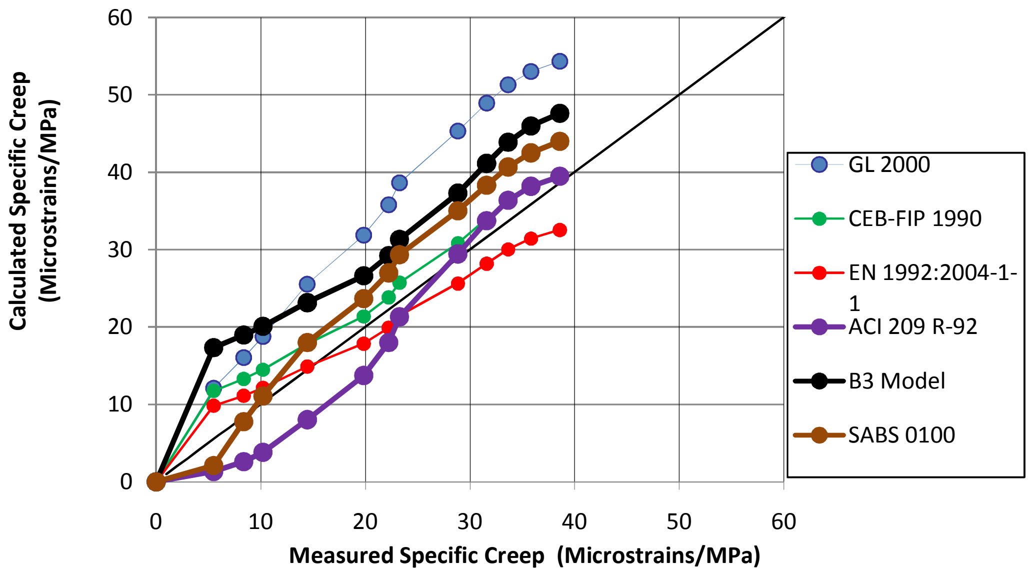

Figure 7.18 b) Calculated vs. Measured specific creep - data set K

Table 7.18: Properties of tested concrete, statistical results and visual observation for creep prediction of data set K

Data set Name	Experiment Names	t_c (days)	t_o (days)	T (°C)	RH (%)	$f_{cm\,28}$ (MPa)	E_{cm28} (GPa)	H (mm)	V/S (mm)
Data set K	K1	32	32	22	65	54	39	50	20

Models	GL 2000	CEB-FIP 1990	EN 1992 - 1-1: 2004	ACI 209 R-92	B3 Model	SABS 0100
BP-COV (%)	68.3	16.8	**16.4**	21.9	46.7	24.7
CEB-MSE (%)	71.0	40.0	27.0	38.7	83.1	**25.8**
Observation	Over Predicts	Over Predicts	Under Predicts	Mixed Behaviour	Over Predicts	Over Predicts

7.4. Summary of results

The statistical errors (BP-COV and CEB-MSE) of each data set that are shown above were subsequently used to compile the accuracy of the models to the entire data. This was achieved through equations 3.1 and 3.5 respectively which are replicated here for convenience.

$$\bar{w} = \sqrt{\frac{1}{N}\sum_{J=1}^{N} w_j^2} \qquad [7.1]$$

$$F_{CEB} = \sqrt{\frac{1}{N}\sum_{j=1}^{N} F_j^2} \qquad [7.2]$$

where

w_j = BP-COV of each data set shown from table 7.1 to 7.18

F_j = CEB-MSE of each data set shown from table 7.1 to 7.18

N = number of data sets under consideration

This was repeated for the coefficient of variation and mean square errors found in the individual experiments and the resulting accuracy of the models to the shrinkage and creep data are shown in table 7.19 and 7.20 respectively.

Table 7.19: Accuracy of the shrinkage results for the models

Using data set results					
Models	GL 2000	CEB-FIP 1990	EN 1992-1-1: 2004	ACI 209 R-92	B3 Model
BP-COV (%)	152.9	64.7	66.2	**47.5**	105.0
CEB-MSE (%)	268.5	147.1	119.6	**45.2**	183.0
Using individual experiment results					
Models	GL 2000	CEB-FIP 1990	EN 1992-1-1: 2004	ACI 209 R-92	B3 Model
BP-COV (%)	151.7	68.8	68.9	**48.3**	102.7
CEB-MSE (%)	294.9	173.5	141.2	**49.8**	205.6

Table 7.20: Accuracy of the creep results for the models

Using data set results						
Models	GL 2000	CEB-FIP 1990	EN 1992-1-1: 2004	ACI 209 R-92	B3 Model	SABS 0100
BP-COV (%)	46.2	32.4	33.1	38.2	62.7	**31.8**
CEB-MSE (%)	57.5	53.6	50.1	42.4	113.2	**29.8**
Using individual experiment results						
Models	GL 2000	CEB-FIP 1990	EN 1992-1-1: 2004	ACI 209 R-92	B3 Model	SABS 0100
BP-COV (%)	66.2	46.7	44.4	43.9	66.2	**43.3**
CEB-MSE (%)	73.1	62.4	56.8	44.0	119.1	**37.8**

CHAPTER 8
ANALYSIS OF RESULTS

8.1. Introduction

In this chapter, the results presented in chapter 7 are analysed. The performance of the models is grouped in categories cement type and compressive strength of the tested concrete. These observations are subsequently used as a tool to recommend of the most suitable model for the design of water retaining structures in South Africa.

8.2. Analysis of shrinkage results

The model performances for shrinkage prediction are divided in six groups and are presented in table 8.1 and 8.2. The assessment on the most accurate prediction model within these groups is presented in table 8.3.

Table 8.1: BP-COV of shrinkage prediction models according to cement type and concrete strength of concrete tested

Category	GL 2000	CEB-FIP 1990	EN 1992-1-1: 2004	ACI 209 R-92	B3 Model
CEM I 30-40 MPa	179.4	83.8	78.5	**54.0**	111.9
CEM I 40-50 MPa	67.8	**30.7**	32.7	41.3	48.6
CEM I 50-60 MPa	82.7	**18.8**	23.3	21.4	58.8
CEM II 30-40 MPa	287.4	124.8	134.6	**66.9**	204.0
CEM II 40-50 MPa	204.5	75.8	84.5	**69.1**	145.4
CEM II 50-60 MPa	93.8	**8.6**	13.0	27.8	83.3

Table 8.2: CEB-MSE of shrinkage prediction models according to the cement type and concrete strength of concrete tested

Category	GL 2000	CEB-FIP 1990	EN 1992-1-1: 2004	ACI 209 R-92	B3 Model
CEM I 30-40 MPa	377.7	228.6	196.2	**54.2**	249.3
CEM I 40-50 MPa	72.5	**33.4**	37.2	47.4	52.0
CEM I 50-60 MPa	125.2	50.7	33.2	**26.1**	84.0
CEM II 30-40 MPa	479.5	238.3	162.5	**48.7**	336.7
CEM II 40-50 MPa	281.9	125.5	94.1	**47.4**	199.8
CEM II 50-60 MPa	93.9	**13.5**	15.9	30.3	79.4

Table 8.3: Most accurate shrinkage prediction model according to cement type and concrete strength of concrete tested

Category	Most accurate shrinkage prediction model
CEM I 30-40 MPa	ACI 209 R-92
CEM I 40-50 MPa	CEB-FIP 1990
CEM I 50-60 MPa	CEB-FIP 1990 / ACI 209 R-92
CEM II 30-40 MPa	ACI 209 R-92
CEM II 40-50 MPa	ACI 209 R-92
CEM II 50-60 MPa	CEB-FIP 1990

The shrinkage performance results were also divided into three groups based in compressive strength only, shown in table 8.4 and 8.5.The assessment on the most accurate prediction model within these groups is presented in table 8.6

Table 8.4: BP-COV of shrinkage prediction models according to concrete strength of concrete tested

Compressive strength	GL 2000	CEB-FIP 1990	EN 1992-1-1: 2004	ACI 209 R-92	B3 Model
30-40 MPa	211.6	95.7	95.6	**57.5**	140.7
40-50 MPa	117.9	**46.3**	50.9	49.7	84.0
50-60 MPa	86.6	**16.2**	20.4	23.7	68.0

Table 8.5: CEB-MSE of shrinkage prediction models according to concrete strength of concrete tested

Compressive strength	GL 2000	CEB-FIP 1990	EN 1992-1-1: 2004	ACI 209 R-92	B3 Model
30-40 MPa	405.5	231.0	188.3	**52.9**	273.8
40-50 MPa	214.7	149.3	132.3	119.4	**109.6**
50-60 MPa	115.7	42.1	28.6	**27.6**	82.5

Table 8.6: Most accurate shrinkage prediction model according to concrete strength of concrete tested

Compressive strength	Most accurate shrinkage prediction model
30-40 MPa	ACI 209 R-92
40-50 MPa	CEB-FIP 1990 / B3 Model
50-60 MPa	CEB-FIP 1990

The shrinkage prediction models have significant high coefficient of variation and CEB mean square errors for the data analysed. Reference is made to table 7.11 to observe this behaviour. It was identified that concretes that contain greywacke from the Western cape (data sets A and I) are over predicted by the models, resulting in high statistical errors.

Table 8.7 shows the performance of the models to the entire data, when these concretes are removed. The table indicates that the statistical errors reduce considerably when greywacke aggregates (with cape flat sands) are not included. Under the new performance, the most accurate prediction model changes to CEB-FIP 1990 model, using Bažant and Panula coefficient of variation method, but remains the ACI 209 R-92 using the CEB mean square error.

Table 8.7: Accuracy of the models to shrinkage results

Concretes with greywacke aggregate (and cape flat sands) analysed(i.e. data set A and I)					
Models	GL 2000	CEB-FIP 1990	EN 1992-1-1: 2004	ACI 209 R-92	B3 Model
BP-COV (%)	152.9	64.7	66.2	**47.5**	105.0
CEB-MSE (%)	268.5	147.1	119.6	**45.2**	183.0
Excluding concretes with greywacke aggregate (and cape flats sands)					
Models	GL 2000	CEB-FIP 1990	EN 1992-1-1: 2004	ACI 209 R-92	B3 Model
BP-COV (%)	99.1	**32.0**	37.3	33.8	67.3
CEB-MSE (%)	123.1	50.2	41.9	**35.2**	83.7

8.3. Analysis of creep results

The model performances for creep prediction are also divided in six groups and are presented in table 8.8 and 8.9. The assessment on the most accurate prediction model within these groups is presented in table 8.10.

Table 8.8: BP-COV of creep prediction models according to cement type and concrete strength of concrete tested

Category	GL 2000	CEB-FIP 1990	EN 1992-1-1: 2004	ACI 209 R-92	B3 Model	SABS 0100
CEM I 30-40 MPa	**20.5**	25.9	25.7	41.1	39.2	29.7
CEM I 40-50 MPa	152.7	108.8	94.3	44.3	83.7	**34.3**
CEM I 50-60 MPa	61.1	**14.8**	17.0	21.1	50.4	26.6
CEM II 30-40 MPa	79.0	65.2	62.5	17.7	142.1	**17.5**
CEM II 40-50 MPa	**25.6**	36.3	42.6	44.3	36.7	48.2
CEM II 50-60 MPa	68.3	16.8	**16.4**	21.9	46.7	24.7

Table 8.9: CEB-MSE of creep prediction models according to the cement type and concrete strength of concrete tested

Category	GL 2000	CEB-FIP 1990	EN 1992-1-1: 2004	ACI 209 R-92	B3 Model	SABS 0100
CEM I 30-40 MPa	29.2	42.1	41.3	39.2	70.2	**27.1**
CEM I 40-50 MPa	379.3	432.6	395.5	48.5	370.6	**42.4**
CEM I 50-60 MPa	65.4	33.8	**22.8**	38.8	83.9	27.9
CEM II 30-40 MPa	103.2	106.1	103.3	30.2	236.3	**26.3**
CEM II 40-50 MPa	58.2	57.9	52.2	45.0	127.9	**33.7**
CEM II 50-60 MPa	71.0	40.0	27.0	38.7	83.1	**25.8**

Table 8.10: Most accurate creep prediction model according to cement type and concrete strength of concrete tested

Category	Most accurate creep prediction model
CEM I 30-40 MPa	GL 2000 / SABS 0100
CEM I 40-50 MPa	SABS 0100
CEM I 50-60 MPa	CEB-FIP 1990 / EN 1992-1-1:2004
CEM II 30-40 MPa	SABS 0100
CEM II 40-50 MPa	GL 2000 / SABS 0100
CEM II 50-60 MPa	EN 1992-1-1:2004/ SABS 0100

The creep performance results were also divided into three groups based in compressive strength only, shown in table 8.11 and 8.12.The assessment on the most accurate prediction model within these groups is presented in table 8.13

Table 8.11: BP-COV of creep prediction models according to concrete strength of concrete tested

Compressive strength	GL 2000	CEB-FIP 1990	EN 1992-1-1:2004	ACI 209 R-92	B3 Model	SABS 0100
30-40 MPa	50.0	45.7	44.3	42.3	90.9	**31.4**
40-50 MPa	125.6	91.3	80.8	44.3	71.5	**39.5**
50-60 MPa	79.2	**12.1**	15.1	24.7	68.8	18.8

Table 8.12: CEB-MSE of creep prediction models according to concrete strength of concrete tested

Compressive strength	GL 2000	CEB-FIP 1990	EN 1992-1-1:2004	ACI 209 R-92	B3 Model	SABS 0100
30-40 MPa	66.4	74.3	72.6	42.9	153.4	**31.1**
40-50 MPa	311.5	354.8	324.3	47.4	311.5	**39.7**
50-60 MPa	80.9	25.7	**19.7**	34.8	81.7	35.8

Table 8.13: Most accurate creep prediction model according to concrete strength of concrete tested

Compressive strength	Most accurate creep prediction model
30-40 MPa	SABS 0100
40-50 MPa	SABS 0100
50-60 MPa	CEB-FIP 1990 / EN 1992-1-1:2004

8.4 General discussion on creep and shrinkage results

The observations on the results of the comparison between the data and the calculations revealed ranges to which the models are expected to over predict or display a mixed behaviour. Model mixed behaviour is of particular importance because it may imply better accuracy if the model predicts close to the real value, however it may also mean a large variance of inaccurate values and a greater risk of obtaining under predicted values.

In general, it was found that for concretes under 45 MPa of compressive strength, the models over predict creep and shrinkage experimental results, however beyond this threshold, there is a trend of mixed behaviour, hence a higher risk of model under prediction exists. WRS are generally made of concretes of compressive strength below 45 MPa, thus models are likely to over predict the actual strains of WRS if only this criteria is taken under consideration.

Beyond 55 % RH, shrinkage results are largely over predicted, while at 50 % RH creep results tend to be over predicted. Note that, the inside face and inside members (i.e. columns) of WRS are exposed to large RH beyond 55 %, hence model over prediction may be expected.

Lastly, at curing times beyond 28 days, the risk of under prediction of creep and shrinkage results increases as mixed behaviour is more frequent. It is unlikely that WRS are cured for periods longer than 7 days, therefore for low curing periods such as these, over prediction is also expected.

In summary, WRS are generally made of concretes of compressive strength below 45 MPa, cured to lower curing times than 28 days and exposed to high RH (higher than 55%). In all three scenarios, the models over predicted results significantly, therefore it is expected that the actual strains of WRS would be over predicted for most cases, thus providing a not necessarily economical but safe design.

However, the selected experiments may not represent the full extent of concretes used in WRS (discussed further in section 10.2.1). Also, a change of aggregate or concrete composition, element dimensions or other exposure conditions may trigger a different outcome to the predictions, thus the engineer should consider the above paragraph while being aware that it may not always be the case. The causes for this change, should be further investigated because it is logical to believe that under-estimation may be the cause of problems for this type of structures. Note that, this is beyond the scope of this investigation which aims to identify a model capable of achieving larger accuracy through appropriate characteristics and mechanisms considered, while obeying engineering principles.

CHAPTER 9

SELECTION OF THE MOST SUITABLE PREDICTION MODEL FOR WRS DESIGN

9.1 Introduction

In this chapter, a selection of the most suitable prediction model to be used in the design of WRS is made based on the analysed results of chapter 7 and the findings of chapter 5 and 6 regarding mechanisms considered, features and Irregularities of the models. To achieve this, a *multi-criteria decision analysis (MCDA)* is considered. This is a system aimed at supporting decision makers when numerous or complex criteria are involved. The selected MCDA is a *weighted sum model* (WSM) in which the mechanisms considered, features and irregularities of models are the weighted criteria.

9.2 Deliberation

A point system is proposed here in which points are attributed to the models according to each criterion. Subsequently, the WSM is performed using four deliberation criteria which are weighted according to their importance. The subjective nature of the weights is later mitigated by an objectivity study.

Table 9.1: Levels and weights of deliberation criteria; deliberation equation

Level	Criteria	Weight	Max. non-normalized points	Max. normalized points
Level 1	Mechanisms considered (*Input*)	1	15	10
Level 1	Features of the models (*Characteristics*)	0.25*	4	10
Level 2	Irregularities (*Errors*)	2	0 (Negative)	0 (Negative)
Level 3	Performance (*Accuracy*)	3	12	10
Equation 9.1 (deliberation equation)				
Points = Input + 0.25 x Characteristics – 2 x Errors + 3 x Accuracy				

*Legend: *- Explained at a later stage*

The following set of equations are required to compute equation 9.1 (in table 9.1):

Input = 1 point for each basic mechanism considered + 1 point for each additional mechanism considered – 1 point for each not considered additional mechanism that is used by another model + 3 bonus points for considering all basic mechanisms. [9.2]

Characteristics = 1 point for each positive feature of the model – 1 point for each negative feature of the model [9.3]

Errors/ Irregularities = 1 point for every error/ Irregularity + 1 penalty point for every error/ irregularity/ negative feature on a sensitive input parameter [9.4]

"Error" points are converted negative by Equation 9.1

Accuracy = Most accurate prediction points + 0.5 $\times$ 2nd most accurate prediction points [9.5]

Most accurate prediction points = 1 point for most accurate result on a large group (i.e. compressive strength only) + 0.5 point for most accurate result on a small group (i.e. CEM Type and compressive strength) [9.6]

2nd most accurate prediction points = 1 point for 2nd most accurate result on a large group + 0.5 point for 2nd most accurate result on a small group [9.7]

Note that equation 9.7 enables models with good results in certain groups to score points regardless of not achieving the most accurate calculation of creep and shrinkage strains in the group. Models within 2% of accuracy to the most accurate model in a group received the maximum number of points. Also, models within 5% of the 2nd most accurate model were attributed the same number of points that a 2nd most accurate model received.

The number of mechanisms considered (Input) is significantly larger than the number of characteristics (features/ Properties) that the models have. Hence the number of points expected from the Input criterion is larger than those originating from the Characteristics, as indicated in table 9.1. With the normalization, to a total of 10 for both criteria, the number of points deriving from the Input reduces whilst the Characteristics points increase. A measure is therefore required to manage the extent to which the Characteristics points influence the overall level 1 points since these are based on the author's observation while the Input is based on counting mechanisms considered. It was therefore decided to limit Characteristics contribution to 20% of the level 1 points.

Calculating the weight of "Characteristics" criterion

Maximum weighted and Normalized points of Input = Max Normalized Input points x weight of Input = 10 x 1 = 10
Maximum weighted and Normalized points of Characteristics = y

For 20 % influence in total level 1 points: $100\left(\frac{y}{y+10}\right) = 20 \therefore y = 2.5$

Max weighted and Normalized point = Max Normalized points of characteristics x weight of characteristic $\Leftrightarrow$ $2.5 = 10 \times x \therefore x = 0.25$

Taking the GL 2000 as an example, the weighted criteria and point system is demonstrated below in tables 9.2 and 9.3.

Table 9.2: Summary of features and good results of GL 2000 model

GL 2000			
Good Feature or result	type	Bad Feature	type
Simple	C*	High sensitivity to humidity	C
All minimum mechanisms considered	I**	Irregularity to V/S change	E*4
f_{cm} & E_{cm} can be substituted	C	Irregularity to curing time change	E
Found more accurate in one of the CEM type and compressive group – creep model	PR ***		

Legend: *- Characteristic criterion   *** - Performance/Accuracy criterion
** - Input criterion   *4 - Error Criterion

Table 9.3: Attributed points for GL 2000 model based on table 9.2

GL 2000 model		
CHARACTERISTICS		
Shrinkage model	good characteristics	2
	bad characteristics	1
	total of characteristics - shrinkage	1
	Total normalized Characteristic points - shrinkage	**2.5**
Creep model	good characteristics	2
	bad characteristics	1
	total of characteristics - creep	1
	Total normalized Characteristic points - creep	**2.5**
PERFORMANCE		
Shrinkage model	CEM and f_{cm} groups - shrinkage	0
	f_{cm} groups - shrinkage	0
	Total performance points - shrinkage	0
	Total normalized Performance points - shrinkage	**0**
Creep model	CEM and f_{cm} groups - creep	1
	f_{cm} groups -creep	0
	Total performance points -creep	0.5
	Total normalized Performance points - shrinkage	**1.04**
INPUT		
Shrinkage model	shrinkage required parameters	5
	shrinkage additional parameters	0
	not achieved add. parameters	0
	bonus points for achieving required parameters - shrinkage	3
	Total input points - shrinkage	8
	Total normalized Input points - shrinkage	**6.15**
Creep model	creep required parameters	7
	creep additional parameters	0
	not achieved add. parameters	
	bonus points for achieving required parameters - creep	3
	Total input result - creep	**10**
	Total normalized Input points -creep	**6.66**
ERRORS		
Creep model	Errors found	2
	Additional penalty for error on a sensitive parameter	0
	Total Error points	2
	Normalized total Error points	**2**
Final Shrinkage model points (using equation 9.1)		**6.78**
Final Creep model points (using equation 9.1)		**6.42**

The above was repeated for the other models. The detailed assessments are accessible in the appendix, while table 9.4 and 9.5 report the normalized points attributed to shrinkage and creep models for every criterion as well as the final normalized points.

Note that it is possible that a model achieves the maximum number of points for the Input, Characteristics or Error criteria. For instance, the in EN 1992:2004-1-1 shrinkage model achieves that for the Characteristics and Error criteria. On the other hand, it is unlikely that a model achieves the maximum number of points for the Performance criterion, because that would imply that the model was the most accurate in all groups of data. For example, the SABS 0100 model, (which achieved the highest Performance rating in creep calculation), received 6.46 points after normalization, that means it achieved 64.6 % of the total achievable points.

While the data used in this project may be replaced or enlarged by a future researcher, which would mean that the Performance rating could change, the Input, Characteristics and Error ratings would remain unchanged for the range of selected models. Therefore this system provides a basis for comparison of these models against other databases or new concretes resulting from advances in concrete technology. It also enables the same basis of comparison for future models.

Table 9.4: Normalized points attributed to shrinkage models

Shrinkage						
Prediction Model	Input (pts*)	Characteristics (pts)	Errors (pts)	Accuracy (pts)	Result** (pts)	Ranking
GL 2000 model	6.15	2.5	0	0	**6.78**	***1.CEB-FIP 1990***
CEB-FIP 1990	6.15	7.5	0	5.42	**24.28**	2. EN 1992-1-1:2004
EN 1992-1-1:2004	6.15	10	0	3.75	**19.90**	3. ACI 209 R-92 4. RILEM B3 model
ACI 209 R- 92	3.08	-5	0	5.63	**18.70**	5. GL 2000
RILEM B3	8.46	0	0	0.83	**10.98**	

Legend: *- Points

**- Result, calculated according to equation 9.1:

Input + 0.25 x Characteristics – 2 x Errors + 3 x Accuracy

Table 9.5: Normalized points attributed to creep models

Creep						
Prediction Model	Input (pts)	Characteristics (pts)	Errors (pts)	Accuracy (pts)	Result (pts)	Ranking
GL 2000 model	6.67	2.5	2	1.04	**6.42**	***1. SABS 0100-1 adj***
CEB-FIP 1990	4	5	0	2.29	**12.13**	2. EN 1992-1-1:2004
EN 1992-1-1:2004	4	7.5	0	2.92	**14.63**	3. CEB-FIP 1990 4. ACI 209 R-92
ACI 209 R- 92	4	2.5	2	2.29	**7.50**	5. RILEM B3 model
RILEM B3	8.67	0	1	0.21	**7.29**	6. GL 2000 model
SABS 0100	3.33	-2.5	1	6.46	**20.08**	

Other weights were also attributed to the deliberation criteria, and except for the case where the weights are changed to unity, the CEB-FIP 1990 remains highest ranked shrinkage model and the SABS 0100-1 adj. the highest ranked creep model. This highlights some objectivity to the answers provided by this system. In particular to creep ranking, it was observed that an increase in the weight of accuracy/performance criteria increases the point difference between the SABS 0100-1 and the other models, with the SABS 0100-1 model benefiting from the change.

On the other hand, if the criteria weights were changed to unity for all four deliberation criteria (i.e. considering all equally important, see table 9.6) the EN 1992-1-1:2004 model achieves the highest points in both creep and shrinkage ranking.

These different sets of results reflect that there is no clear answer. Nevertheless, the EN 1992-1-1:2004 and the CEB-FIP 1990 are consistently placed in the top three positions, for the range of weights considered.

Table 9.6: Un-weighted normalized points attributed to creep and shrinkage models

<table>
<tr><th>Prediction Model</th><th>Un-weighted* Shrinkage Result</th><th>Un-weighted* Creep Result</th><th>Resulting Shrinkage Ranking</th><th>Resulting Creep Ranking</th></tr>
<tr><td>GL 2000 model</td><td>8.65</td><td>8.21</td><td rowspan="6"><u>1.EN 1992-1-1: 2004</u>
2. CEB-FIP 1990
3. RILEM B3
4. GL 2000 model
5. ACI 209 R-92</td><td rowspan="6"><u>1.EN 1992-1-1: 2004</u>
2. CEB-FIP 1990
3. GL 2000 model
4. RILEM B3
5. ACI 209 R-92
6. SABS 0100-1 adj</td></tr>
<tr><td>CEB-FIP 1990</td><td>19.07</td><td>11.29</td></tr>
<tr><td>EN 1992-1-1:2004</td><td>19.90</td><td>14.42</td></tr>
<tr><td>ACI 209 R- 92</td><td>4.12</td><td>6.79</td></tr>
<tr><td>RILEM B3</td><td>9.29</td><td>7.88</td></tr>
<tr><td>SABS 0100</td><td>N/A</td><td>6.29</td></tr>
</table>

Legend: *- all weights equal to 1

Of note is that the only two models that have no inherent flaws with respect to shrinkage and creep prediction are the EN1992-1-1:2004 and CEB-FIP 1990. This, together with their consistent top three places in the weighted evaluation make them strong contenders for use in a South African standard for water retaining structures.

Note further that this work focussed on evaluation in the current form, and did not proceed to correcting flaws or recalibration to increase accuracy. It is proposed that the EN1992-1-1:2004 model is adopted and that a follow-up study is devoted to recalibration to local data.

CHAPTER 10
DISCUSSIONS and CONCLUSION

10.1 Introduction

This chapter presents a summary of the methods used in this project and their limitations, a discussion on the findings, and the selection of the most suitable prediction model. To conclude, recommendations for further research are also provided.

The research was conducted to identify the most suitable prediction model to be used in the design of WRS in South Africa. To achieve this, the following plan of action was proposed and carried out.

Phase 1: Experimental data acquisition phase

Phase 2: Experimental data processing phase

Phase 3: Selection of Prediction models and model processing phase

Phase 4: Statistical analysis and comparison of prediction models to WRS data

In Phase 1, data sources were identified and data was collected thereafter. The data was acquired from reliable experiments with extensive duration and a countrywide origin to provide relevance to the research.

In phase 2, data was selected to represent the concretes used in the construction of water retaining structures throughout South Africa. The selected data was later compared with the prediction models' results.

The assessment of the contents of prediction models was done in phase 3. The formulas and remarks which are published in the models were studied and its relevance to South African conditions was noted. Also in phase 3, the models were programmed through a careful selection of a software package and extensive verification of the quality of the programming.

In the last phase, the WRS data (obtained in phase 2) and the programmed models (obtained in phase 3) were used to compute a statistical evaluation on the accuracy of model predictions to the data.

10.2. Discussion

10.2.1 Phase 1 and Phase 2

The risk of acquiring unreliable data was mitigated through a careful selection of data sources. The sources are experiments done at a reputable university by an academic personnel member, an academic research experiment at a reputable university and local industry requested experiments also performed at a reputable university.

Despite the above, experimental errors may exist due to the nature of these experiments and the long durations required to perform it. It is also possible that these errors may have been carried through to phase 2 of the project when the selection of WRS data took place, and is therefore, important to acknowledge this limitation on the findings of this research.

The range of concrete mix proportions used to select the WRS data in phase 2, were merely an attempt to represent the maximum number of concretes used in WRS. However, it is unable to represent the full set of WRS concretes used in practice. That is, it is possible that a particular concrete mix does not fall within the range utilized yet it is still used in the WRS construction.

10.2.2 Phase 3 and Phase 4

10.2.2.1. Selection of models

Models were selected based on their complexity, region and date of origin as well as reported accuracy in the literature. Two levels of accuracy were considered, the entry/basic and advanced level.

The entry level represents models that are ideal for conceptual and tender stage while the advanced level represents those required for more accurate studies and higher confidence levels. Comparing these two types of models using the same data and statistical indicators, indicated the extent to which the advanced models are more accurate than the entry models. In shrinkage and creep calculation, the GL 2000 (an entry level model) was the least accurate in many occasions due to its simplicity. On the other hand, the SABS 0100 (also an entry level model) which had been adjusted previously achieved very accurate results in many creep calculations, indicating that the entry level models have a huge potential for improvement. Indeed, calibration of these models to South African data may result in simple models that are more accurate than complex advanced level models. However, it is clear that such simple models cannot distinguish between creep and shrinkage levels based on mechanisms not included in their formulations.

Many models in the literature are measured against international data, such as the RILEM data base (e.g. Goel *et al.* 2007). Although such data may be reliable, the model's may achieve good results when compared with this data, but fail to replicate local South African data accurately (e.g. the RILEM B3 model).

The region and date of origin of the models were considered to account for recent advances in creep and shrinkage prediction. Other models may exist which are more recent and that do not originate from the same the region of the models analysed in this project. However the extensive number of models considered and the relative recent date of origin of models was regarded acceptable for the purposes of this project.

10.2.2.2 Model processing and accuracy assessment

The accuracy of the models compared to the selected data may not be the sole criterion for the selection of the most suitable prediction model for WRS design. This is the case due to the above discussion on reliability of the data, but also because all the models have positive as well as negative features that need to be considered in this selection.

The GL 2000 presents a simple approach whilst containing all basic input requirements. Provision is made for the engineer to incorporate f_{cm28} and E_{cm28} tested values in the prediction, which improves accuracy. This model was found to compute good creep results in the CEM II 40-50 MPa group during creep prediction. On the other hand, the same model presents a high sensitivity to small changes of relative humidity as well as errors in its response to V/S and curing time change. These errors are showed in derivation 5.1 and 5.3 respectively, in chapter 5. It was also observed that the model was overly conservative in many of its predictions.

The CEB-FIP 1990 and the EN 1992-1-1:2004 have low sensitivity to small input parameter changes and the ability to incorporate f_{cm28} and E_{cm28} tested values in its prediction amongst other positive features listed in chapter 6. The CEB-FIP 1990 had the most accurate results in four *small groups* (i.e. CEM type and compressive strength categories) and three *large groups* (i.e. compressive strength category only) for both creep and shrinkage prediction which is a noteworthy performance. The EN 1992-1-1: 2004 had the most accurate results in three small groups and one large group for creep prediction.

However, both models do not consider drying before curing, curing type and their provision for temperature effects may be regarded as unrealistic since precise temperature duration may not be known at design stage.

The ACI 209 R-92 is a simple model based on correction factors to the ultimate strain and unlike the previous described models, it considers the curing method as an input parameter. It also uses mix proportions to describe the concrete which is useful when the mix design has been finalized. It shows good results in the 30-40 MPa group and four CEM type-compressive strength groups during shrinkage prediction.

Despite these good results and features, the ACI 209 R-92 model is highly sensitive to a small change of curing time, which is aggravated by incorrect model responses when curing time is changed. This error is shown in figure 5.14 of chapter 5. Also, the model does not consider temperature effects to creep or shrinkage and not all basic input requirements are considered for shrinkage calculation.

The RILEM B3 model contains all the basic input requirements and an extensive range of additional input parameters. The model also shows low sensitivity to small changes of these parameters and the possibility to incorporate tested values of f_{cm28} and E_{cm28} for better accuracy. It is a unique model because it is able to distinguish the basic creep from drying creep which is not possible in the other models. With regard to its accuracy, it shows good results in the 30-40 MPa group for shrinkage prediction.

On the downside, the B3 model is a very complex model with some parameters which are not readily available at design stage (e.g. cement content). Despite its complexity it does not consider temperature effects to creep or shrinkage. Most importantly, the model responds incorrectly to a change in V/S or curing time as indicated in derivation 5.2 and figure 5.15 respectively.

The last model analysed was the SABS 0100 creep model. This is a simple model capable of considering aggregate type and tested values of f_{cm28} and E_{cm28} for better accuracy. In spite of its simplicity, it achieved good results in five small groups and two big groups. However, the model needs the creep coefficient to be manually read off a graph, which prevents automation. Furthermore, it shows high sensitivity to this coefficient in its calculations.

10.2.3 Relevance of the findings to WRS design

It is clear from the findings of this research that not all models are immune of problems. Some models have characteristic problems (such as high sensitivity to small change of parameters) whilst others show problems in engineering principles which is a more severe fault. Whichever the case may be, creep and shrinkage models should be implemented with caution because of these shortcomings.

In general, the prediction models over predicted creep and shrinkage of concretes that have compressive strength lower than 45 MPa, cured to lower curing times than 28 days and exposed to high RH (higher than 55%). Considering that these are the type of concrete and exposure conditions experienced by WRS, the models may be expected to over-predict the actual strains. Beyond those thresholds, limited conclusions can be drawn as mixed behaviour is pertinent.

However, as mentioned earlier the selected experiment may not represent the full extent of concretes used in WRS. Additionally, a change of aggregate or concrete composition, element dimensions or other exposure conditions may trigger a different outcome to the prediction, therefore the engineer should consider the above paragraph while aware that it may not always be the case. In fact, this should be investigated further in future research, as it is logical to believe that under-estimation may be the cause of problems for this type of structures.

10.3 Conclusion

It is proposed that the EN1992-1-1:2004 model is adopted for creep and shrinkage prediction of WRS in South Africa. In the objectivity study of the deliberation system proposed in this project, this model consistently achieved top three positions in both creep and shrinkage rankings regardless of the weights considered. It is also one of the models that have no inherent flaws with respect to shrinkage and creep prediction, and its use has recently been recommended in other countries which implies that improvements to the model are foreseen in the long term. On this note, it is recommended that a follow-up study focuses in recalibration to local data which would improve prediction of creep and shrinkage of local concretes.

10.4 Recommendations for further research

The following recommendations are made for further research to complement this research and address aspects excluded from this research to limit the scope.

- A larger amount of experimental data should be collected. . A continuous extension of the new South African data base for creep and shrinkage is recommended, in order to enable recalibration of the adopted models to improve accuracy.
- Some experiments may be done by the researcher over a period of a year, which would increase the quantity of reliable data for the database created in this project. This is likely to benefit other researchers as well.
- Suggestions from the industry regarding the ranges used for WRS data selection is advisable: this may be achieved through an internet survey. The author's suggested webpage for this purpose is "www.surveymonkey.com".
- Flaws identified in the various models in this report may be corrected by definition of appropriate formulations for particular mechanisms, which follow correct, physical trends.
- Recalibration of a selection of corrected models to local data, to improve accuracy, should be performed.
- A suitable evaluation method should be devised by expert opinion and/or reliability concepts, in order to improve the objectivity of model selection.
- Once an accurate model has been identified, simplification to an entry level model may be useful. In this manner an entry level version is available for preliminary design, while the extended version allows accurate consideration of specific environmental conditions, concrete ingredients and proportions and loading conditions.

REFERENCES

1. Acker, P. *Comportment méchanique du béton: apports de l'approche phisyco-chimique. Rapport de Recherche LPC,* Nº 152, 1988.

2. Alexander and Davis, *The Influence of Aggregates on the Compressive Strength and Elastic Modulus of Concrete*, J Die Siviele Ingenieur in Suid-Afrika, South Africa, 1992, pp 161-170.

3. Alexander, M.G, *Deformation and volume change of hardened concrete, Chapter 13, Fultons Concrete Technology*, Addis B.J, Owens G, (Eds), Cement and Concrete Institute, 8th edn, Midrand, 2001

4. American Concrete Institute Committee, *ACI 209.2R-08: Guide for Modeling and Calculating Shrinkage and Creep in Hardened Concrete,* American Concrete Institute Committee, 2008

5. American Concrete Institute Commitee, *ACI 209R-92: Prediction of Creep, Shrinkage, and Temperature Effects in Concrete Structures,* American Concrete Institute Commitee, 1992.

6. Ballim, Y. *The concrete making properties of the andesite lavas from the Langgeleven formation of the Ventersdorp Supergrou*p, MSc Thesis, University of the Witwatersrand, Johannesburg, 1983.

7. Ballim, Y. *Localizing international concrete models – the case of creep and shrinkage prediction*, Fifth International Conference in Concrete, New Dehli, 1999

8. Bamforth P.B., *Early-age thermal crack control in concrete, CIRIA 660,* CIRIA London, MWL Digital,UK, 2007.

9. Bažant, Z.P., *Creep and Shrinkage prediction model for analysis and design of concrete structures - model B3*, J Materials and Structures Nº28, 1995, pp. 357-365.

10. Bažant, Z.P. & Panula L., *Practical prediction of time-dependent deformations of concrete – Part 6 ,* J Matériaux et constructions Nº 69 (Vol 12), 1978, pp175- 183

11. Bhatt P, MacGinley TJ & Choo BS, *Reinforced concrete: Design theory and Examples,* 3rd edn, Taylor & Francis, London, 2007.

12. Blaine, R.L., Arni, H.T. & Evans, D.N. *Interactions between cement and concrete properties, II, National Bureau of Standards, Building Science Series, No.5,* 1966, pp.44

13. BS8007, *Code of Practice for the Design of Concrete Structures for retaining aqueous liquids*, British Standards Institution, London, 1987

14. *BS 8110, Structural use of concrete – Part 2: Code of Practice for Special Circumstances, British Standards Institution, London, 1985*

15. *BS EN 1992-3: 2006, British Standard, EuroCode 2 – Design of concrete Structures – Part 3: Liquid retaining and Containment Structures, British Standards Institution, 2006*

16. CEB - FIP 1970, Model Code 1970. Comité Euro-International du Béton, Lausane, France, 1970

17. CEB - FIP 1990, Model Code 1990. Comité Euro-International du Béton, Lausane, France, 1990

18. EN1992-1-1:2004, EuroCode 2:Design of concrete structures- Part 1-1: General Rules and Rules for Buildings, European Committee for Standardisation, Brussels, 2004

19. Department of water affairs & Forestry of the Republic of South Africa, *National Water Resource Strategy*, South Africa, 2004

20. Fanourakis, G.C. & Ballim Y., *An Assessment of the Accuracy of Nine Design Models for Predicting Creep in Concrete, J South African Institution of Civil Engineering, Nº 608 (Vol 48-4),* 2006, pp. 2-8

21. Feldman, R.F. & Sereda P.J., *A new model for hydrated Portland cement paste and its practical implications,* Eng. J , Vol 53, No. 8,9, 1970, pp. 53-59

22. Ferreira, R.M., *Probability based durability analysis of concrete structures in marine environment*, University of Minho, 2004.

23. *Gardner, N.J. & Lockman, M.J., GL2000: "Design Provisions for Drying Shrinkage and Creep of Normal-Strength Concrete", ACI Mater. J 98(2), 2000, pp.159-165*

24. Goel, R., Kumar, R. & Paul, D.K.,*Comparative Study of Various Creep and Shrinkage Prediction Models for Concrete*, J Mat Civil Engrg Nº 19(3), 2007, pp. 249-260

25. Hammer, T.A., Test methods for Linear Measurement of Autogenous Shrinkage Before setting, Autogeneous Shrinkage of concrete, Ei-ichi Tazawa (eds), E & FN Spoon, London, 1999, pp. 143-154.

26. Holt, E. E., *Early Age Autogenous Shrinkage of concrete*, Technical Research Centre of Finland, Finland, 2001.

27. Hobbs, D.W. & Parrot L.J., *Prediction of Drying shrinkage*, J Concrete,London,1979, pp. 19-24

28. Hsu,T.C., Slate, F.O., Sturman, G.M. & Winter, G., J. American Concrete Institute, Vol.60, Nº 2, 1963, pp. 209-223.

29. Illston, J.M. & Domone, P.L.J. (eds) 2006, *Construction Materials: Their nature and Behaviour*, 3rd edn, Spon Press, London & New York.

30. Institute of Structural Engineering – Stellenbosch University, *SANS 10100 Part 3 - Design of Concrete Water Retaining Structures (Draft),* 2010.

31. Ishai, O. *The time-dependent deformation behavior of cement paste, mortar and concrete, in* Proceedings of conference on structures of concrete and its behavior under load, Cement and Concrete Association, London, 1965,pp. 345-364

32. Japan Concrete Institute, Technical Committee on Autogenous Shrinkage of concrete, *Committee Report, Autogenous Shrinkage of* Concrete, Ei-ichi Tazawa (eds), E & FN Spoon, London, 1999, pp. 1-62.

33. Jaufeerally H, *Performance and Properties of Structural Concrete Made with Corex Slag*, M.Sc. Thesis, University of Cape Town, 2001.

34. Lerch W. *The Influence of Gypsym on the Hydration of Portland Cement Pastes,* Research Laboratories of the Portland Cement Association, Bulletin Nº 12,1946, pp. 41

35. Mehta, P.K. & Monteiro, P.J.M. 2006, *Concrete: structure, properties, and materials,* 3rd edn, Prentice Hall, New Jersey.

36. Messner, H.S., *Optimum Gypsum Content of Portland Cement*, ASTM Bulletin, Nº 169, 1950, pp. 39-45.

37. Mucambe, E.S.D., *Permeability and Durability of Concrete Water Retaining Structures in South Africa*, BSc Civil Engineering edn, University of KwaZulu-Natal, School of Civil Engineering, Surveying and Construction, Durban, 2007

38. Mucambe, E.S.D. & van Zijl G.P.A.G, *Creep and Shrinkage Prediction Models for Concrete Water Retaining Structures in South Africa, Fourth International Conference of the* Structural Engineering, Mechanics and Computation, *Taylor and Francis, London, 2*010, pp. 223

39. Neville, A. M., *Properties of concrete,* 3rd edn, Pitman Publishing Limited, London, 1981

40. Neville, A.M., *Properties of concrete,* 4th edn, Pearson Education Asia, Essex, 2000

41. Paulini P., *A Weighting Method for Cement Hydration*, 9th International Congress on Chemistry of Cement, New Delhi, 1992, pp. 248- 254.

42. Pickett, G., Effect of Aggregate on Shrinkage of Concrete and a Hypothesis Concerning Shrinkage, J ACI, № 52-36, 1956, pp. 581-590

43. Powers, T.C., *Mechanisms of Shrinkage and Reversible Creep of Hardened Cement Paste*, Proceedings of an International Conference, Cement and Concrete Association, London,1965, pp. 319-343.

44. Richardson MG, *Carbonation of Reinforced Concrete: Its Causes and Management,* CITIS LTD, Dublin, 1988.

45. Roper, H., *Cement Paste Shrinkage – Relationship to Hydration, Young's Modulus and Concrete Shrinkage,* Proceedings of the Fifth International Sympodium on Chemistry of Cements, Tokyo, 1968, pp. 92-99

46. SABS 0100-1*: South African Standard: The Structural Use of Concrete (Part 1: Design),* The South African Bureau of Standards, 2.2nd edn, Pretoria, 2000

47. Sokota, I., *Portland Cement Paste and Concrete.*Macmilan, London, 1979

48. Swayze, M.A., *Volume Changes in Concrete*, J Materials Research and Standards, Vol 1, 1961, pp. 700-704

49. The Concrete Society, *Report of a Working Party of the Materials Technology Divisional Committee*, London, 1973

50. Troxell, G.E., Raphael, J.M., Davis R.E., *Long Term Creep and Shrinkage Tests of Plain and Reinforced Concrete.* Proceedings of the American Society of Testing Materials, Vol 58, 1958, pp. 1101- 1120.

51. van Zijl, G.P.A.G., *Computational Modelling of Masonry Creep and Shrinkage*, Delft,1999.

52. van Zijl, G.P.A.G., *Structural Concrete: Post tensioned slabs (S841), Class notes edn,* Stellenbosch,University, Structural Department, Stellenbosch, *2005*

53. Wagner, O., *Das Kriechen Unbewehrten Betons (Creep of Plain Concrete)*, J Deutscher Ausschuss fu□r Stahlbeton № 131, 1958, pp. 74

54. Wittmann, F.H., *Surface Tension, shrinkage and strength of cement paste*, J Mater. Struct., Vol 1, No. 6, 1968, pp. 547-552

55. Wittmann, F.H., Beltzung F., Zhao T., *Shrinkage Mechanisms, Crack Formation and Service Life of Reinforced Concrete Structures*, Int. J. Structural Engineering, Vol 1, No. 1, 2009, pp. 13- 28.

APPENDIX

derivation 5.2 (Complete derivation)

1. as V/S tends to infinity, the specimen becomes bulkier

D= 2 x V/S, therefore D tends to infinity as V/S tends to infinity and since $\tau_{sh} = k_t k_s D$ then τ_{sh} tends to infinity as well.

$$\varepsilon_{sh\infty} = \varepsilon_{s\infty} + \frac{E(7+600)}{E(t_c + \tau_{sh})}$$

where $E(t)$ is defined as $E(t) = E_{cm28}\sqrt{\frac{t}{4+0.85t}}$

$$\therefore E(t_c + \tau_{sh}) = E_{cm28}\sqrt{\frac{t_c + \tau_{sh}}{4+0.85(t_c + \tau_{sh})}} \Leftrightarrow E(t_c + \tau_{sh}) = E_{cm28}\sqrt{\frac{\infty}{4+\infty}} = E_{cm28} \times \sqrt{1} = E_{cm28}$$

$$\therefore \varepsilon_{sh\infty} = \varepsilon_{s\infty} \times \frac{E(7+600)}{E_{cm28}} = number\ \ A = A$$

Also $q_5 = \frac{7.57\times10^5}{f_{cm28}\varepsilon_{sh\infty}^{0.6}} = \frac{7.57\times10^5}{f_{cm28}\times A^{0.6}} = number\ \ B = B$

$$H(t) = 1-(1-h)S(t)$$

With $S(t) = \tanh\left(\frac{t-t_c}{\tau_{sh}}\right)^{1/2} = \tanh\left(\frac{t-t_c}{\infty}\right)^{1/2} = \tanh 0 = 0 \therefore H(t) = 1$

$$H(t_0) = 1-(1-h)S(t_0)$$

With $S(t_0) = \tanh\left(\frac{t_0-t_c}{\tau_{sh}}\right)^{1/2} = \tanh\left(\frac{t-t_c}{\infty}\right)^{1/2} = \tanh 0 = 0 \therefore H(t_0) = 1$

Hence $C_d = q_5\sqrt{e^{-8H(t)} - e^{-8H(t)}} = B\times\sqrt{e^{-8\times 1} - e^{-8\times 1}} = B\times\sqrt{0} = 0$

In other words as V/S tends to infinity, specimen becomes bulkier and drying creep becomes 0

Since $J(t,t_0,t_c) = q_1 + C_0(t,t_0) + C_d(t,t_0,t_c)$

$$J(t,t_0,t_c) \rightarrow q_1 + C_0(t,t_0) + 0 \;\; as \;\; V/S \rightarrow 0$$

as V/S tends to zero, the specimen becomes slender

D= 2 x V/S, therefore D tends to zero as V/S tends to zero and since $\tau_{sh} = k_t k_s D$ then τ_{sh} tends to zero

2. as V/S tends to zero, the specimen becomes slender

D= 2 x V/S, therefore D tends to zero as V/S tends to zero and since $\tau_{sh} = k_t k_s D$ then τ_{sh} tends to zero as well.

$$\varepsilon_{sh\infty} = \varepsilon_{s\infty} + \frac{E(7+600)}{E(t_c + \tau_{sh})}$$

where $E(t)$ is defined as $E(t) = E_{cm28}\sqrt{\frac{t}{4+0.85t}}$

$$\therefore E(t_c + \tau_{sh}) = E_{cm28}\sqrt{\frac{t_c + \tau_{sh}}{4+0.85(t_c + \tau_{sh})}} \Leftrightarrow E(t_c + \tau_{sh}) = E_{cm28}\sqrt{\frac{t_c}{4+0.85t_c}} = number \;\; F = F$$

$$\therefore \varepsilon_{sh\infty} = \varepsilon_{s\infty} \times \frac{E(7+600)}{F} = number \;\; G = G$$

Also $q_5 = \frac{7.57\times 10^5}{f_{cm28}\varepsilon_{sh\infty}^{0.6}} = \frac{7.57\times 10^5}{f_{cm28}\times G^{0.6}} = number \;\; L = L$

$H(t) = 1 - (1-h)S(t)$

With $S(t) = \tanh\left(\frac{t - t_c}{\tau_{sh}}\right)^{\frac{1}{2}} = \tanh\left(\frac{t - t_c}{0}\right)^{\frac{1}{2}} = \tanh(\infty) = 1 \therefore H(t) = h$

$H(t_0) = 1 - (1-h)S(t_0)$

With $S(t_0) = \tanh\left(\frac{t_0 - t_c}{\tau_{sh}}\right)^{\frac{1}{2}} = \tanh\left(\frac{t - t_c}{0}\right)^{\frac{1}{2}} = \tanh(\infty) = 1 \therefore H(t_0) = h$

Hence $C_d = q_5\sqrt{e^{-8H(t)} - e^{-8H(t)}} = B \times \sqrt{e^{-8\times h} - e^{-8\times h}} = L \times \sqrt{0} = 0$

In other words as V/S tends to infinity, specimen becomes slender and drying creep becomes 0, which is not correct

Since $J(t, t_0, t_c) = q_1 + C_0(t, t_0) + C_d(t, t_0, t_c)$

$J(t, t_0, t_c) \to q_1 + C_0(t, t_0) + 0 \;\; as \;\; V/S \to 0$

as V/S tends to zero, the specimen becomes slender

D= 2 x V/S, therefore D tends to zero as V/S tends to zero and since $\tau_{sh} = k_t k_s D$ then τ_{sh} tends to zero

Table A1: Design mixes from which ranges for selecting the WRS were created

Design mixture 1		Design mixture 2	
Material	**Quantity**	**Material**	**Quantity**
Cement	*315 Kg*	Cement	319 Kg
Slag	*69 Kg*	Slag	65 Kg
Water	*192 L*	Water	192 L
19,0 mm Stone	*896 Kg*	19mm Stone	870 Kg
9,5 mm Stone	*224 Kg*	9.5 mm Stone	330 Kg
River Sand	*730 Kg*	Crusher Sand	192 Kg
Plasticizer	*1344 ml*	River Sand	435 Kg

Table A2: Reported properties of the concrete in experiments of data set A

Property	A1	A2	A3	Units
t_c	7	7	7	days
Tª	23	23	23	ºC
RH	50	50	50	%
f_{cm28}	33	36	36	MPa
E_{cm28}	33	33	33	GPa
SIZE	300x51x51	300x51x51	300x51x51	mm x mm x mm
Volume	780300	780300	780300	mm^3
Total S area	66402	66402	66402	mm^2
Ac	2601	2601	2601	mm^2
u	204	204	204	mm
h	25.5	25.5	25.5	mm
V/S	11.75	11.75	11.75	mm
t_o	14	14	14	days
Constant Stress	87	87	87	MPa
Class of cement	N	N	N	
Type of cement	1	1	1	
Type of curing	water	water	water	
water Q.	182	194	191	kg/mm^3

Slump	75	85	70	mm
Fine Aggr.	41.27	40.86	41.11	%
Cement content	300	300	300	kg/mm^3
Sand content	773	760	768	kg/mm^3
Stone content	1100	1100	1100	kg/mm^3
Aggregate	1873	1860	1868	kg/mm^3

Table A3: Reported properties of the concrete in experiments of data set B

Property	B1	B2	B3	B4	B5	Units
t_c	14	14	14	14	14	days
Tª	23	23	22	23	23	ºC
RH	55	55	50	60	55	%
f_{cm28}	34	34	37	38	36	MPa
E_{cm28}	21	21	N/Av	N/Av	N/Av	GPa
SIZE	100x100x 200	100x100x 200	100x100x 200	100x100x 200	100x100 x200	mm x mm x mm
Volume	2000000	2000000	2000000	2000000	2000000	mm^3
Total S area	100000	100000	100000	100000	100000	mm^2
Ac	10000	10000	10000	10000	10000	mm^2
u	400	400	400	400	400	mm
h	50	50	50	50	50	mm
V/S	20	20	20	20	20	mm
t_o	N/Av	N/Av	N/Av	N/Av	N/Av	days
Constant Stress	N/Av	N/Av	N/Av	N/Av	N/Av	MPa
Class of cement	N	N	N	N	N	
Type of cement	1	1	1	1	1	
Type of curing	water	water	water	water	water	
water Q. kg/m3	200	200	195	200	200	kg/mm^3
Slump	50	50	45		70	mm
Fine Aggr. %	41.70	41.70	35.68	41.71	41.70	%
Cement content	333	333	390	333	333	kg/mm^3
Sand content	787	787	652	787.3	787	kg/mm^3

Stone content	1100	1100	1175	1100	1100	kg/mm^3
Aggregate	1887	1887	1827	1887.3	1887	kg/mm^3

Table A4: Reported properties of the concrete in experiments of data set C

Property	C1	C2	C3	C4	Units
t_c	29	28	28	28	days
Tª	21	23	23	24	ºC
RH	66	55	60	50	%
f_{cm28}	35	34	36	39	MPa
E_{cm28}	39	27	30	29	GPa
SIZE	100x100x 200	cylinder d=100 ; h=300	100x100x 200	cylinder d=100 ; h=200	mm x mm x mm
				cylinder	
Volume	2000000	2356194	2000000	1570796	mm^3
Total S area	100000	102101.8	100000	70685.8	mm^2
Ac	10000	7854	10000	7854	mm^2
u	400	314.1593	400	314.2	mm
h	50	50	50	50	mm
V/S	20	23.1	20	22.2	mm
t_o	28	28	N/Av	28	days
Constant Stress	7	10	N/Av	12	MPa
Class of cement	N	N	N	N	
Type of cement	1	1	1	1	
Type of curing	water	water	water	water	
water Q. kg/m3	195	180	207	195	kg/mm^3

Table A5: Reported properties of the concrete in experiments of data set E and F

Property	E1	E2	E3	F1	G1
t_c	29	28	28	49	7
Tª	23	24	24	21	25
RH	65	50	50	43	50
f_{cm28}	46	40	42	41	52
E_{cm28}	40	34	30	26	-
SIZE	100x100 x 200	cylinder d=100, h=200mm	cylinder d=100, h=200mm	102 x 102 x 230	285x75 x 75
Volume	2000000	1570796.3	1570796.3	2392920	1603125
Total S area	100000	70685.8	70685.8	114648	96750
Ac	10000	7854	7854	10404	5625
u	400	314.2	314.2	408	300
h	50	50	50	51	37.5
V/S	20	22.2	22.2	20.9	16.6
t_o	29	28	28	49	N/Av
Constant Stress	11	12	12	6	N/Av
Class of cement	N	N	N	N	N
Type of cement	1	1	1	1	1
Type of curing	water	water	water	water	water
water Q. kg/m3	200	180	180	210	180
Slump	85	80	85	75	55
Fine Aggr. %	37.3	42.1	42.1	42.7	42.2
Cement content	333	300	240	378	360
Sand content	655	803	803	772	804
Stone content	1100	1104	1104	1036	1100
Aggregate	1755	1907	1907	1808	1904

Table A6: Reported properties of the concrete in experiments of data set G and H

Property	G1	H1	H2	H3	H4	Units
t_c	7	30	29	29	28	days
Tª	25	23	23	21	23	ºC
RH	50	65	65	66	60	%
f_{cm28}	52	55	50	52	55	MPa
E_{cm28}	-	44	39	36	39	GPa
SIZE	285x75 x 75	100x100x 200	100x100x 200	100x100x 200	100x100x 200	mm x mm x mm
Volume	1603125	2000000	2000000	2000000	2000000	mm^3
Total S area	96750	100000	100000	100000	100000	mm^2
Ac	5625	10000	10000	10000	10000	mm^2
u	300	400	400	400	400	mm
h	37.5	50	50	50	50	mm
V/S	16.6	20	20	20	20	mm
t_o	N/Av	30	29	29	286	days
Constant Stress	N/Av	12	13	14	10	MPa
Class of cement	N	N	N	N	N	
Type of cement	1	1	1	1	1	
Type of curing	water	water	water	water	water	
water Q. kg/m3	180	195	205	210	185	kg/mm^3
	55					mm
	42.2					%
	360					kg/mm^3
	804					kg/mm^3
	1100					kg/mm^3
	1904					kg/mm^3

Table A7: Reported properties of the concrete in experiments of data set I, J and K

Property	I1	J1	K1	K2
t_c	28	29	31	33
Tª	21	21	23	21
RH	61	61	65	65
f_{cm28}	36	42	57	51
E_{cm28}	35	39	39	39
SIZE	100x100x 200	100x100x 200	100x100x 200	100x100x 200
Volume	2000000	2000000	2000000	2000000
Total S area	100000	100000	100000	100000
Ac	10000	10000	10000	10000
u	400	400	400	400
h	50	50	50	50
V/S	20	20	20	20
t_o	29	10	31	33
Constant Stress	10	N/Av	12	12
Class of cement	N	N	N	N
Type of cement	2	2	2	2
Type of curing	water	water	water	water
water Q. kg/m3	200	195	205	200

Table A8: BP-COV of prediction models to individual shrinkage experiments

Series	GL 2000	CEB-FIP 1990	EN 1992: 2004 -1-1	ACI 209 R- 92	B3 Model
A1	249.7	131.1	114.2	80.6	147.3
A2	253.4	136.5	121.7	84.5	180.7
A3	275.2	151.4	133.8	97.3	194.2
B1	66.6	14.2	10.5	44.2	16.7
B2	111.8	17.3	28.6	28.5	50.0
B3	231.9	87.1	107.2	38.7	141.7
B4	59.3	20.9	26.0	46.8	21.7
B5	182.1	56.3	74.8	34.2	107.7
C1	97.8	15.8	21.3	12.4	44.9
C2	128.0	43.8	56.6	22.4	56.7
C3	53.7	90.6	20.5	38.6	27.1
C4	200.9	89.8	111.9	45.6	150.2
D1	39.5	34.6	37.6	54.6	21.9
D2	24.2	61.2	58.9	73.7	42.9
E1	20.7	36.4	33.8	41.8	8.8
E2	143.1	51.6	68.0	24.3	81.8
E3	119.9	38.5	54.1	16.4	68.8
F1	72.9	9.1	19.0	15.3	59.6
G1	72.4	25.7	29.9	15.3	37.8
H1	82.7	11.6	13.4	29.1	65.5
H2	131.4	30.6	40.6	43.3	115.5
H3	71.1	14.3	7.5	18.3	67.6
I1	287.4	124.8	134.6	66.9	204.0
J1	204.5	75.8	84.5	69.1	145.4
K1	102.8	12.7	21.4	40.2	100.2
K2	86.9	12.4	9.5	19.5	69.1
COV	**151.7**	**68.8**	**68.9**	**48.3**	**102.7**

Table A9: CEB- MSE of prediction models to individual shrinkage experiments

Series	GL 2000	CEB-FIP 1990	EN 1992: 2004 -1-1	ACI 209 R- 92	B3 Model
A1	424.0	251.8	219.6	57.0	253.7
A2	962.6	616.5	496.8	118.9	686.0
A3	690.7	433.9	373.7	99.2	480.5
B1	66.9	11.5	19.4	49.4	22.0
B2	104.9	19.2	24.7	39.4	48.1
B3	202.8	76.9	72.6	31.3	121.7
B4	46.4	23.4	34.5	53.8	19.0
B5	152.8	46.1	49.5	34.1	87.5
C1	109.4	25.8	27.9	27.6	53.6

C2	118.5	44.1	50.2	31.3	53.5
C3	62.8	15.9	19.6	31.8	34.9
C4	336.6	193.8	126.9	41.8	264.9
D1	29.9	36.3	43.5	58.5	23.0
D2	24.6	55.3	58.5	71.1	40.8
E1	14.9	33.9	38.1	50.9	9.3
E2	216.3	113.4	68.0	19.7	144.1
E3	106.7	37.8	44.0	21.4	62.4
F1	67.2	11.2	26.4	33.8	52.7
G1	157.3	71.4	43.1	15.6	101.2
H1	69.5	10.3	21.1	36.6	52.2
H2	117.2	29.2	35.8	39.3	98.6
H3	77.2	13.0	15.3	31.1	68.5
I1	479.5	238.3	162.5	48.7	336.7
J1	281.9	125.5	94.1	47.4	199.8
K1	87.1	12.4	26.9	39.1	81.5
K2	144.4	50.8	16.1	19.3	115.8
MSE	**294.9**	**173.5**	**141.2**	**49.8**	**205.6**

Table A10 : BP-COV of prediction models to individual creep experiments

Series	**GL 2000**	**CEB-FIP 1990**	**EN 1992-1-1:2004**	**ACI 209 R-92**	**B3 Model**	**SABS 0100**
A1	32.2	29.7	29.3	40.4	47.3	13.0
A2	24.7	37.0	34.3	30.1	48.5	16.4
A3	116.9	116.8	116.8	28.5	63.3	23.9
C1	57.8	66.7	66.8	68.4	52.7	80.8
C2	16.0	18.4	18.5	58.0	22.8	62.1
C4	48.4	28.0	21.4	42.2	89.6	21.4
E1	35.9	9.4	18.5	43.1	45.5	21.2
E2	13.6	22.3	27.2	59.5	19.6	38.4
E3	18.2	10.6	17.1	59.1	14.7	42.7
H1	74.7	18.3	12.2	33.0	70.5	48.9
H2	133.6	66.9	42.5	40.9	119.9	70.5
H3	20.5	24.9	39.1	43.8	19.6	28.8
I1	79.0	65.2	62.5	17.7	142.1	17.5
J1	25.6	36.3	42.6	44.3	36.7	48.2
K1	140.8	59.4	28.2	52.4	101.0	72.1

K2	29.0	21.1	35.0	31.8	23.7	17.2
COV	**66.2**	**46.7**	**44.4**	**43.9**	**66.2**	**43.3**

Legend:

No reported creep values for experiment C3

Table A11: CEB- MSE of prediction models to individual creep experiments

Series	GL 2000	CEB-FIP 1990	EN 1992-1-1:2004	ACI 209 R-92	B3 Model	SABS 0100
A1	28.1	53.3	52.8	32.3	79.2	17.3
A2	26.3	55.4	52.8	25.7	78.8	24.5
A3	99.9	99.8	99.8	23.4	89.9	28.7
C1	84.3	98.0	97.8	51.0	205.9	48.5
C2	23.0	30.2	30.0	61.0	34.2	51.1
C4	56.9	54.3	48.3	43.1	148.3	23.5
D1	0.0	0.0	0.0	0.0	0.0	0.0
E1	29.9	12.0	13.6	54.0	59.3	34.3
E2	13.7	16.8	18.9	59.3	26.7	36.2
E3	18.7	16.1	16.5	58.0	28.1	42.0
H1	67.8	27.1	15.1	41.8	89.2	40.5
H2	164.1	115.0	88.6	33.3	206.1	69.9
H3	27.8	20.2	27.2	51.7	40.5	32.0
I1	103.2	106.1	103.3	30.2	236.3	26.3
J1	58.2	57.9	52.2	45.0	127.9	33.7
K1	138.5	81.7	53.9	46.9	151.0	53.3
K2	38.5	20.6	23.6	44.6	54.6	24.6
MSE	**73.1**	**62.4**	**56.8**	**44**	**119.1**	**37.8**

Legend:

No reported creep values for experiment C3

Table A12: Table of positive and negative features of prediction models

Good Feature			Bad Feature		
GL 2000					
Feature	type	Qty	Feature	type	Qty
Simple	C		High sensitivity	C	1
Has minimum requirements	I		Irregularity to V/S change	E	
Fcm & Ecm can be substituted	C		Irregularity to curing time change	E	
Found more accurate in one of the CEM type and compressive categories – creep	PR	1			
CEB- FIP 1990					
simple	C		Not all minimum requirements are considered - creep	I	1
Fcm & Ecm can be substituted	C		Type of curing not considered	AI	1
Low sensitivity	C		Use of temperature is unrealistic – creep only	C	
Additional inputs considered (Temperature) – creep only	AI	1			
All required inputs - shrinkage	I				
Found more accurate in one of the CEM type and compressive categories - shrinkage	PR	3			
Found more accurate in one of the compressive strength categories - shrinkage	PR	2			
Found more accurate in one of the CEM type and compressive categories - creep	PR	1			
Found more accurate in one of the compressive strength categories - creep	PR	1			
EN 1992-1-1:2004					
simple	C		Not all minimum requirements are considered	I	1
Fcm & Ecm can be substituted	C		Type of curing not considered	AI	1
Low sensitivity	C		Use of temperature is unrealistic	C	

			– creep only		
Additional input considered (Temperature)	AI	1			
All required inputs - shrinkage	I				
Correction factors for high strength concretes	C				
Found more accurate in one of the CEM type and compressive categories - creep	PR	3			
Found more accurate in one of the compressive strength categories - creep	PR	1			
ACI 209 R-92					
simple	C		Not all minimum requirements considered – shrinkage only	I	1
Fcm & Ecm can be substituted – Creep only	C		Fcm & Ecm cannot be substituted – Shrinkage only	C	
Minimum requirements considered – creep only	C		Temperature not considered	AI	1
Additional input considered (curing type)	AI	1	High sensitivity to curing	C	1
Found more accurate in one of the CEM type and compressive categories - shrinkage	PR	4	Irregularity to curing change	E	
Found more accurate in one of the compressive strength categories - shrinkage	PR	1	high sensitivity on an irregular parameter	C&E	1
			Unrealistic parameters at design phase (e.g. slump)	C	
RILEM B3					
Has minimum requirements	I		Too complex	C	
Additional input considered	AI	4	Temperature not considered	AI	1
Low sensitivity	C		Unrealistic parameters at design phase	C	
Fcm & Ecm can be substituted	C		Not a general form to account for specimen shape	C	

Distinguish between basic and drying creep	C		Irregularity on V/S change	E	
Found more accurate in one of the compressive strength categories - shrinkage	PR	1			
SABS 0100					
simple	C		Not fully programmable	C	
Additional input considered (Aggregate type)	AI	1	High sensitivity	C	1
Fcm & Ecm can be substituted	C		Not all basic parameters are considered	I	2
Found more accurate in one of the CEM type and compressive categories - creep	PR	5	No provision for smaller specimen (V/S)	I	1
Found more accurate in one of the compressive strength categories - creep	PR	2	Creep coefficient is a input parameter (reading off a graph)	C	
			high sensitivity on an irregular parameter	C&I = E	1

Table A13: Attributed points for GL 2000 model

GL 2000 model		
CHARACTERISTICS		
Shrinkage model	good characteristics	2
	bad characteristics	1
	total of characteristics - shrinkage	**1**
Creep model	good characteristics	2
	bad characteristics	1
	total of characteristics - creep	**1**
PERFORMANCE		
Shrinkage model	CEM and Fcm categories - shrinkage	0
	fcm categories - shrinkage	0
	Total performance value - shrinkage	**0**
Creep model	CEM and Fcm categories - creep	1
	fcm categories -creep	0
	Total performance value -creep	**0.5**
INPUT		
Shrinkage	shrinkage required parameters	5

model	shrinkage additional parameters	0
	not achieved add. parameters	0
	bonus points for achieving required parameters - shrinkage	3
	TOTAL input result - shrinkage	**8**
Creep model	creep required parameters	7
	creep additional parameters	0
	not achieved add. parameters	
	bonus points for achieving required parameters - creep	3
	TOTAL input result - creep	**10**
ERRORS		
Creep models	Errors found	2
	Additional penalty for error on a sensitive parameter	0
	TOTAL Error value	**2**
Shrinkage points		**5**
Creep points		**8.5**

Table A14: Attributed points for CEB-FIP 1990

CEB-FIP 1990		
CHARACTERISTICS		
Shrinkage model	good characteristics	3
	bad characteristics	0
	total of characteristics - shrinkage	**3**
Creep model	good characteristics	3
	bad characteristics	1
	total of characteristics - creep	**2**
PERFORMANCE		
Shrinkage model	CEM and Fcm categories - shrinkage	3
	fcm categories - shrinkage	2
	Total performance value - shrinkage	**3.5**
Creep model	CEM and Fcm categories - creep	1
	fcm categories -creep	1
	Total performance value -creep	**1.5**
INPUT		
Shrinkage model	shrinkage required parameters	5
	shrinkage additional parameters	1
	not achieved add. parameters	1
	bonus points for achieving required parameters - shrinkage	3

	TOTAL input result - shrinkage	**8**
Creep model	creep required parameters	6
	creep additional parameters	1
	not achieved add. parameters	1
	bonus points for achieving required parameters - creep	0
	TOTAL input result - creep	**6**
ERRORS		
Creep models	Errors found	0
	Additional penalty for error on a sensitive parameter	0
	TOTAL Error value	**0**
Shrinkage points		**21.5**
Creep points		**12.5**

Table A15: Attributed points for EN 1992-1-1:2004

EN 1992-1-1:2004		
CHARACTERISTICS		
Shrinkage model	good characteristics	4
	bad characteristics	0
	total of characteristics - shrinkage	**4**
Creep model	good characteristics	4
	bad characteristics	1
	total of characteristics - creep	**3**
PERFORMANCE		
Shrinkage model	CEM and Fcm categories - shrinkage	0
	fcm categories - shrinkage	0
	Total performance value - shrinkage	**0**
Creep model	CEM and Fcm categories - creep	3
	fcm categories -creep	1
	Total performance value -creep	**2.5**
INPUT		
Shrinkage model	shrinkage required parameters	5
	shrinkage additional parameters	1
	not achieved add. parameters	1
	bonus points for achieving required parameters - shrinkage	3
	TOTAL input result - shrinkage	**8**
Creep model	creep required parameters	6
	creep additional parameters	1
	not achieved add. parameters	1

	bonus points for achieving required parameters - creep	0
	TOTAL input result - creep	**6**
ERRORS		
Creep models	Errors found	0
	Additional penalty for error on a sensitive parameter	0
	TOTAL Error value	**0**
Shrinkage points		**12**
Creep points		**16.5**

Table A16: Attributed points for ACI 209 R-92

ACI 209 R-92		
CHARACTERISTICS		
Shrinkage model	good characteristics	1
	bad characteristics	3
	total of characteristics - shrinkage	**-2**
Creep model	good characteristics	3
	bad characteristics	2
	total of characteristics - creep	**1**
PERFORMANCE		
Shrinkage model	CEM and Fcm categories - shrinkage	4
	fcm categories - shrinkage	1
	Total performance value - shrinkage	**3**
Creep model	CEM and Fcm categories - creep	0
	fcm categories -creep	0
	Total performance value -creep	**0**
INPUT		
Shrinkage model	shrinkage required parameters	4
	shrinkage additional parameters	1
	not achieved add. parameters	1
	bonus points for achieving required parameters - shrinkage	0
	TOTAL input result - shrinkage	**6**
Creep model	creep required parameters	1
	creep additional parameters	1
	not achieved add. parameters	0
	bonus points for achieving required parameters - creep	0
	TOTAL input result - creep	**6**
ERRORS		

Creep models	Errors found	1
	Additional penalty for error on a sensitive parameter	1
	TOTAL Error value	**2**
Shrinkage points		**7**
Creep points		**3**

Table A17: Attributed points for RILEM B3 model

RILEM B3 model		
CHARACTERISTICS		
Shrinkage model	good characteristics	3
	bad characteristics	3
	total of characteristics - shrinkage	**0**
Creep model	good characteristics	3
	bad characteristics	3
	total of characteristics - creep	**0**
PERFORMANCE		
Shrinkage model	CEM and Fcm categories - shrinkage	0
	fcm categories - shrinkage	1
	Total performance value - shrinkage	**1**
Creep model	CEM and Fcm categories - creep	0
	fcm categories -creep	0
	Total performance value -creep	**0**
INPUT		
Shrinkage model	shrinkage required parameters	5
	shrinkage additional parameters	4
	not achieved add. parameters	1
	bonus points for achieving required parameters - shrinkage	3
	TOTAL input result - shrinkage	**11**
Creep model	creep required parameters	7
	creep additional parameters	4
	not achieved add. parameters	1
	bonus points for achieving required parameters - creep	3
	TOTAL input result - creep	**13**
ERRORS		
Creep models	Errors found	1
	Additional penalty for error on a sensitive parameter	0
	TOTAL Error value	**1**

Shrinkage points	**12**
Creep points	**11**

Table A18: Attributed points for SABS 0100-1 mod. creep model

RILEM B3 model		
CHARACTERISTICS		
Creep model	good characteristics	2
	bad characteristics	3
	total of characteristics - creep	**-1**
PERFORMANCE		
Creep model	CEM and Fcm categories - creep	5
	fcm categories -creep	2
	Total performance value -creep	**4.5**
INPUT		
Creep model	creep required parameters	4
	creep additional parameters	1
	not achieved add. parameters	0
	bonus points for achieving required parameters - creep	0
	TOTAL input result - creep	**5**
ERRORS		
Creep model	Errors found	0
	Additional penalty for error on a sensitive parameter	1
	TOTAL Error value	**1**
Creep points		**14.5**